

DebriSat Pre Preshot Laboratory Analyses

March 27, 2015

Paul M. Adams¹ and Patti M. Sheaffer²
¹Space Materials Laboratory
²Space Science Applications Laboratory
Physical Sciences Laboratories

Prepared for:

Space and Missile Systems Center
Air Force Space Command
483 N. Aviation Blvd.
El Segundo, CA 90245-2808

Contract No. FA8802-14-C-0001

Authorized by: Space Systems Group

Distribution Statement A: Approved for public release; distribution unlimited

Report Documentation Page			Form Approved OMB No. 0704-0188		
Public reporting burden for the collection of information is estimated to average 1 hour per response, including the time for reviewing instructions, searching existing data sources, gathering and maintaining the data needed, and completing and reviewing the collection of information. Send comments regarding this burden estimate or any other aspect of this collection of information, including suggestions for reducing this burden, to Washington Headquarters Services, Directorate for Information Operations and Reports, 1215 Jefferson Davis Highway, Suite 1204, Arlington VA 22202-4302. Respondents should be aware that notwithstanding any other provision of law, no person shall be subject to a penalty for failing to comply with a collection of information if it does not display a currently valid OMB control number.					
1. REPORT DATE 27 MAR 2015	2. REPORT TYPE Final	3. DATES COVERED -			
4. TITLE AND SUBTITLE DebrisSat Pre Preshot Laboratory Analyses		5a. CONTRACT NUMBER FA8802-14-C-0001			
		5b. GRANT NUMBER			
		5c. PROGRAM ELEMENT NUMBER			
6. AUTHOR(S) Paul M. Adams and Patti M. Sheaffer		5d. PROJECT NUMBER			
		5e. TASK NUMBER			
		5f. WORK UNIT NUMBER			
7. PERFORMING ORGANIZATION NAME(S) AND ADDRESS(ES) The Aerospace Corporation 2310 e. El Segundo Blvd. El Segundo, CA 90245-4609		8. PERFORMING ORGANIZATION REPORT NUMBER TOR-2014-03083			
9. SPONSORING/MONITORING AGENCY NAME(S) AND ADDRESS(ES) Space and Missile Systems Center Air Force Space Command 483 N. Aviation Blvd. El Segundo, CA 90245-2808		10. SPONSOR/MONITOR'S ACRONYM(S) SMC			
		11. SPONSOR/MONITOR'S REPORT NUMBER(S)			
12. DISTRIBUTION/AVAILABILITY STATEMENT Approved for public release, distribution unlimited					
13. SUPPLEMENTARY NOTES The original document contains color images.					
14. ABSTRACT In preparation for the DebrisSat hypervelocity impact test a Pre Preshot was conducted to validate the performance of the aluminum projectile to meet the velocity goal of 7 km/s and confirm operational status of test chamber and facility. The target was a multi-shock shield supplied by NASA which consisted of seven bumper panels consisting of fiberglass (E-glass, #1,2,4,5), stainless steel mesh (#3) and Kevlar (#6,7). In contrast to the DebrisSat and Debris-LV impact tests, no soft catch panels were installed. A witness plate assembly was provided by Aerospace in order to catch and sample debris for laboratory analysis, to identify materials produced by the impact and characterize the degree of darkening associated with hypervelocity collisions.					
15. SUBJECT TERMS DebrisSat, hypervelocity impact, space debris					
16. SECURITY CLASSIFICATION OF:			17. LIMITATION OF ABSTRACT UU	18. NUMBER OF PAGES 100	19a. NAME OF RESPONSIBLE PERSON
a. REPORT unclassified	b. ABSTRACT unclassified	c. THIS PAGE unclassified			

Abstract

In preparation for the DebrisSat hypervelocity impact test a Pre Preshot was conducted to validate the performance of the aluminum projectile to meet the velocity goal of 7 km/s and confirm operational status of test chamber and facility. The target was a multi-shock shield supplied by NASA which consisted of seven bumper panels consisting of fiberglass (E-glass, #1,2,4,5), stainless steel mesh (#3) and Kevlar (#6,7). In contrast to the DebrisSat and Debris-LV impact tests, no “soft catch” panels were installed. A witness plate assembly was provided by Aerospace in order to catch and sample debris for laboratory analysis, to identify materials produced by the impact and characterize the degree of darkening associated with hypervelocity collisions.

The material collected on the witness plate as a result of the impact formed a thin continuous layer about 10 microns thick, solidified from molten droplets of two phases that have a complex intermixed flow structure. The material consists of a crystalline Fe-Cr-Ni rich phase and amorphous oxide phases. The relative Fe-Cr-Ni proportions in the Fe-Cr phase are not significantly different from the stainless steel bumper though it also contains significant amounts Al and Si. The Al and Si contents are about equal in early arriving Fe-Cr-Ni while the later arriving Fe-Cr is Si rich and Al is low to absent. In the later droplets there is less flow structure and individual droplets tend to retain their shape implying they were already semi-solidified when deposited. The oxide phases have a range of compositions.

The early oxide phase, mixed with Fe-Cr-Ni in complex flow patterns, is primarily Ca-Al oxide with no Si. Later oxide droplets present on the surface are larger (to 100-200 microns) and show less flow structure but some gas bubbles. Later oxide droplets have significant Si and many have compositions similar to E-glass. The integrated (Ca-Al-Si) composition of the early phases with the complex flow patterns is significantly enriched in Al with respect to E-glass implying much of the Al (to 18%) came from the projectile. Aluminum has the lowest melting point of the starting materials.

The first three bumpers that were perforated were fiberglass (1,2) and stainless steel (3). Molten droplets consisting of Fe-Cr-Ni and Al-Ca oxide may have condensed from a mixed gas phase formed from the bumpers and the projectile. Si and Al from the E-glass dissolved in the Fe-Cr leaving Al and Ca in an oxide phase. Additional Al came from the Al projectile. All Si may have dissolved in the Fe-Cr-Ni phase possibly leaving no Si for the Al-Ca oxide. These droplets arrived first in a very fluid state and physically mixed and flowed together in complex patterns. The fourth and last bumper to be perforated by the decelerated projectile was E-glass. Molten droplets from this bumper arrived latter and some were less fluid and show less flow structure. The droplet size was larger (to 100-200 μm) and the composition was more consistent with E-glass. The later droplets show little to no mixing and the late Fe-Cr-Ni droplets retain their shape. This implies they were cooler and partially solidified when deposited.

Significant darkening of adjacent structures, with a drop from 90-95% to 20-25% reflectance, occurred as a result of impact. The deposition on the witness plate assembly appears to be line of sight since witness plates protected by Whipple shield showed little change. LWIR spectral features from the deposited material are related to silicate and borate from the E-glass bumpers that were penetrated. The silicate feature shifted as a result of a change in composition.

Acknowledgements

DebrisSat Team Members:

J.-C. Liou: NASA Space Debris Program Office, NASA JSC
AEDC Range G Light Gas Gun Staff
Charles Griffice: Aerospace
Marlon Sorge: Aerospace
Gouri Radhakrishnan: Aerospace

Financial Support:

Charles Griffice and Tom Huynh

Discussions with:

Gouri Radhakrishnan
Charles Griffice
C. C. Wan

UV-VIS-NIR Spectroscopy

Dianna Alaan

FIB/TEM Sample Preparation

Miles Brodie

Aerospace Technical Operating Report No.
TOR-2014-03083

DebrisSat Pre Preshot Laboratory Analyses

23 December, 2014

Paul M. Adams¹ and Patti Sheaffer²

¹Materials Processing Department
Space Materials Laboratory

²Remote Sensing Department
Space Science Applications Laboratory

Physical Sciences Laboratories

Introduction

- The DebrisSat test was conducted to better understand the distribution of fragments generated from a hypervelocity impact with a modern satellite.
 - The last such test (SOCIT) was conducted 20 years ago and satellite construction has changed considerably since then.
 - In 2009 a Cosmos 2251 upper stage collided with an Iridium 33 satellite.
 - Produced 2000+ trackable fragments (>10 cm).
 - 8 other known collisions, some only known long after occurrence.
- DebrisSat was a NASA program with support/collaboration from the Air Force Space and Missile Center, University of Florida and Aerospace.
- Tests were conducted at the Arnold Engineering Development Complex, Tullahoma, Tennessee.
 - Two-Stage Light Gas Gun Facility - Range G.
 - Largest such facility in the United States.
 - All tests used a ~600 gram projectile with a nominal velocity of 7 km/s.



Introduction (cont.)

- Two trial tests were conducted prior to DebrisSat.
 - **Pre Preshot**. February 2014
 - Debris-LV (Pre Shot). 1 April 2014
 - DebrisSat. 15 April 2014
- Pre Preshot was conducted February 2014
 - Validated performance of projectile to meet velocity goal of 7 km/s.
 - Confirmed operational status of test chamber and facility.
 - Target was primarily designed to catch the projectile.
 - Multi-shock shield supplied by NASA.
 - Multiple bumper panels of fiberglass, stainless steel mesh and Kevlar.
 - **No “soft catch “ panels were installed** (unlike Debris-LV and DebrisSat).
 - Test conducted with a pressure of ~1-2 Torr nitrogen.
 - A witness plate assembly was provided by Aerospace in order to catch and sample debris.

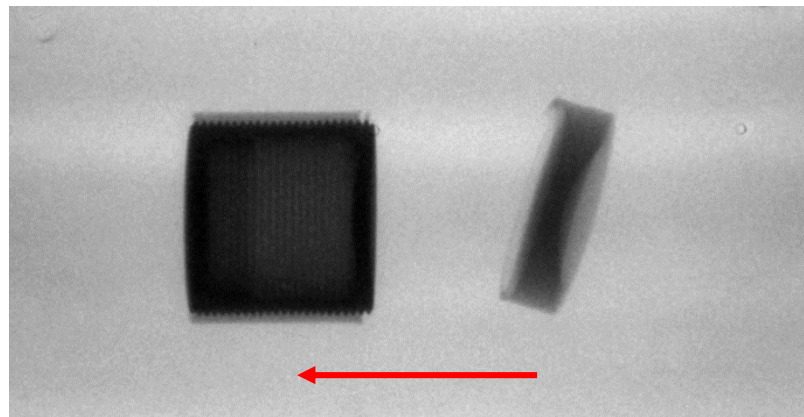


- Background
 - “Darkening” of satellites has been observed as a result of suspected hypervelocity impacts.
 - The material and processes responsible for the darkening is unknown.
- Objectives
 - Materials collected on witness plates in the Pre Preshot test were analyzed in order to identify the source and conditions responsible for the darkening.
 - UV-VIS-NIR-LWIR reflectance spectra were measured of post test debris for comparison with pre test sources to determine the spectral signature of material generated by a hypervelocity impact.
 - Possibly determine if a hypervelocity impact occurred based on remotely sensed spectra?
 - Can the source be identified – does it have a unique signature?



Projectile

Images by AEDC



Flash X-ray of projectile in flight

- Constructed from three pieces:
- Outer Nylon shell (sabot) with 2 part hollow aluminum insert.
- ~600 grams, 8.6 cm diameter X 10.3 cm long – size of a soup can.
- Velocity ~ 6.8-6.9 km/s.
- During flight Nylon base separated from Nylon-aluminum body.
 - In all three tests.



Target being loaded into chamber.

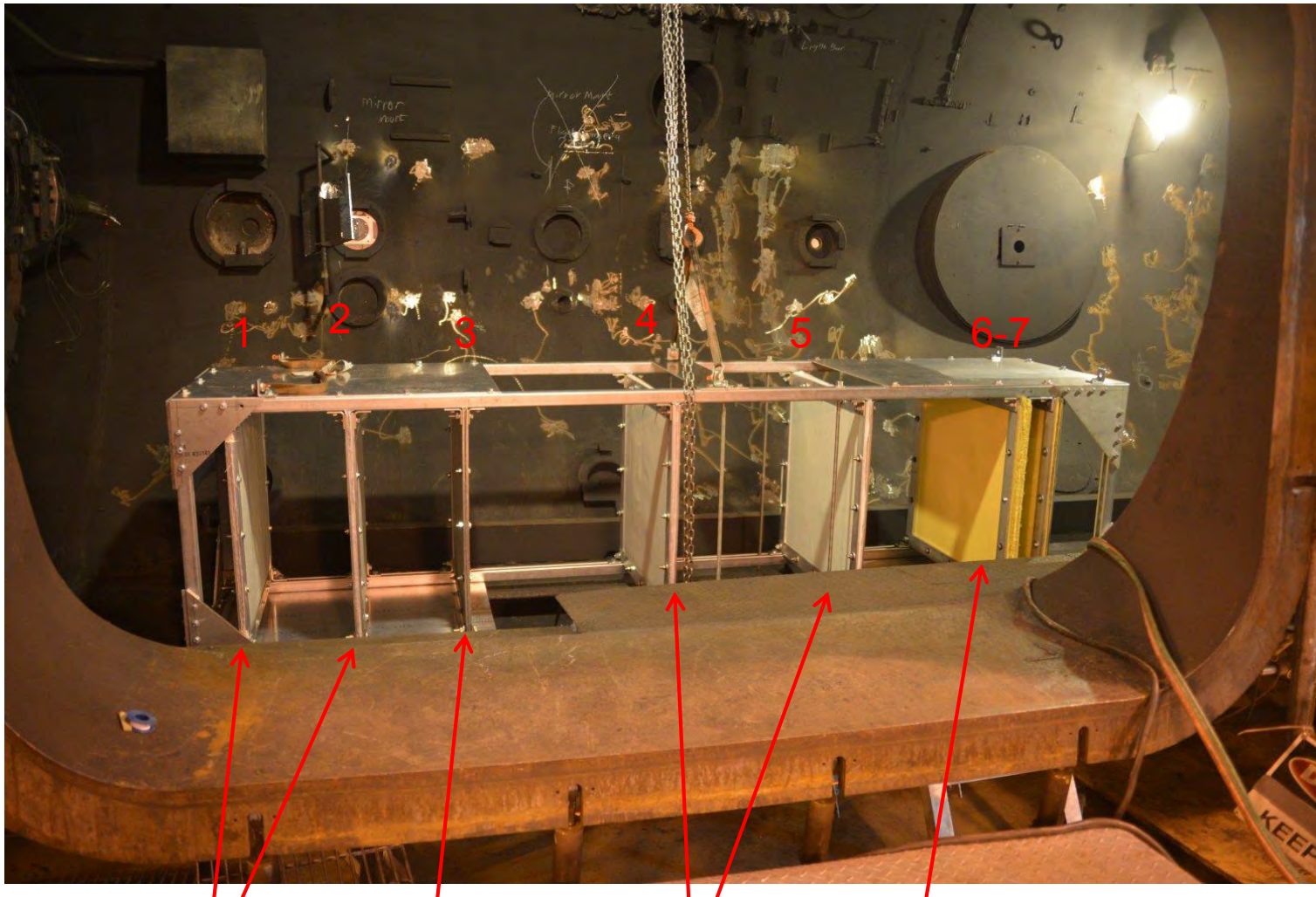


Image by AEDC

E-glass

Steel

E-glass

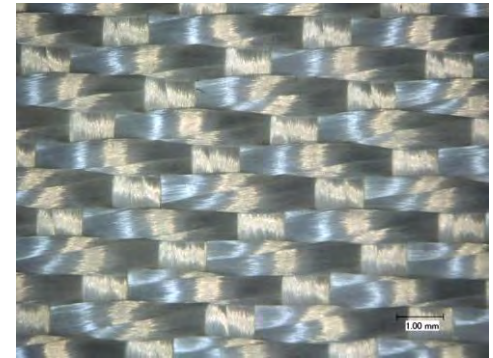
Kevlar

Overall length of the target was 2.65m. Witness plate assembly was mounted on the side of the chamber between bumpers 3 and 4

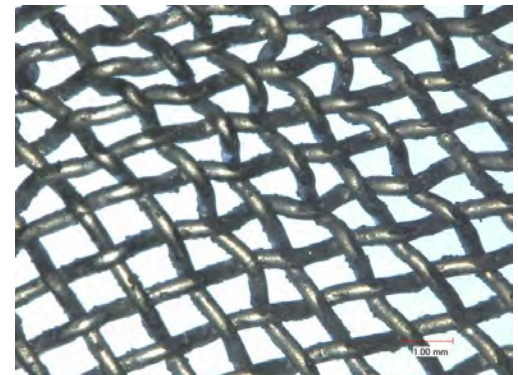


Bumper Materials

- Fiberglass bumpers constructed from FG-3784 satin weave E-glass fabric
 - 22 layers of 26 oz per sq ft fabric for each bumper
 - ~7 micron fiber diameter
 - E-glass is a calcium boro-aluminosilicate
 - Minor Na, Mg
- Steel bumpers constructed from 304 (?) stainless steel (SS) mesh.
 - Filaments are about 0.4 mm dia.
 - Seven sheets were stacked
 - 69.1 % Fe, 18.2% Cr, 10.8% Ni, 1.4 % Mn, 0.5% Si (wt %)



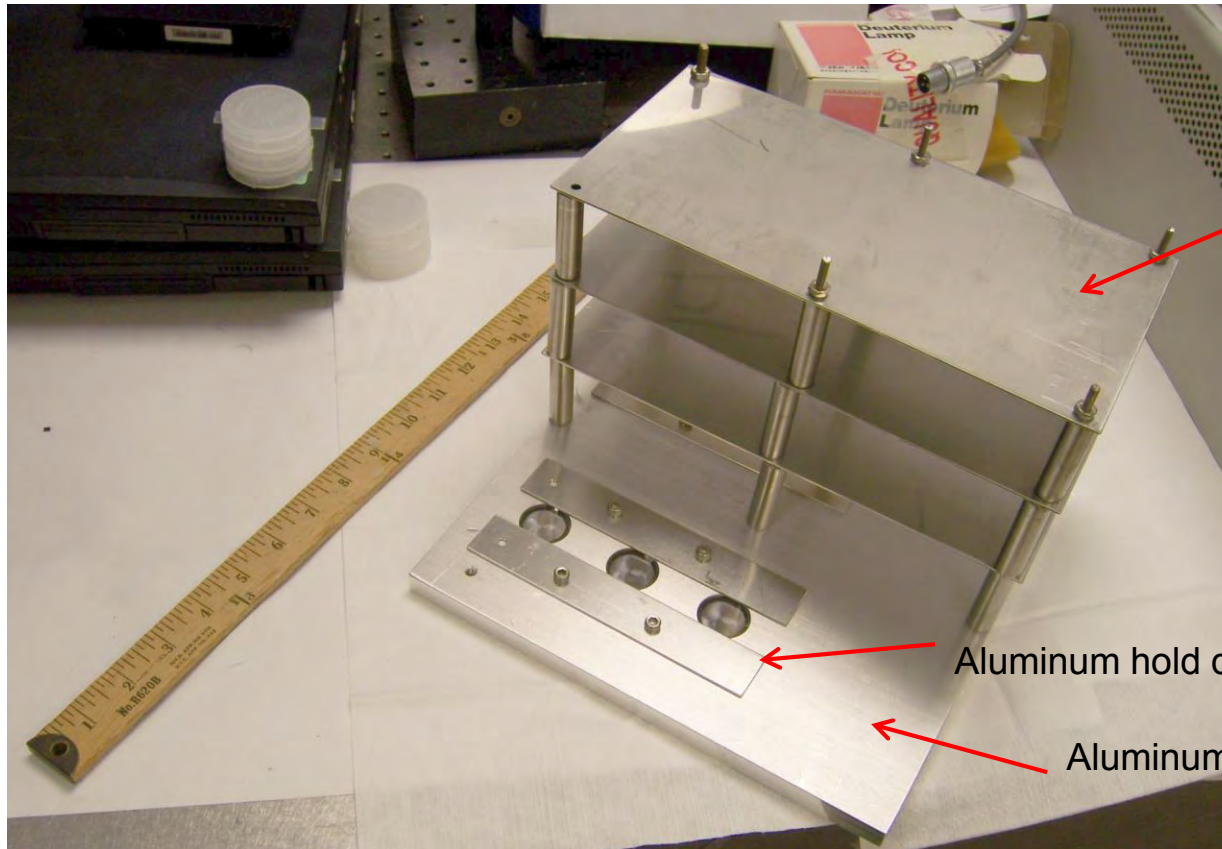
FG-3784 fabric



SS Mesh



Witness Plate Assembly



(3) Stainless steel
Whipple plates

Aluminum hold down plate

Aluminum base plate

(6) 1" diameter fused silica windows – (3) directly exposed and (3) protected under Whipple plates.
Multilayer insulation (MLI) samples added later.

Assembly positioned about 1 meter from center of target

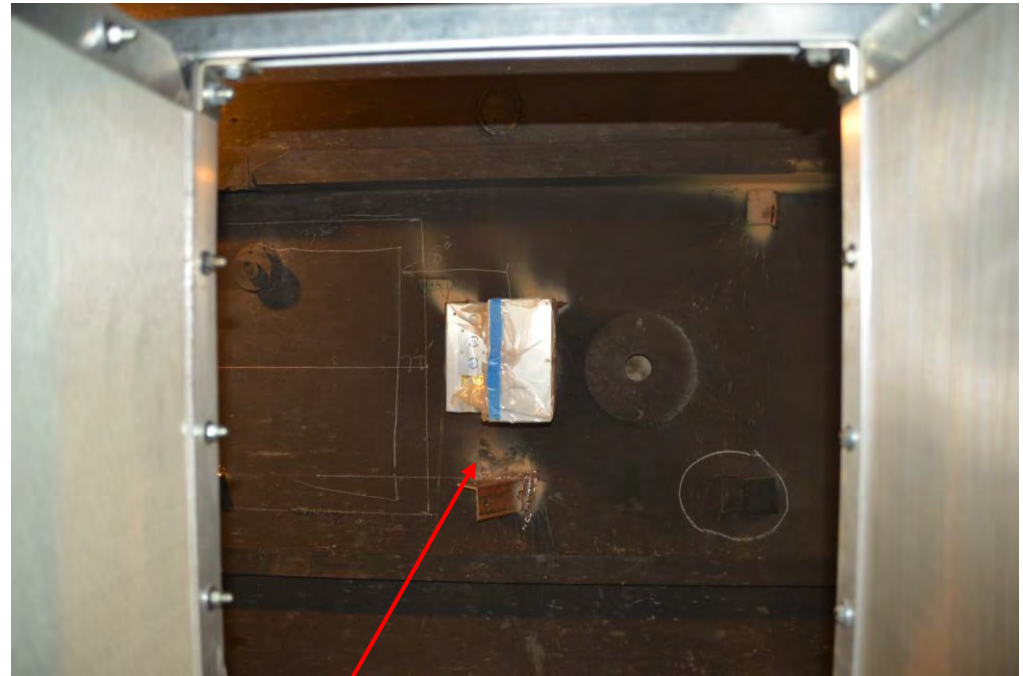


Target and Witness Plate Mounted in Chamber



Looking Down Range

Fiberglass panel (Bumper #1) in front.



Bumper #4
Fiber Glass

Bumper #3
Stainless Steel

Looking between
bumpers #3 and #4

Witness Plate Assembly
covered in plastic

Images by AEDC



SBU Marking Target - Post Test

Back stop

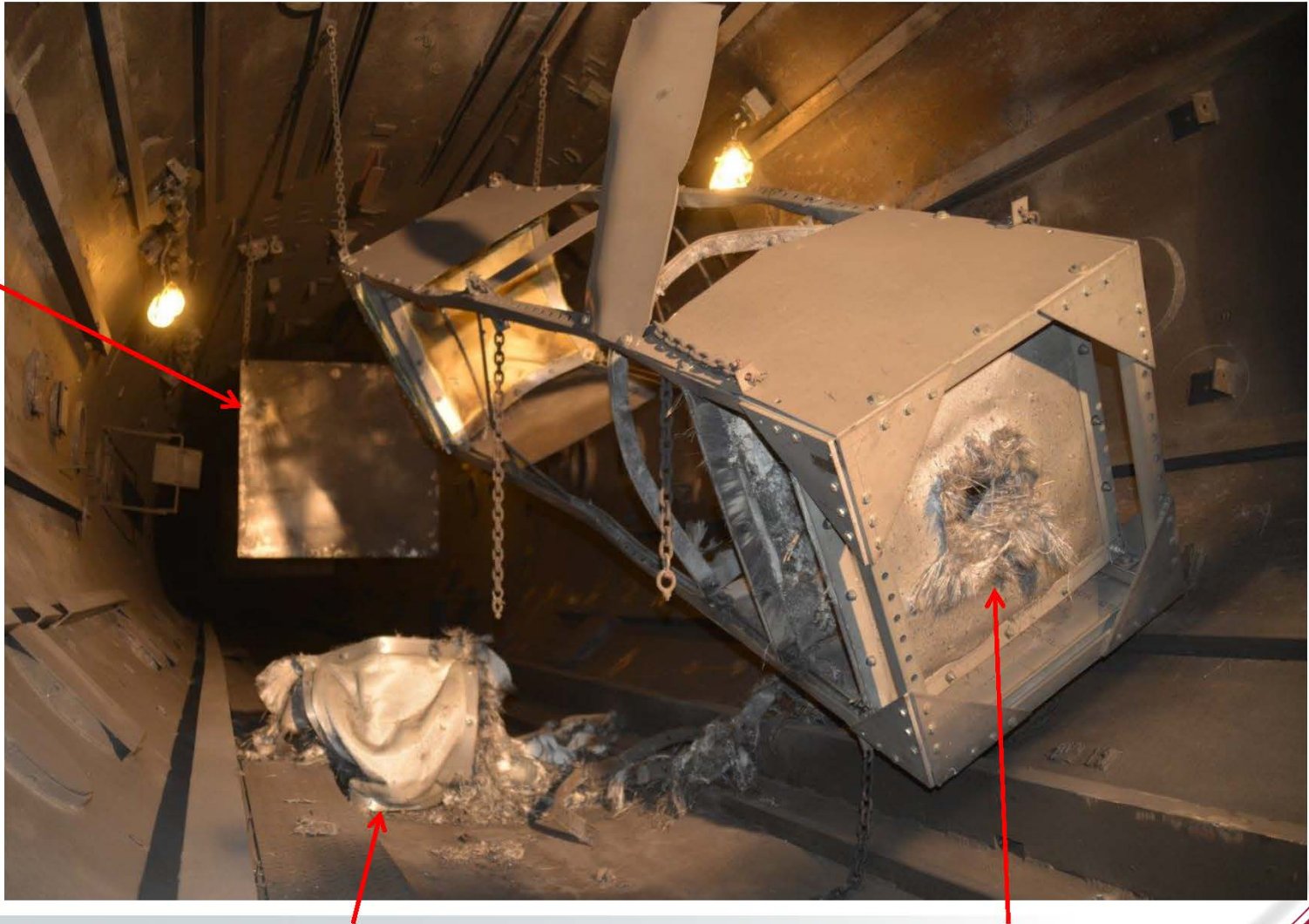


Image by AEDC

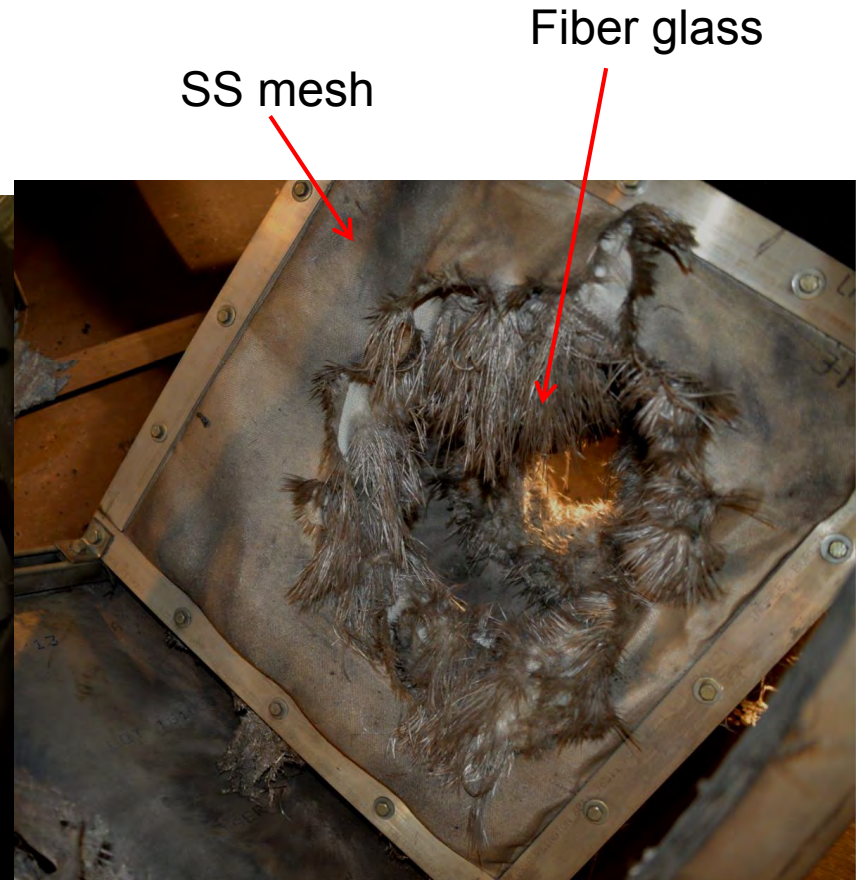
4th and 5th bumpers were dislocated from the frame. 4th bumper was penetrated, 5th was not.

First 3 bumpers were penetrated

Target - Post Test



Front side of 1st bumper.
Note that some fiberglass has ejected up range.



Back side of 3rd bumper.
Note that fiberglass protrudes through SS.

Images by AEDC



SBU Marking Target - Post Test

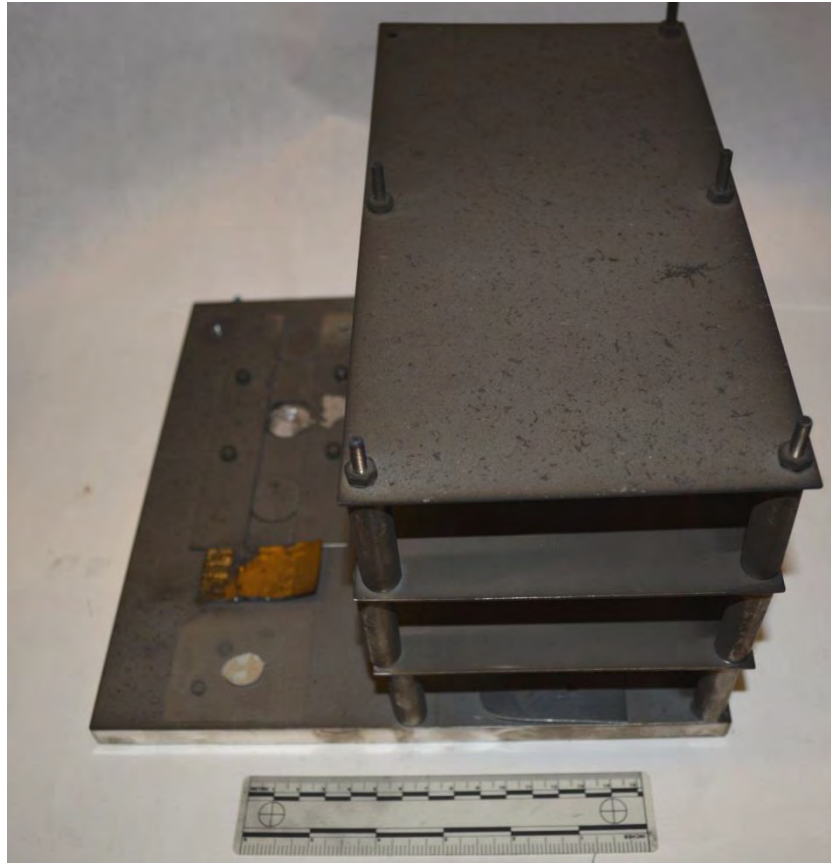


Bumper 1: Fiberglass	Bumper 2: Fiberglass	Bumper 3: steel mesh	Bumper 4: Fiberglass	Bumper 5: Fiberglass	Rear wall 1: Kevlar	Rear wall 2: Kevlar
130 mm diameter perforation	300 mm diameter perforation	600 mm diameter perforation	300 mm diameter perforation (TBD), bumper frame dislocated from shield structure	No complete penetration, bumper frame dislocated from shield structure	Tear on outer fabric layer, no complete penetration	No damage

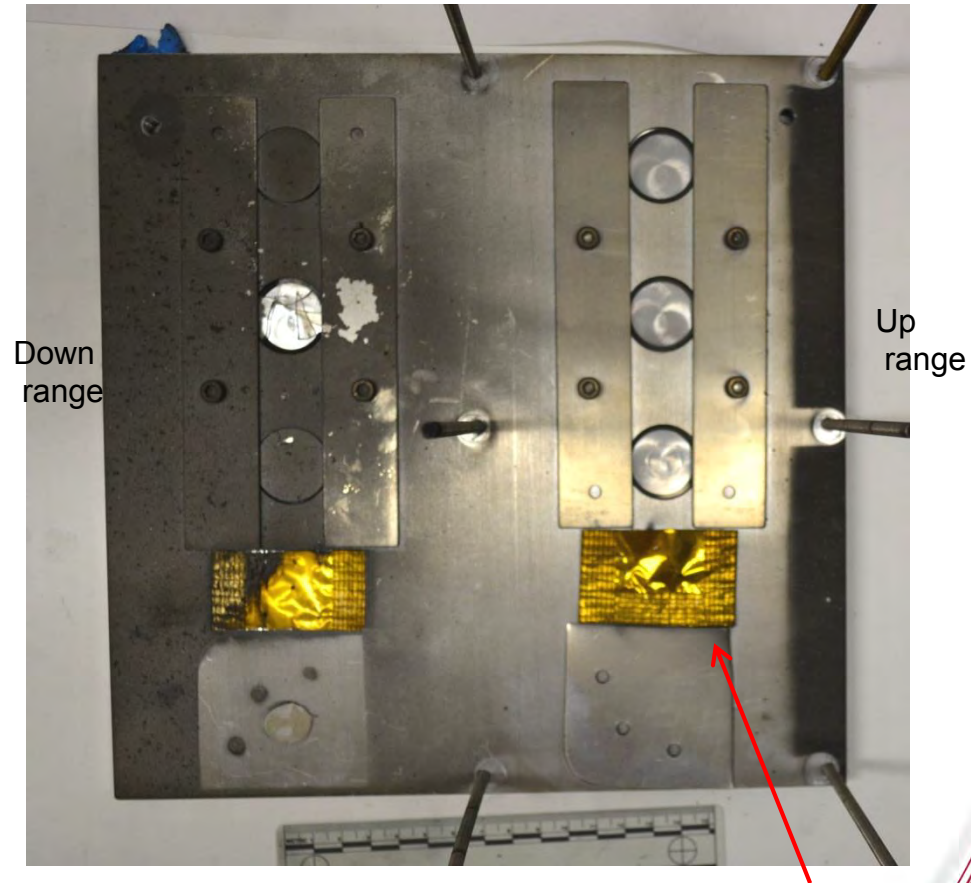
From NASA Orbital Debris Quarterly News V18 #2 2014



Witness Plates: Post Test



With Whipple plate shields



Whipple plates removed

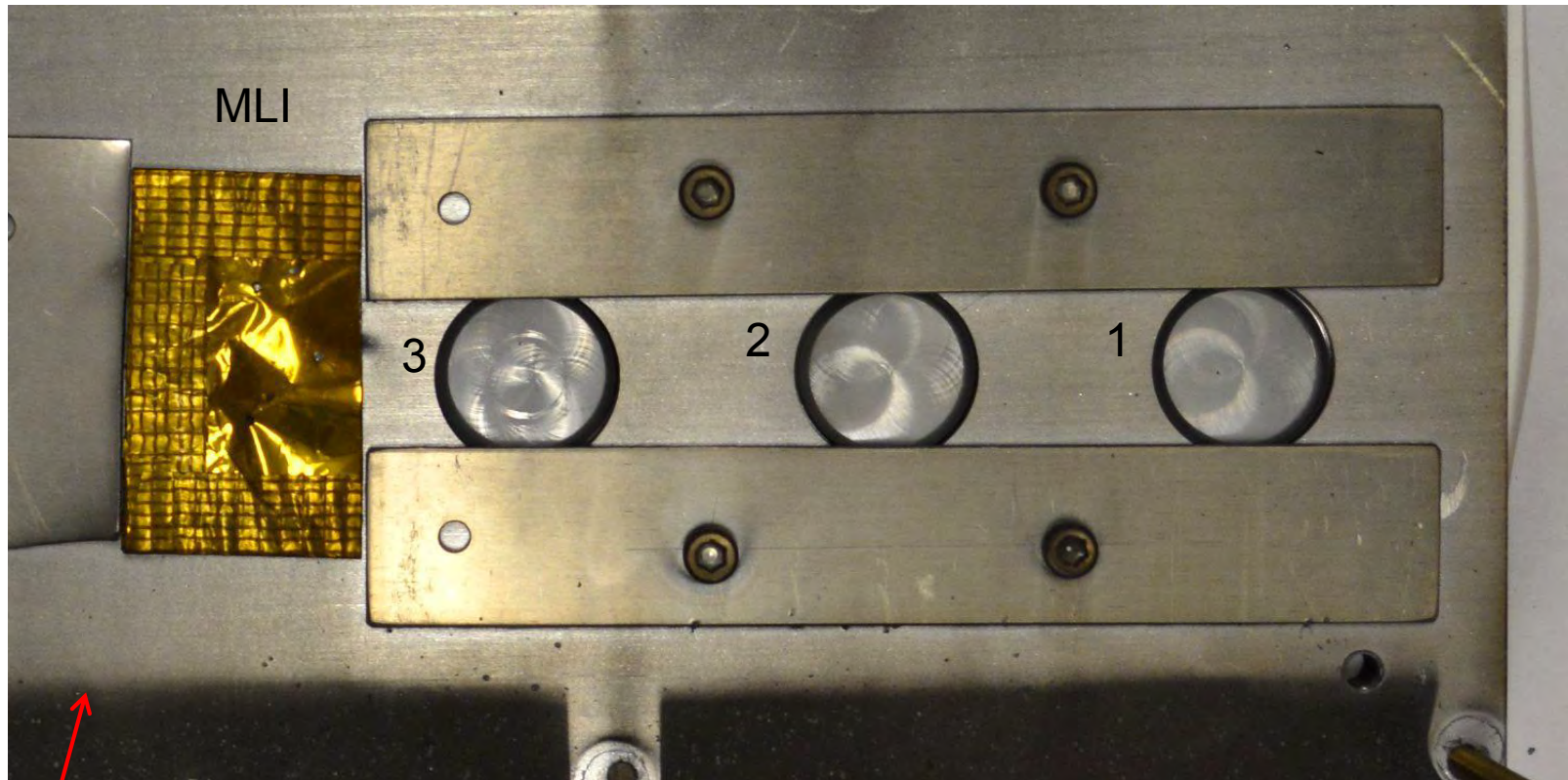
MLI

Exposed surfaces are covered with a matte gray coating and fine debris.
Note thin darker band on base plate on up range side.



Witness Plates: Post Test (protected)

Down range



Up range

Note very sharp boundary between thick up range deposits (dark) and protected area.

Surfaces of samples under Whipple plates are relatively clean.
Deposition appears to be at a very high angle based on sharpness of debris shadow.



Witness Plates: Post Test (unprotected)

Down range



Multi layer
insulation

Hold down plate

Up range

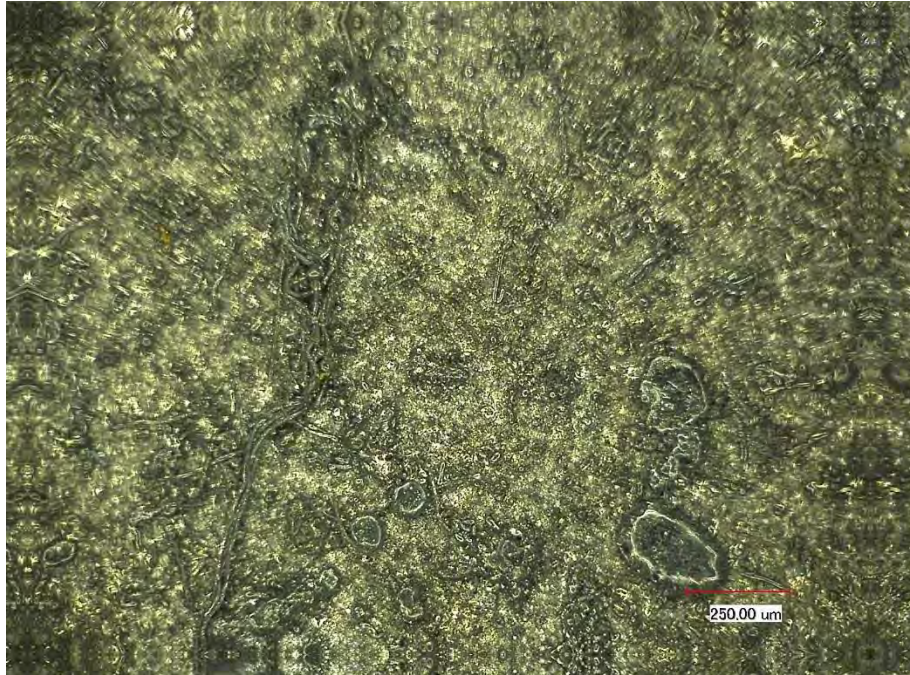
Note blistered and peeled coating and
fractured quartz window

Exposed surfaces are covered with a matte gray coating and fine debris.
Note larger deposits are concentrated toward the down range side of the plate.

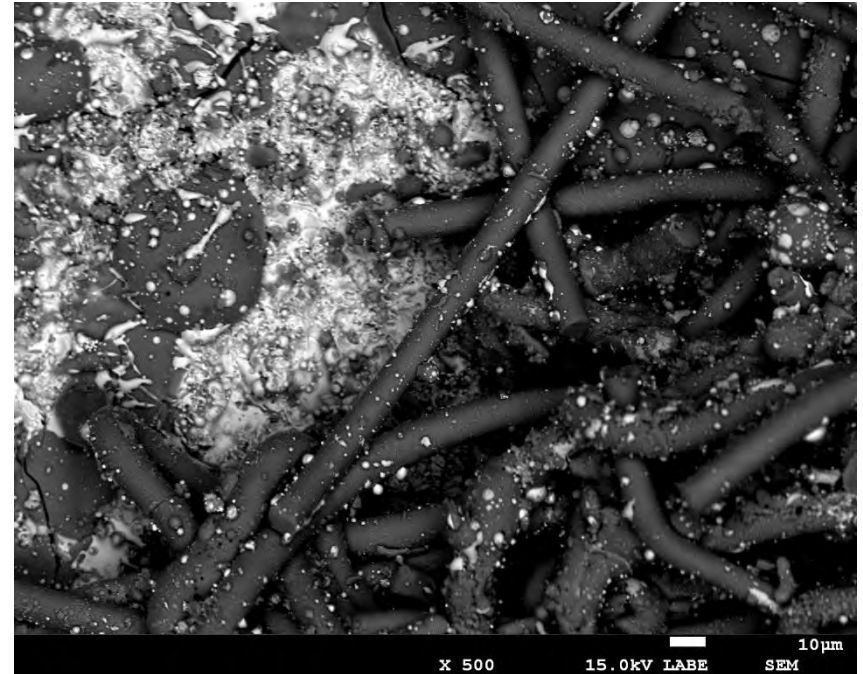


Top Whipple Plate: Post Test

Optical



SEM



Note large molten droplets and unmelted to partially melted glass fibers on the surface.

Laboratory Results

(Supplemental Information and Additional
Analyses in Appendix)



Laboratory Methods

- Scanning Electron Microscopy (SEM)
 - High resolution imaging.
 - Atomic number contrast.
- Energy Dispersive (X-ray) Spectroscopy (EDS) in the SEM
 - Semiquantitative elemental composition.
 - Elemental mapping and line scans.
- Wavelength Dispersive (X-ray) Spectroscopy (WDS) in the SEM
 - Quantitative elemental composition.
 - Standardization with materials of known composition.
 - Light element detection and quantification (boron).
- Electron Backscatter Diffraction (EBSD) and Transmission Kikuchi Diffraction (TKD) in the SEM
 - Mapping of crystalline domains and phase identification/verification.
- Fourier Transform Infrared (FTIR) spectroscopy
 - Identification of chemical functional groups.
 - Correlation with LWIR hyperspectral remote sensing signatures.
- UV-VIS-NIR Spectroscopy
 - Measurement of darkening at UV-VIS-NIR wavelengths.
- X-ray Diffraction
 - Identification of compounds based on crystal structure.



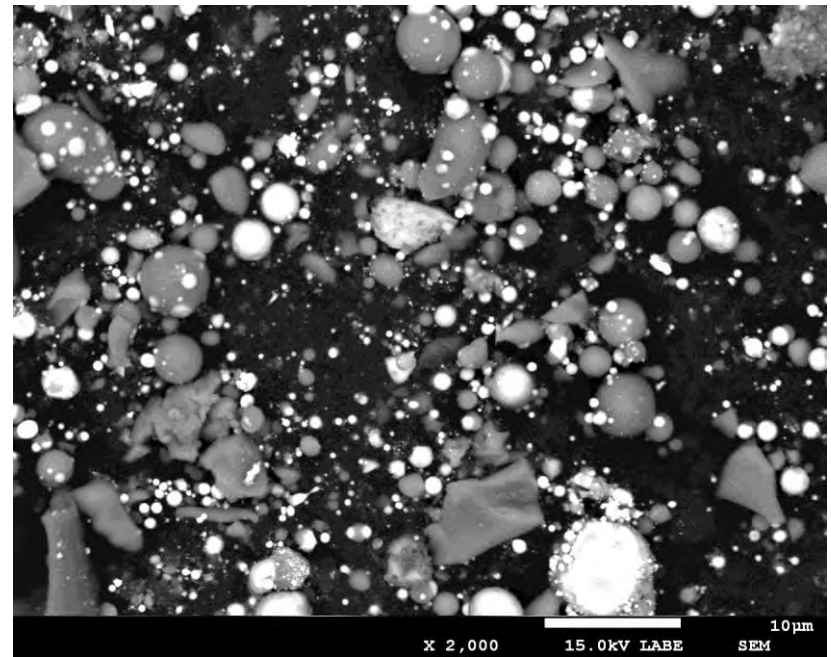
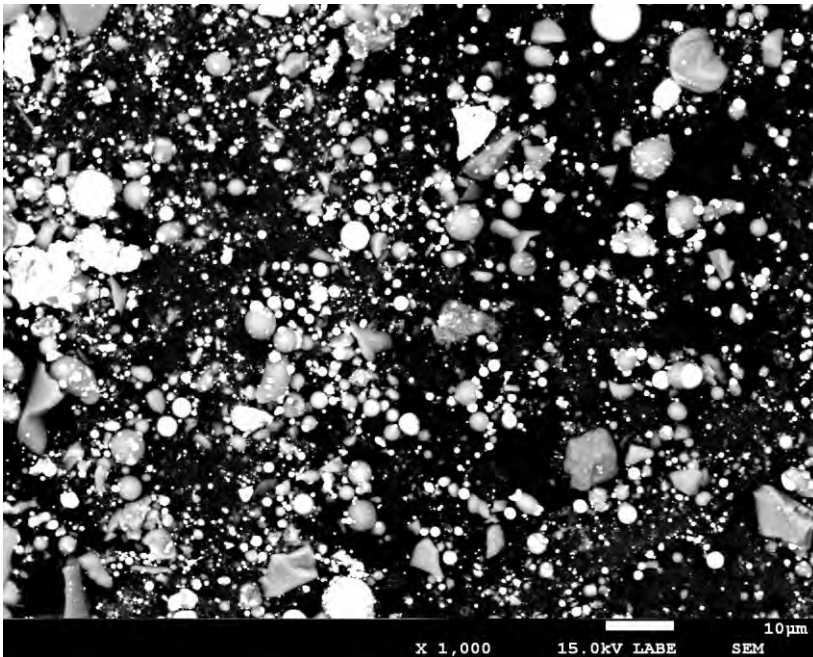
Samples Analyzed

- Top Whipple plate
 - Tape lift, with conductive carbon tape to sample loose debris.
 - SEM-EDS
 - FTIR
 - Hemispherical reflectance
- Hold down plate (directly exposed)
 - SEM-EDS (surface)
 - SEM-EDS (cross section of blistered flake mounted in epoxy)
 - SEM-EBSD-TKD (FIB prepared cross section of blistered flake)
 - SEM-WDS (cross section of blistered flake and baseline E-glass)
 - XRD (blistered coating flake)
 - FTIR
 - Hemispherical reflectance
 - UV-VIS-NIR Spectroscopy
 - Diffuse reflectance
- Witness plate SiO₂ windows
 - UV-VIS-NIR Spectroscopy
 - Transmission and diffuse reflectance



Top Whipple Plate Tape Lift

Backscatter SEM 1KX 2KX

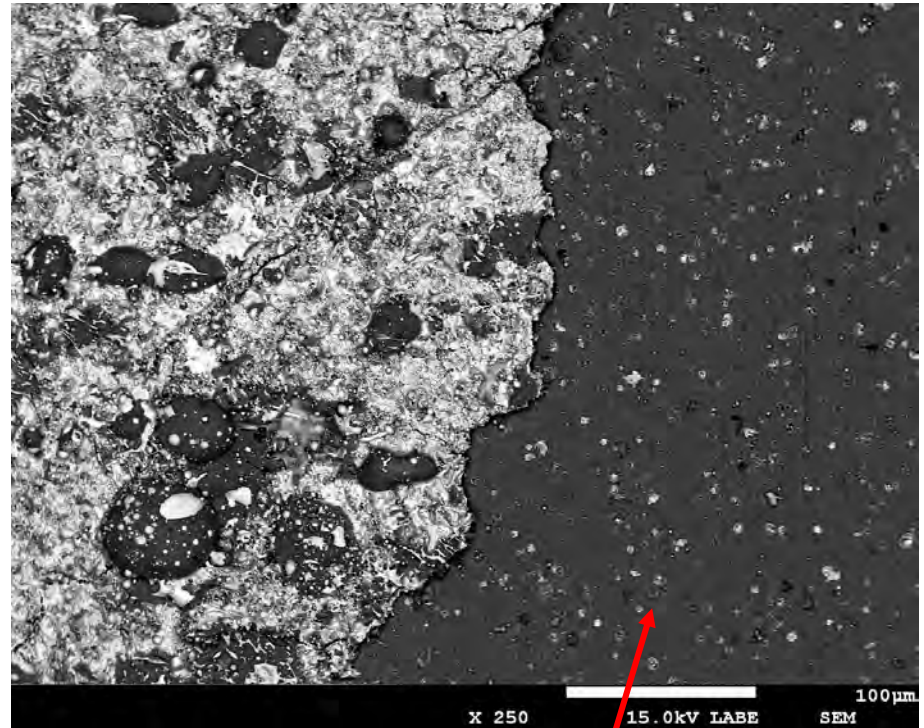
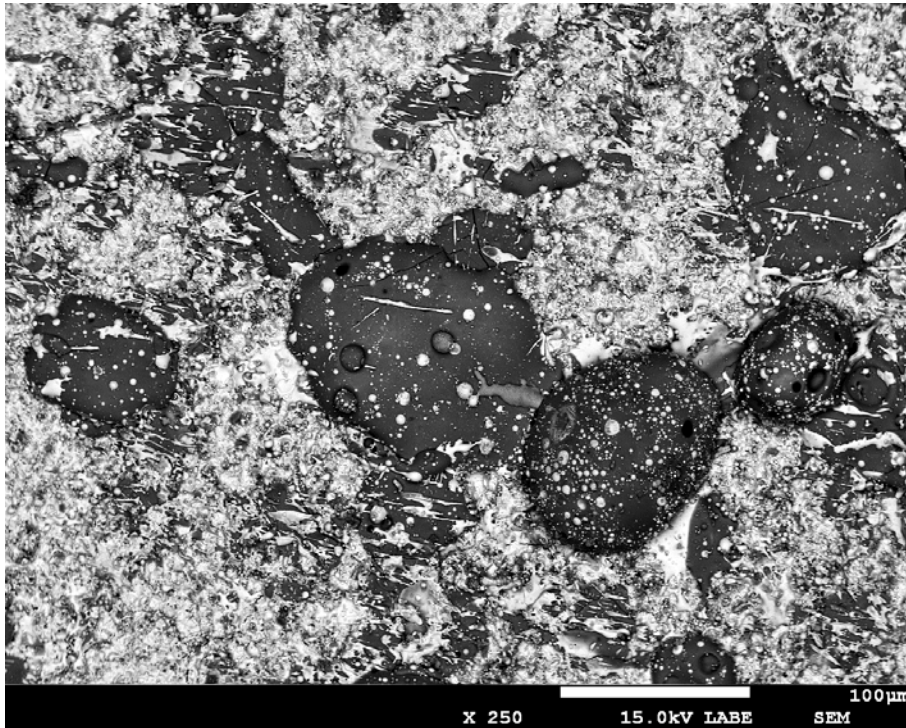


- Transferred material consists of solidified molten droplets.
- Individual droplets range from 10 µm to 10 nm.
- Two families of material are present.
 - Fe-Cr-Ni rich (white – light gray)
 - With major Si and Al
 - With major Si , little Al
 - Silicate – oxide (medium gray)
 - Ca-Al oxide
 - Ca-Al silicate



Exposed Hold Down Plate (Z)

Backscatter SEM 250X



- Surface is covered with coalesced molten droplets.
- Larger low-Z droplets are on top.

Blistered film at right peeled away showing underlying aluminum substrate.

- Two families of material are present.
 - Fe-Cr-Ni rich (white – light gray)
 - With major Si and Al
 - With major Si, little Al

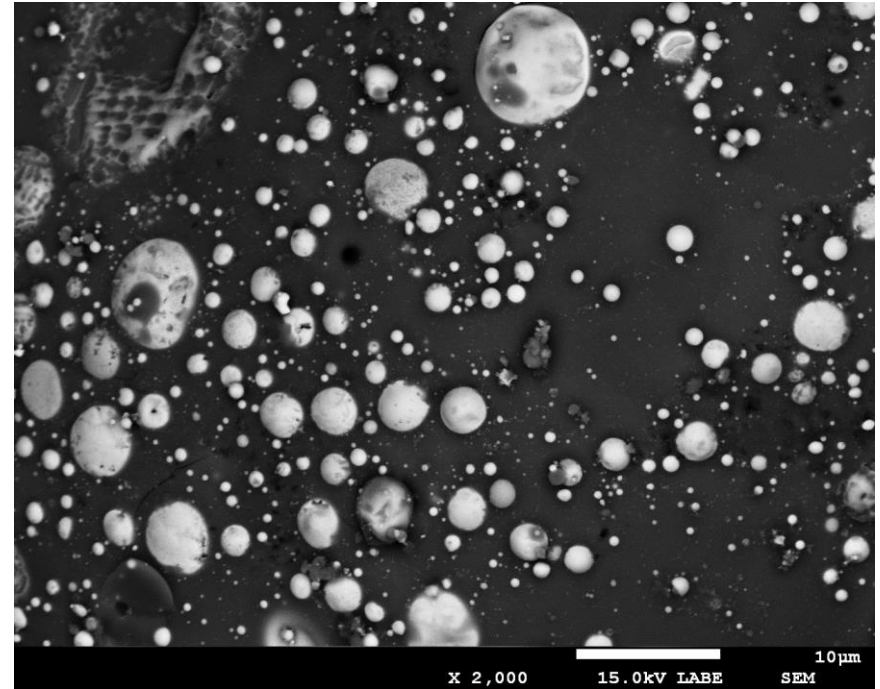
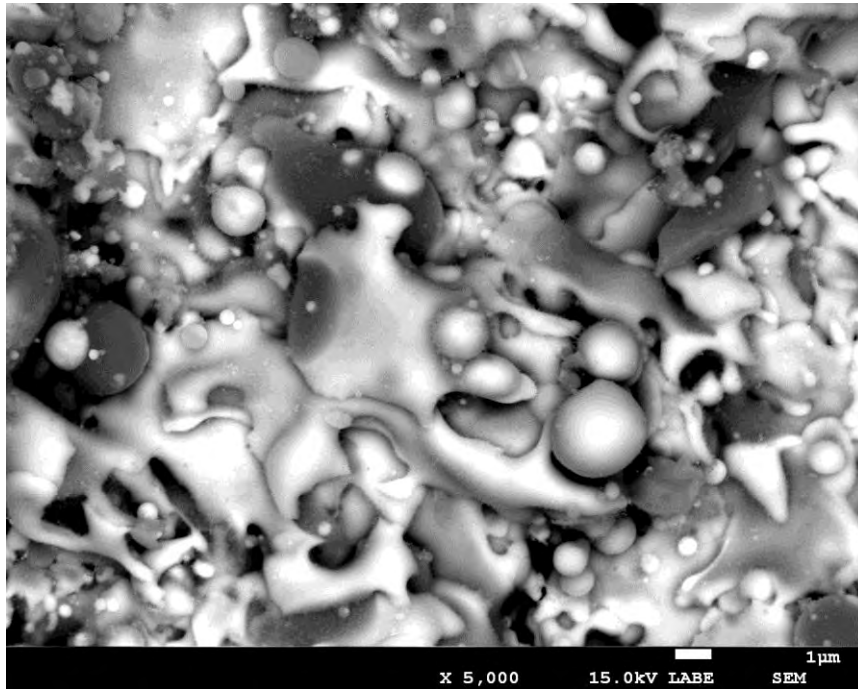
- Silicate – oxide (medium gray)
 - Ca-Al oxide
 - Ca-Al silicate



Exposed Hold Down Plate (Z)

Backscatter SEM

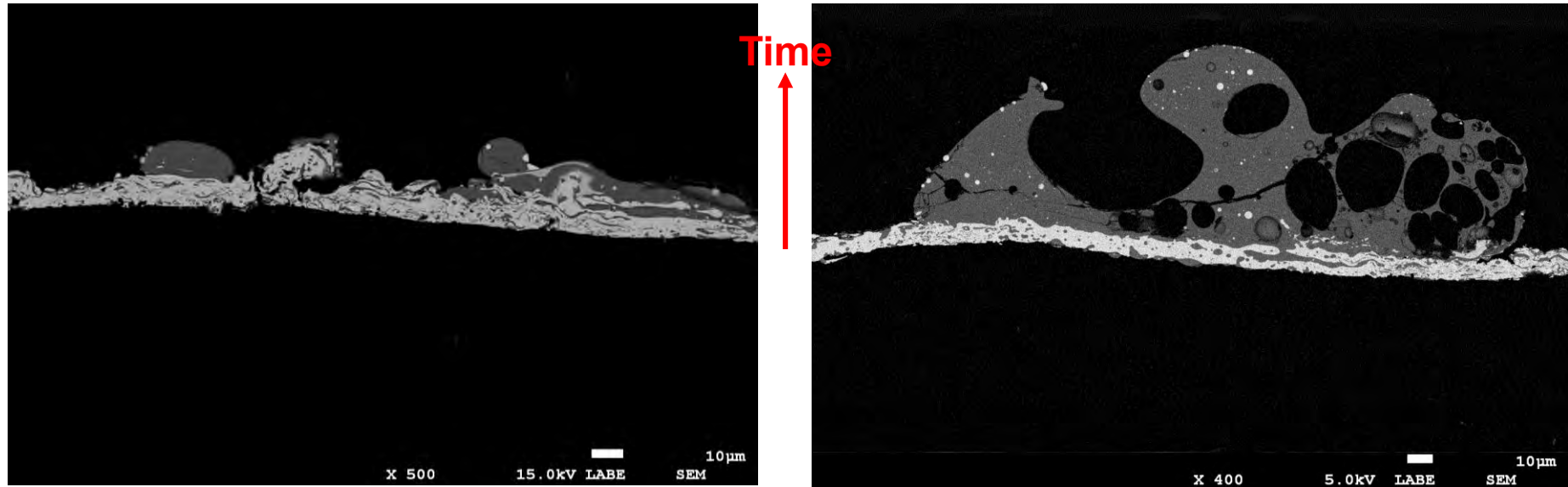
5KX, 2KX



- Coalesced molten droplets with complex flow structure.
- Later droplets are more spherical suggesting they were at least partially solidified when they hit.



Exposed Down Range Hold Down Plate (Z): Cross Sectioned Flake Backscatter SEM 400-500X

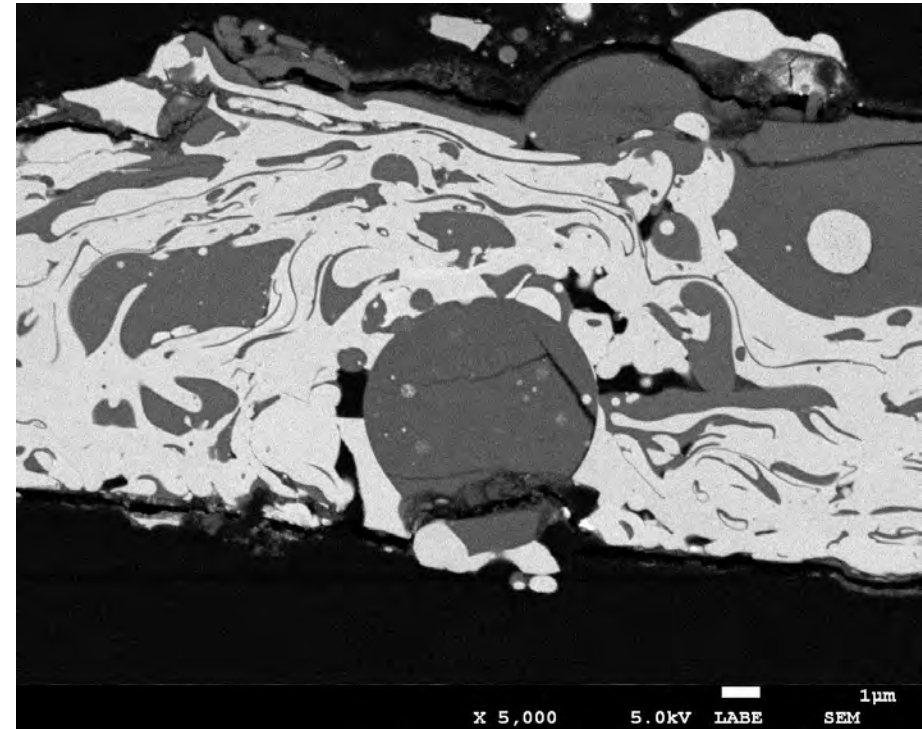
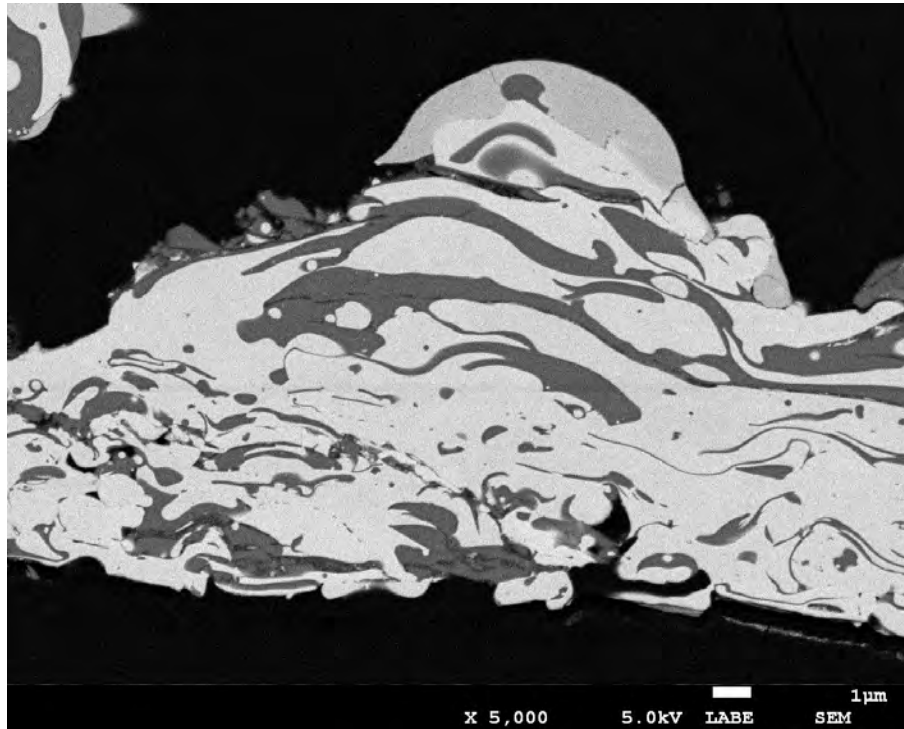


- The cross section records the history of deposition and any changes that occurred over time.
- The flake is about 10 microns thick and has a complex flow structure indicative of coalesced molten droplets (top surface is up).
- Two classes of material : Fe-Cr-Ni rich (bright), silicates/oxides (dark gray)
 - Black = mounting epoxy.
- Large droplets of silicate arrived last.



Exposed Hold Down Plate (Z) Cross Sectioned Flake

Backscatter SEM 5KX



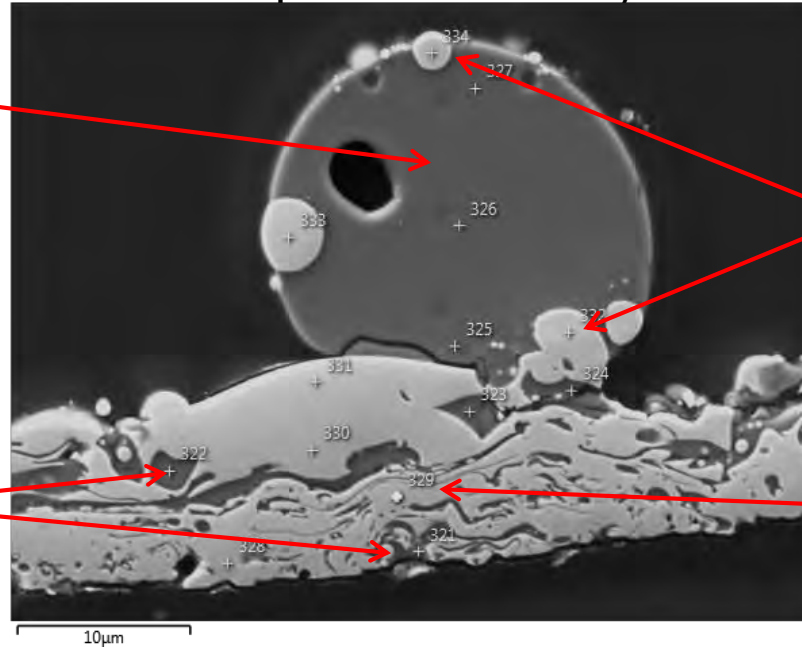
- Note complex flow structure and mixing of droplets.
- Many droplets arrived in a molten state or were impacted while still molten.
- Some more spherical droplets appear to have solidified before deposition.



Exposed Hold Down Plate (Z) Cross Sectioned Flake

EDS Semi-quantitative Analyses

Large late oxide droplet has composition similar to E-glass with significant Si



Later more isolated Fe-Cr-Ni has more Si and little Al

Early Oxide phase mixed with Fe-Cr-Ni is rich in Al and Ca, little Si

Early Fe-Cr-Ni has significant Al and Si

	321	322	323	324	325	326	327	328	329	330	331	332	333	334
O	53.65	58.53	62.50	62.11	64.05	65.60	61.18	3.62	3.96	2.80	4.20	3.31	3.29	4.39
Na					0.31									
Mg			0.69		1.26		0.87							
Al	26.42	29.06	16.21	26.00	7.32	6.04	18.34	14.09	14.18	1.02	12.00	3.68		
Si	1.66	0.68	9.93	0.70	18.67	19.90	10.56	9.01	10.83	33.60	22.53	21.08	16.43	23.22
Ca	9.92	11.73	10.20	11.19	8.38	8.46	9.05	0.54						
Cr	2.19		0.47					13.40	12.59	12.66	12.52	12.97	14.60	13.76
Mn										1.58		1.51		1.55
Fe	6.16							53.86	49.18	42.63	48.76	49.13	55.87	48.09
Ni	0.00							5.48	9.26	5.72	0.00	8.33	9.81	8.99
Total	100.	100.	100.	100.	100.	100.	100.	100.	100.	100.	100.	100.	100.	100.

← Analysis location-see above image

All values are atomic %

Later droplets are not uniformly distributed.



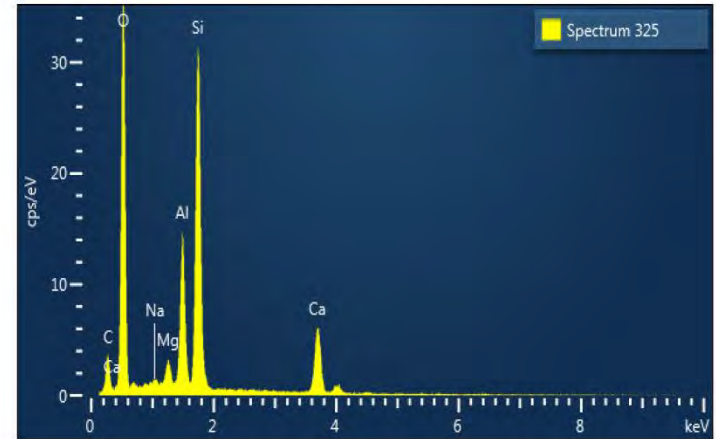
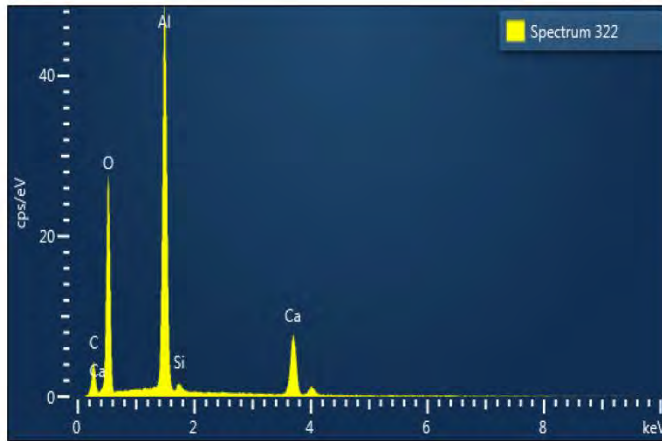
Exposed Hold Down Plate (Z) Cross Sectioned Flake

EDS Spectra (see previous chart for locations)

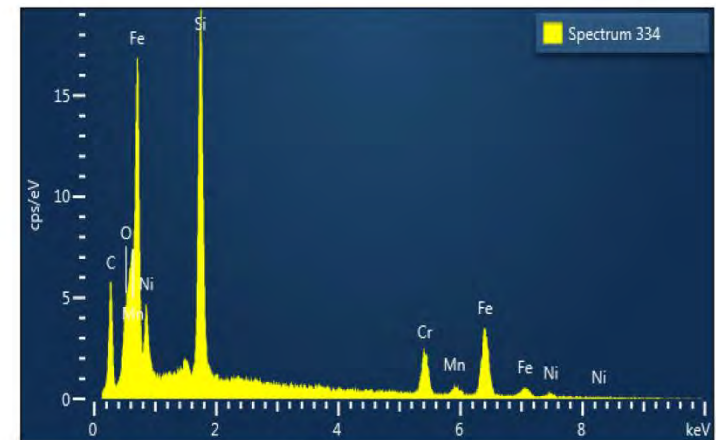
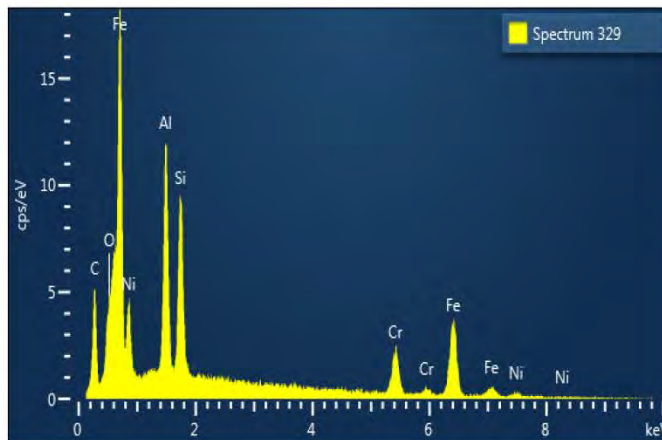
Early

Later

Oxide
Phase

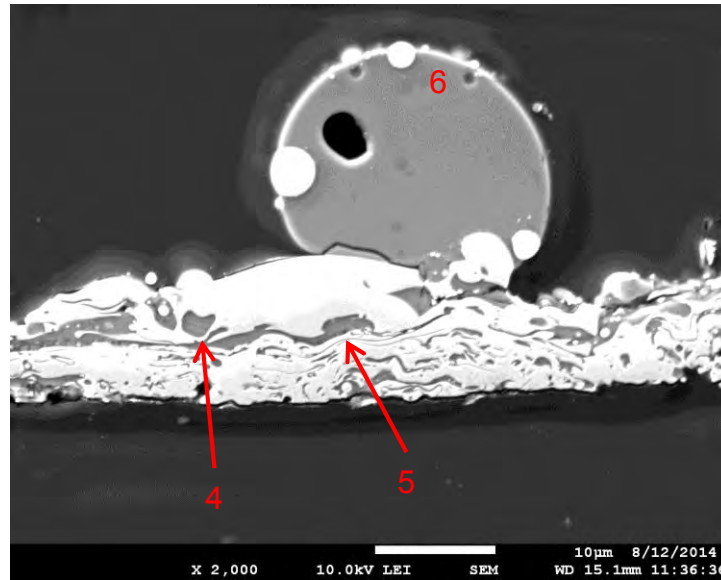
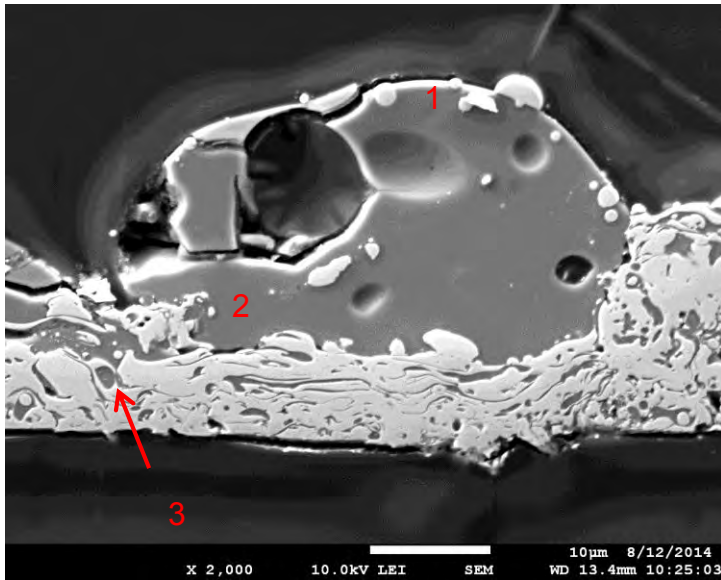


Fe-Cr-Ni
Phase



Exposed Hold Down Plate (Z) Cross Sectioned Flake

WDS Quantitative Analyses (including boron)



	E-Glass	E-Glass	Large1	Large 2	Early 3	Early4	Early5	Large6
B ₂ O ₃	7.83	8.11	8.03	8.03	2.68	2.84	3.99	8.00
Na ₂ O	0.76	0.75	0.72	0.72	0.00	0.01	0.04	0.73
MgO	0.58	0.58	0.60	0.60	0.02	0.05	0.75	0.77
Al ₂ O ₃	13.32	13.15	14.79	14.79	60.99	61.53	42.12	13.31
SiO ₂	53.55	53.59	52.86	52.86	0.99	2.93	14.34	51.32
CaO	22.84	22.65	22.89	22.89	27.74	27.22	22.87	22.38
Total	98.89	98.83	99.89	99.89	92.42	94.59	84.10	96.51

WDS Standards:
 Quartz – Si
 Spinel – Mg, Al
 Danburite – B, Ca
 Albite - Na

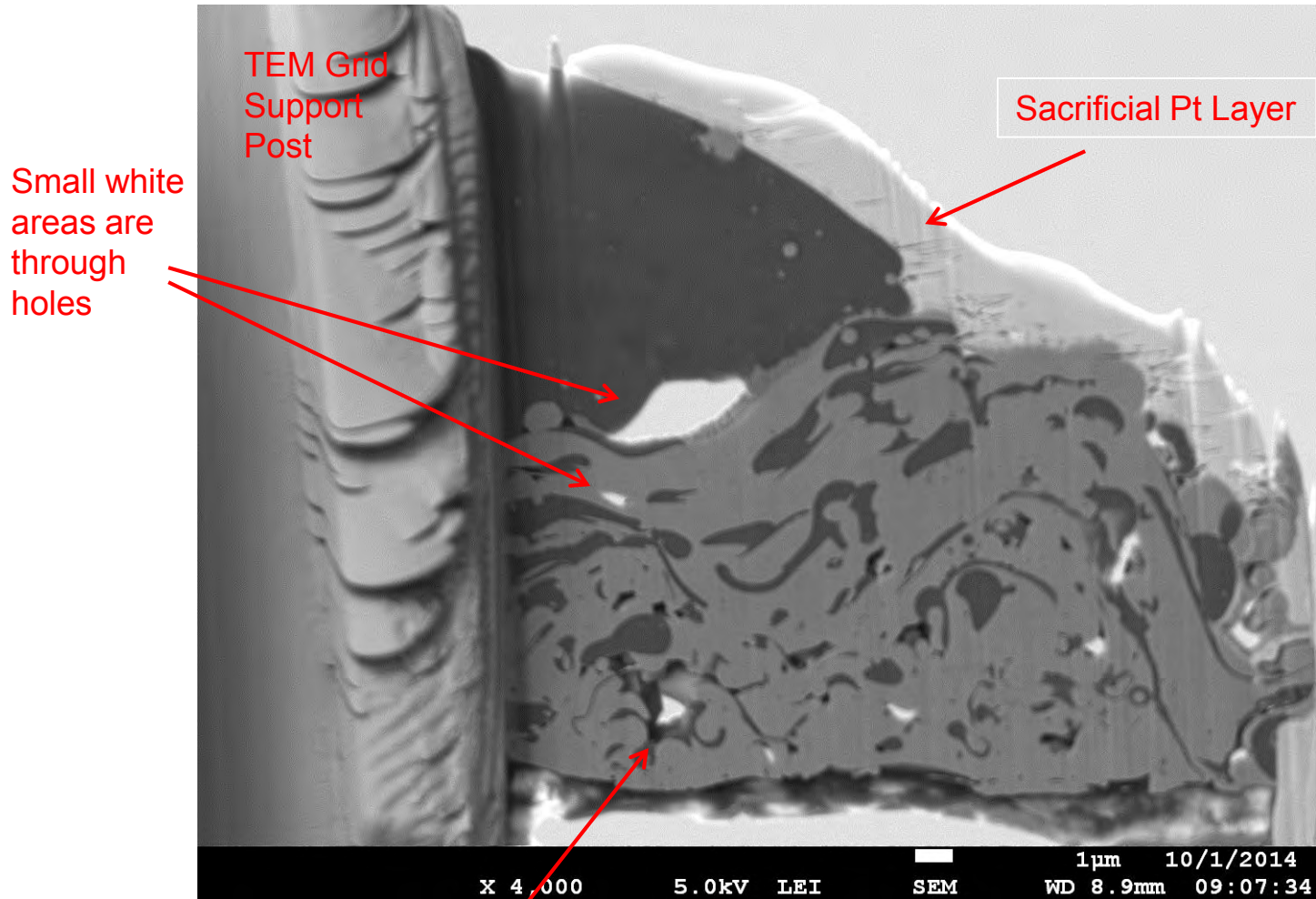
All values are weight %

Large late droplets have compositions similar to E-glass (including B).
 Early oxide phase has little silicon and reduced boron.



Focused Ion Beam (FIB) Prepared Cross Section TEM Sample

Secondary Electron SEM Image

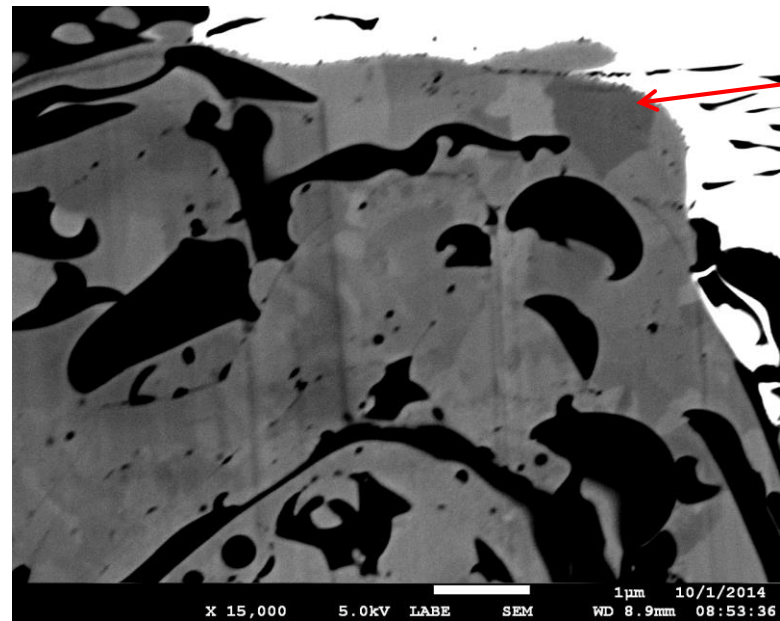
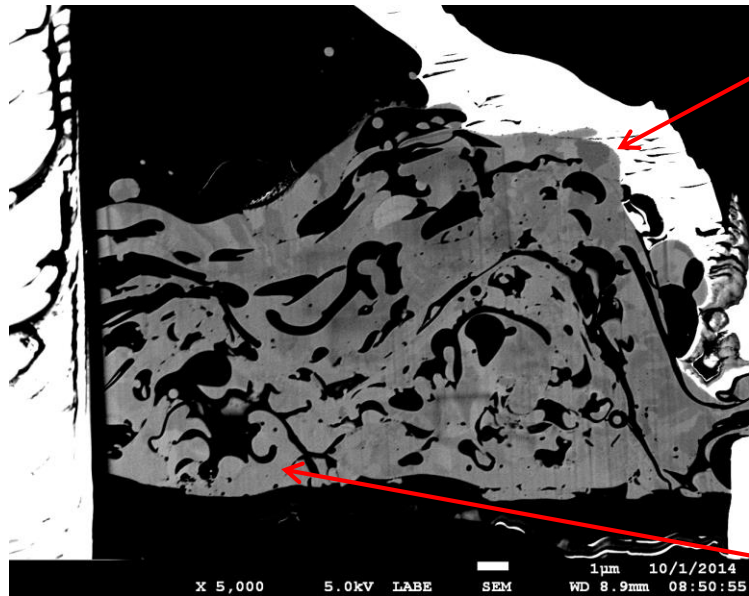


Sample is about 0.1 µm thick



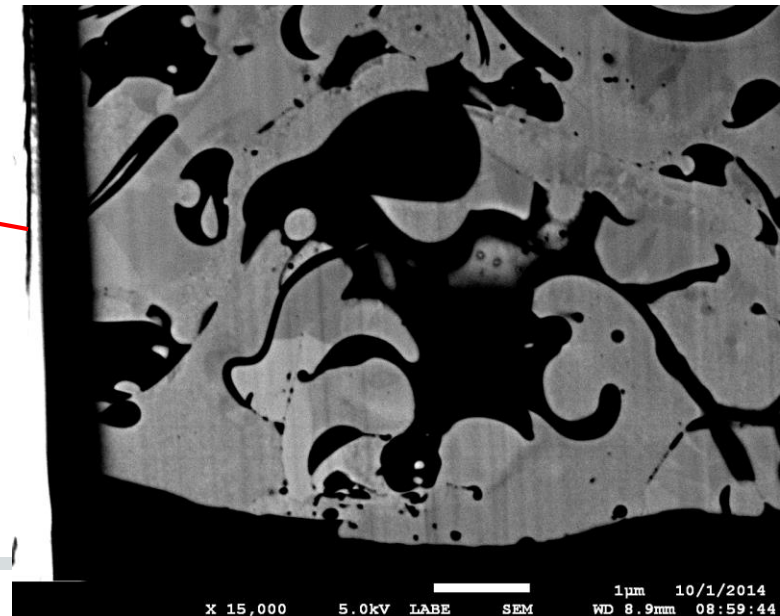
FIB/TEM Cross Section

Backscatter SEM 5KX, 15KX



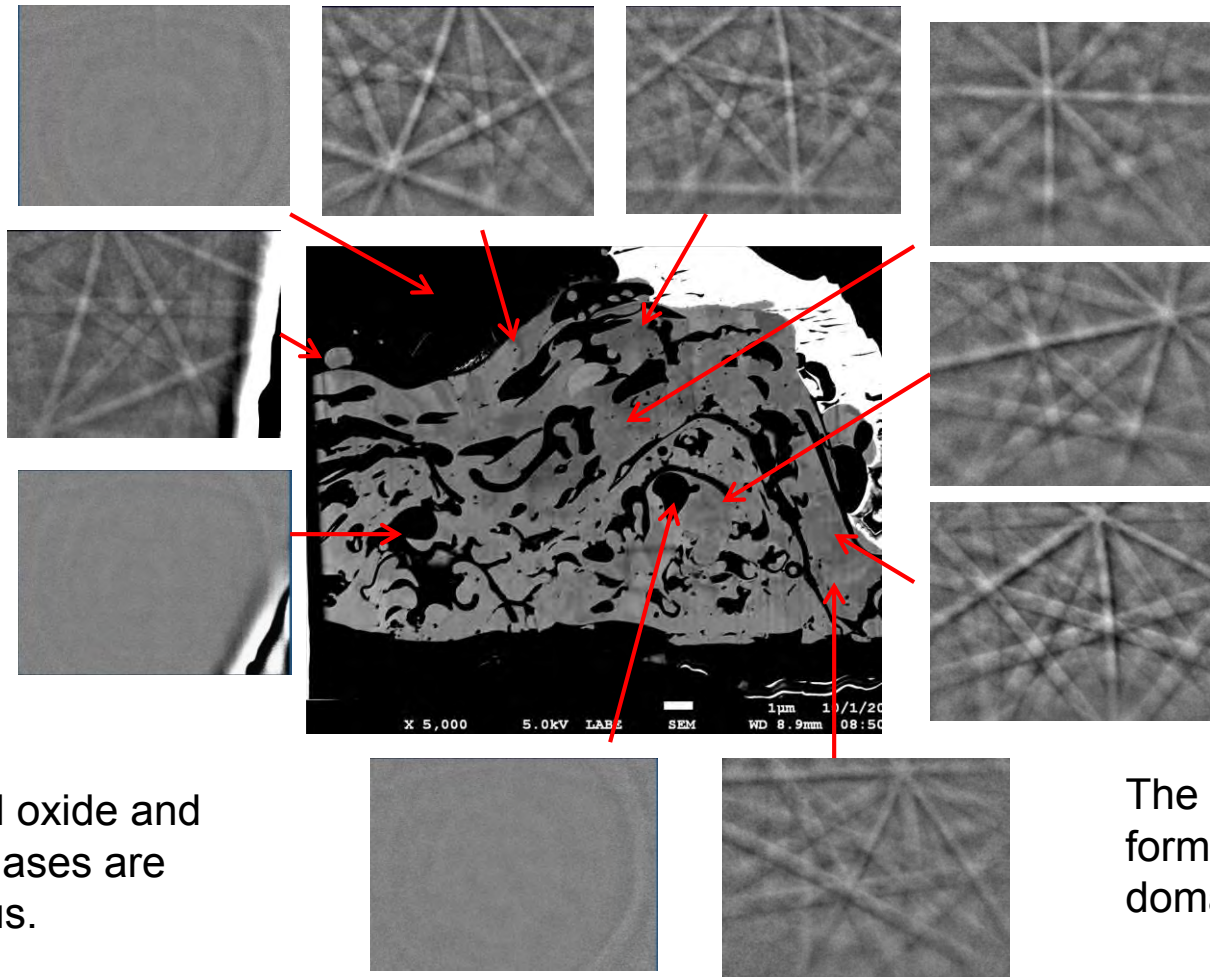
Single
crystal
grain

Channeling contrast in the Fe-Cr-Ni phase shows crystalline grain boundaries. Crystallites are relatively large (to 1 µm) with respect to individual “flows”.



FIB/TEM Cross Section

Backscatter SEM with Electron Backscatter Diffraction Patterns (EBSD)



The Ca-Al oxide and silicate phases are amorphous.

The Fe-Cr-Ni phase forms single crystal domains.

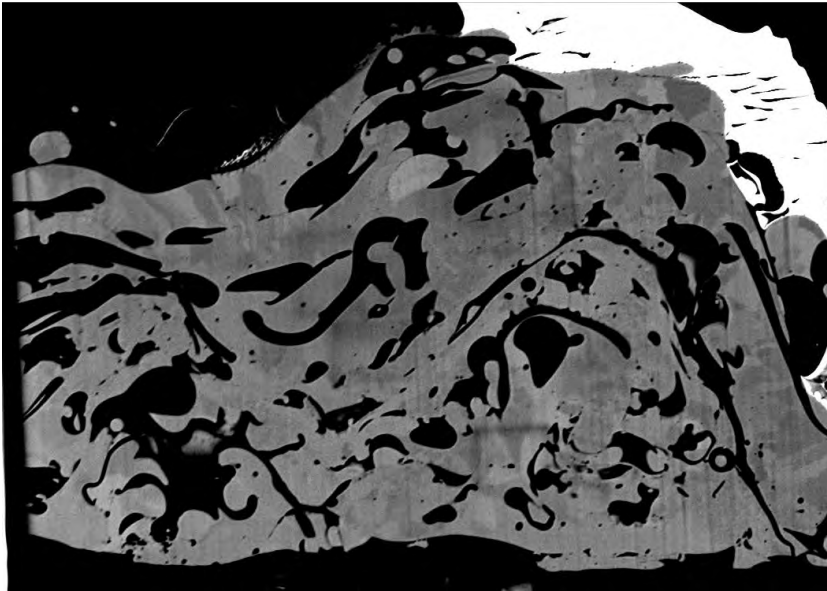
Geometric EBSD patterns are produced by areas that are single crystals.
XRD identified BCC (alpha) Fe phase.

Areas that are amorphous or polycrystalline do not produce EBSD patterns.

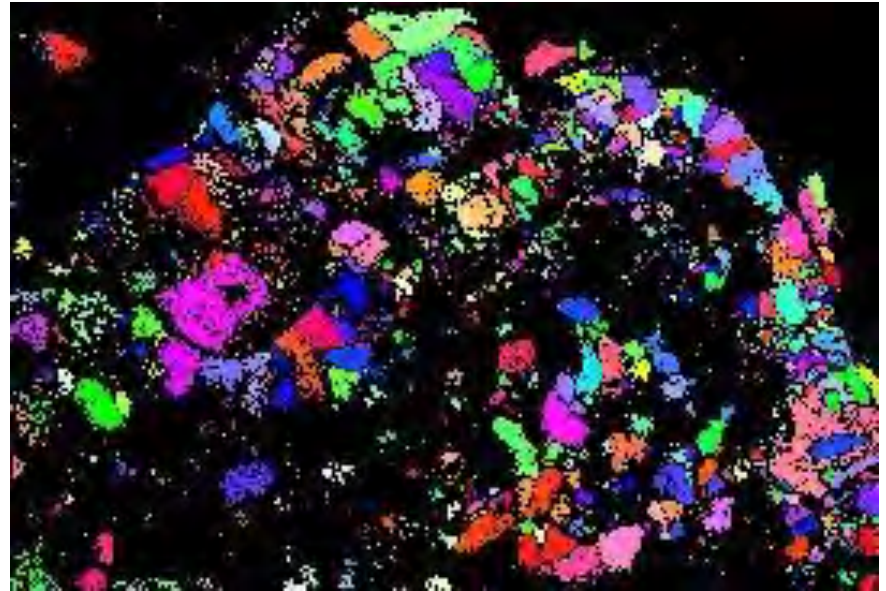


FIB/TEM Cross Section

Backscatter SEM with Transmission Kikuchi Diffraction Patterns (TKD)

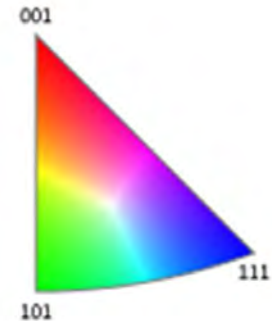


SEM

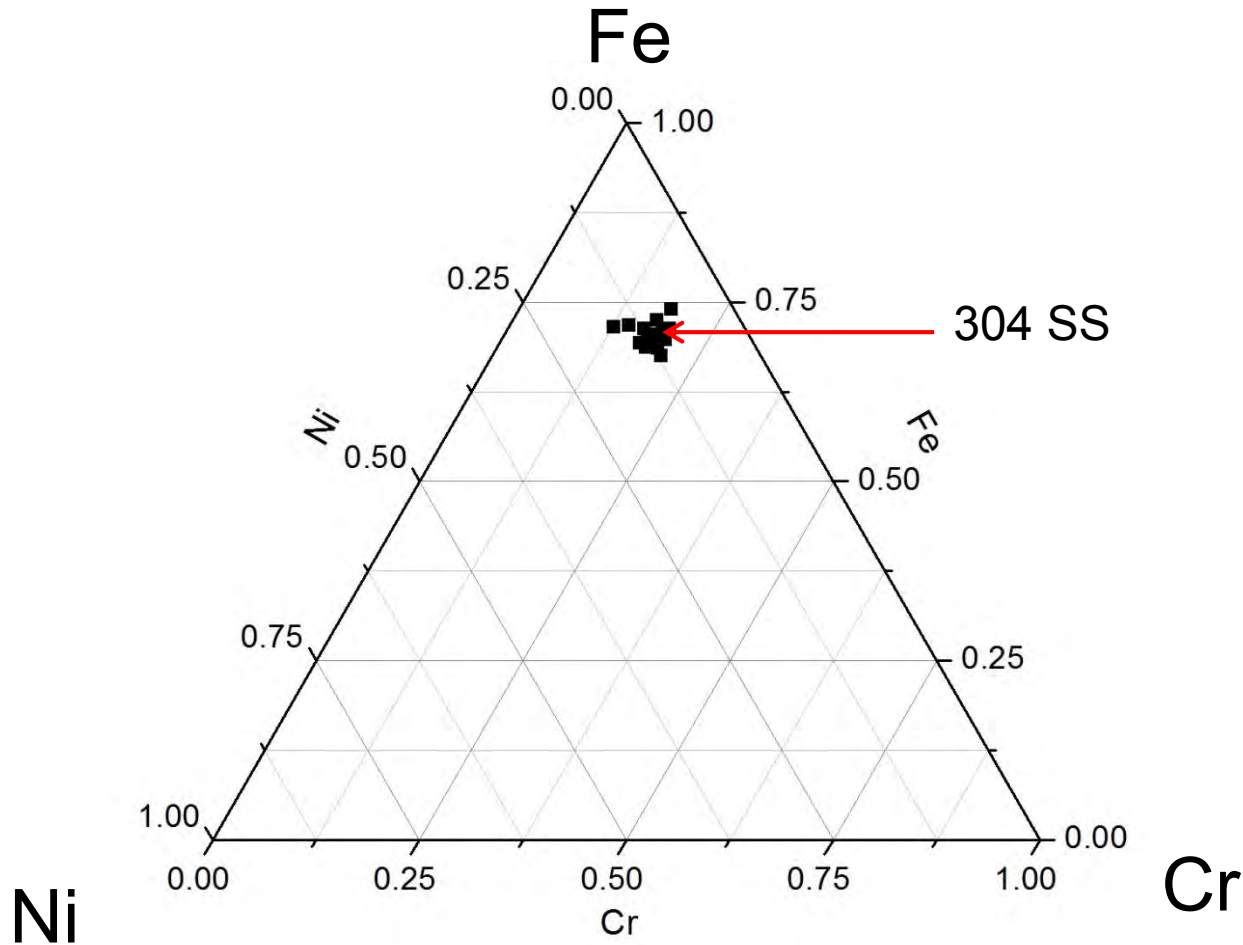


TKD grain orientation map (BBC-Fe).

- TKD has an order of magnitude better spatial resolution than EBSD.
- TKD patterns are analyzed to determine grain orientation (color).
 - Grain orientations are random.
 - Black areas are amorphous or orientation could not be determined.



Relative Composition of the Fe-Cr-Ni Phase



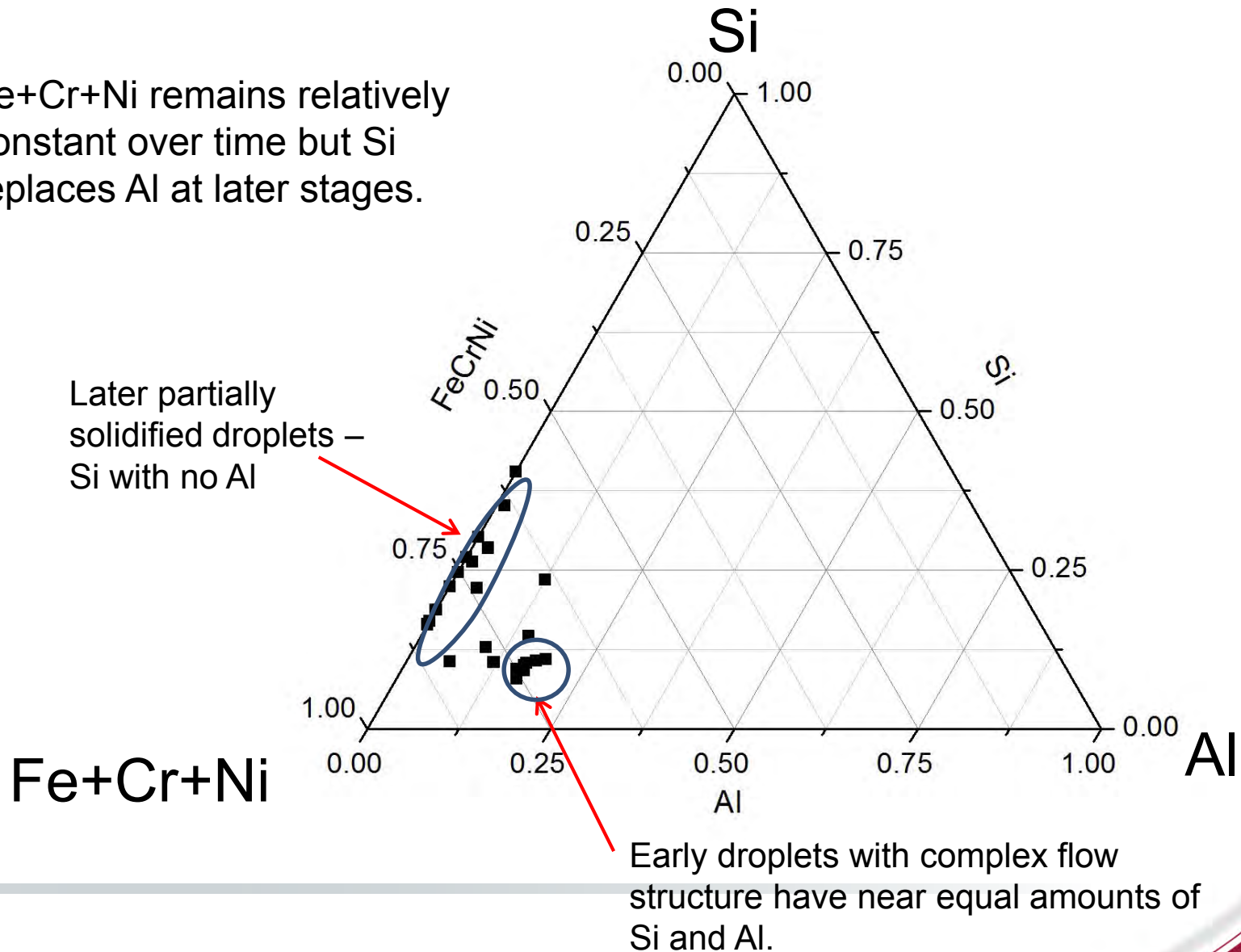
Al and Si are also present in the Fe-Cr-Ni phase.

The relative proportions of Fe-Cr-Ni in the deposits do not change significantly from the SS bumpers. No segregation/partitioning of Fe-Cr-Ni.



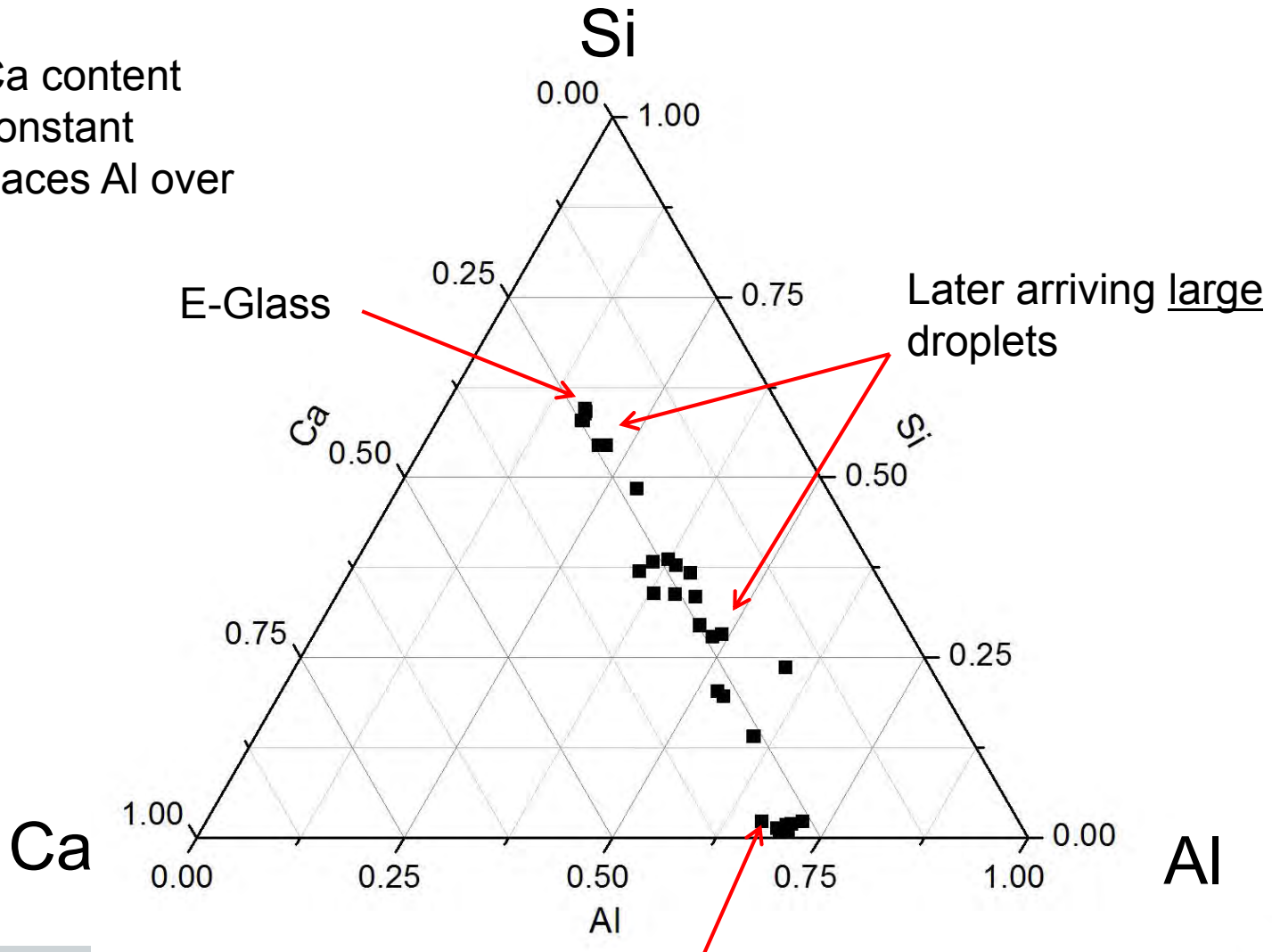
Composition of Fe-Cr-Ni Phase

Fe+Cr+Ni remains relatively constant over time but Si replaces Al at later stages.



Composition of the Oxide-Silicate Phase

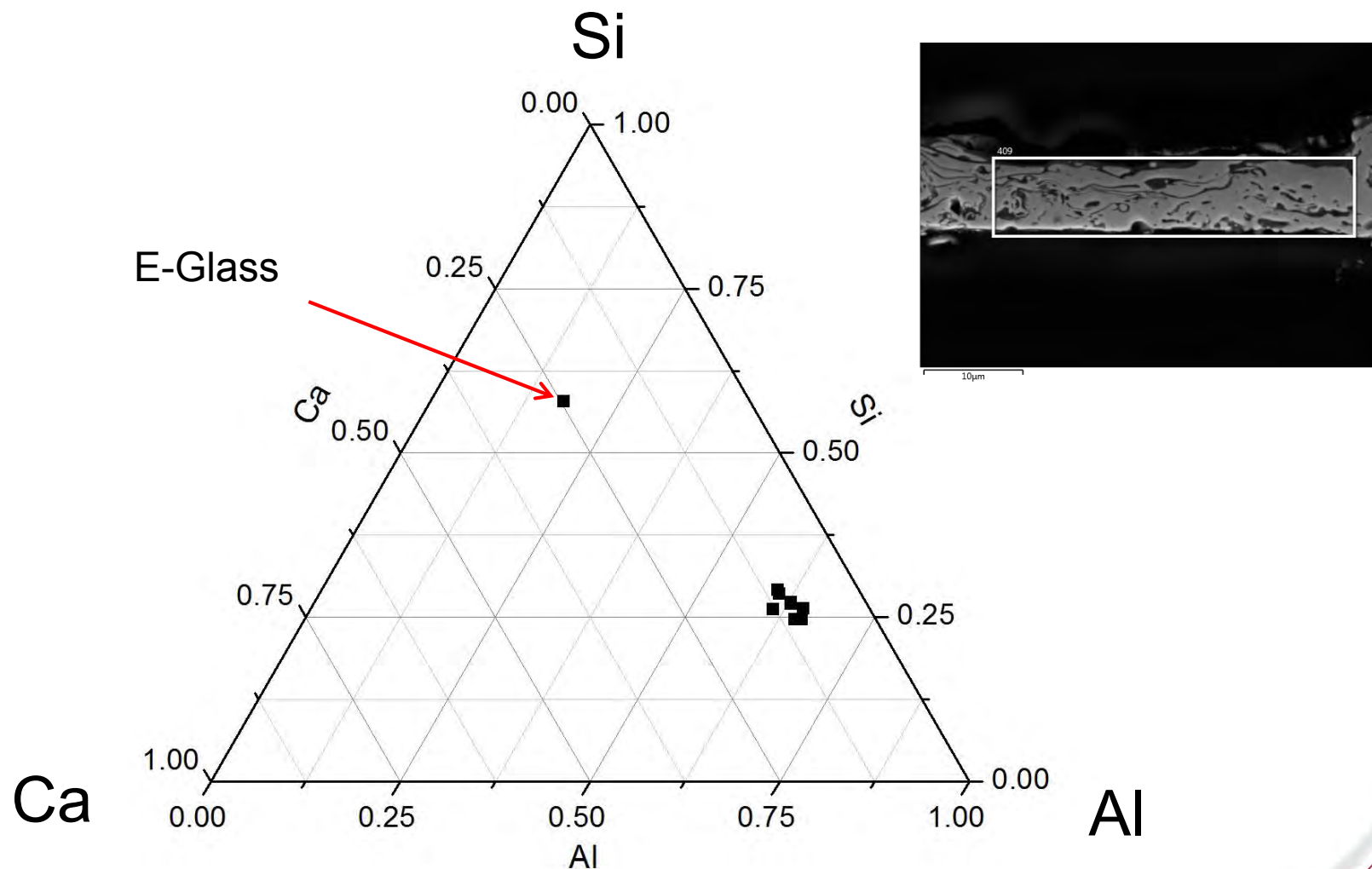
Relative Ca content remains constant but Si replaces Al over time.



Early oxide in complex flow patterns with Fe-Cr-Ni phase has high Al from the projectile?



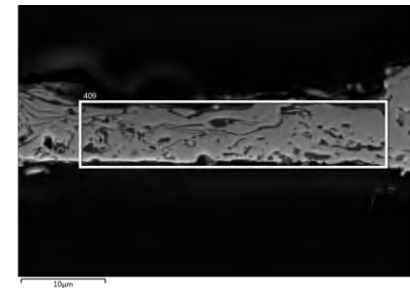
Integrated Ca-Al-Si Content of Fe-Cr-Ni and Ca-Al-Si Phases in Early Complex Flow Structure



In the early deposits there is considerably more aluminum than could have come from just E-glass – must have come from the projectile.



Integrated Composition in Complex Flow Structure



All values in atomic %

	E-glass	Loc 1	Loc 2	Loc 3	Loc 4	Loc 5	Loc 6	Loc 7	Loc 8	SS
O	65.3	17.87	22.03	22.83	29.40	25.68	29.33	26.37	23.52	
Al	5.9	18.64	18.69	20.08	18.63	19.41	18.86	17.81	18.53	
Si	19.4	9.03	8.07	8.62	8.00	7.41	7.13	7.23	8.68	
Ca	8.4	3.30	2.95	3.17	3.86	3.15	2.75	2.39	3.27	
Cr		9.79	9.41	8.65	7.68	8.38	8.17	8.90	8.81	19.3
Fe		36.26	33.95	31.85	28.18	31.63	28.90	32.44	32.54	68.2
Ni		5.11	4.90	4.80	4.23	4.33	4.46	4.49	4.66	10.2
Total	99.0	100.00	100.00	100.00	100.00	100.00	100.00	100.00	100.00	97.7

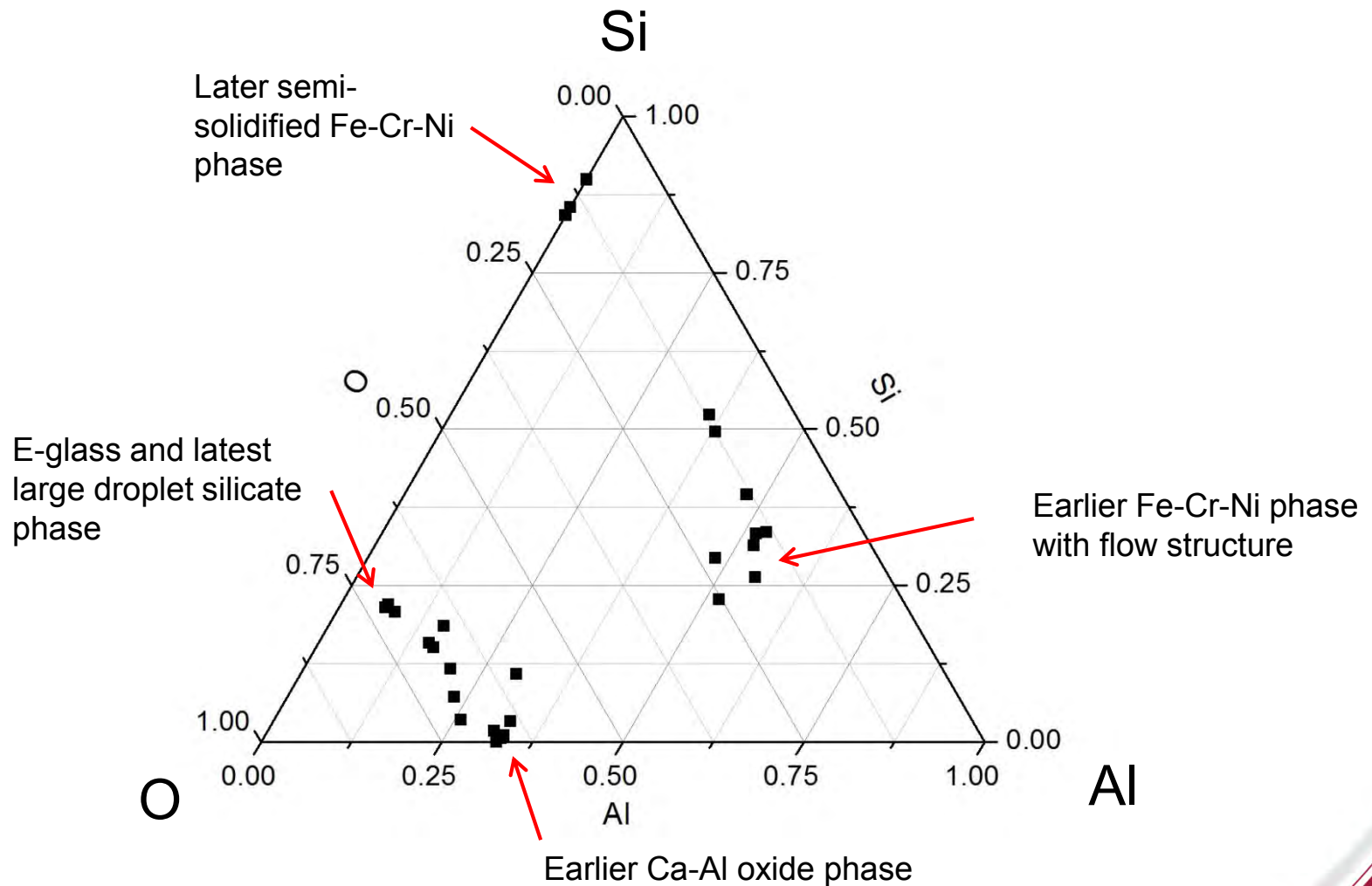
- The Si/Ca, and to lesser extent O/Ca ratios, in the deposits are very similar to that in E-glass (Si/Ca = 2.3 and O/Ca = 7.8).
- The Ca contents above were used to estimate the Al, Si and O required to make E-glass. The calculated and observed Si values were close, those of O – less so, but similar.
- The observed Al greatly exceeded that calculated to make E-glass - the later amount was subtracted from the observed amount. The remainder musty have come from the projectile.

The estimated relative proportions (summed atomic % of constituents) of the starting materials contributing to the deposits were:

SS : 40-51% Aluminum Projectile: 16-18% E-Glass: 34-45%



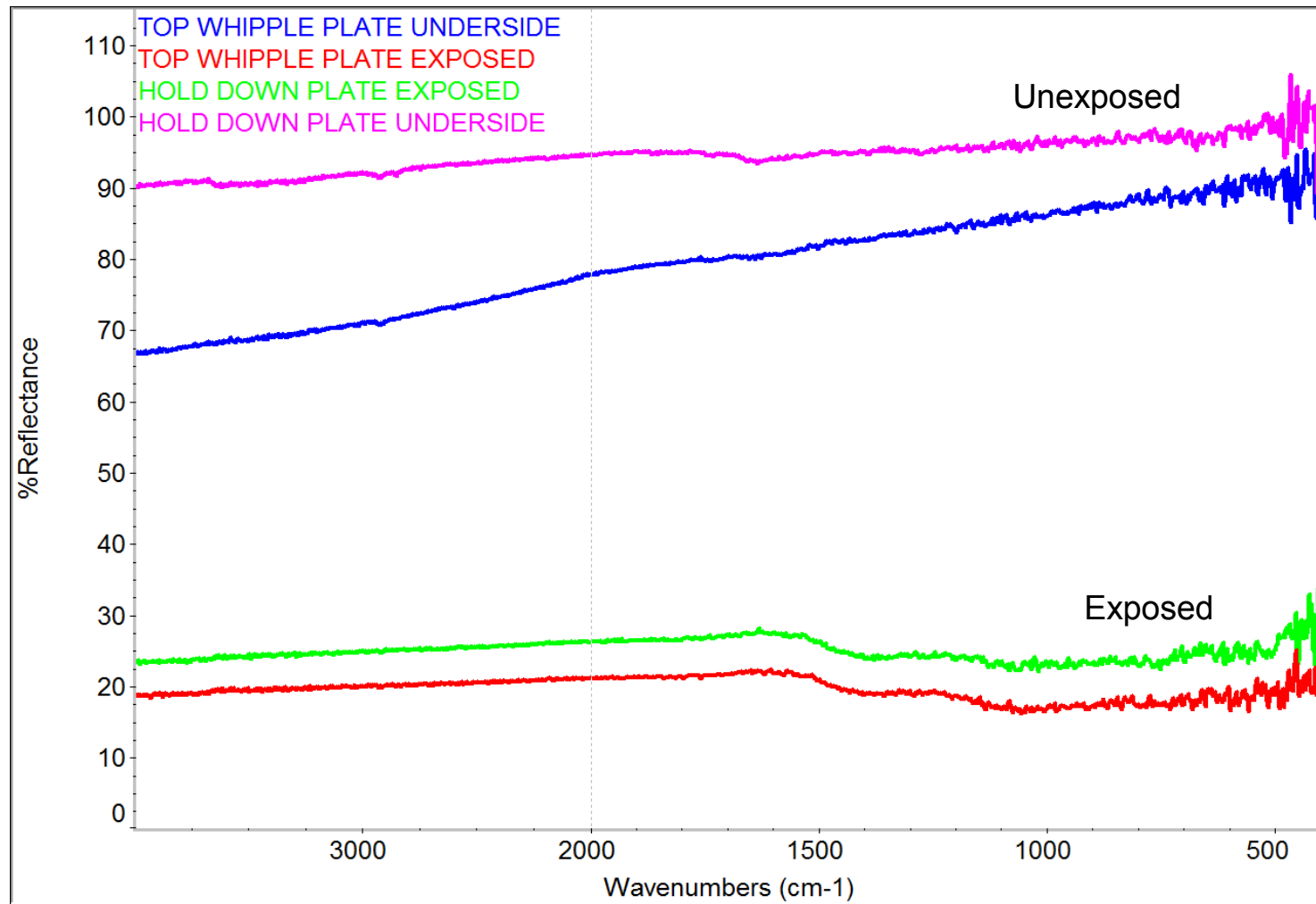
Relative Al-Si-O Contents of Fe-Cr-Ni and oxide/silicate phases



Aluminum content decreases over time – less contribution from the projectile.
Relative oxygen content remains nearly constant. Two episodes of deposition: early with flow structure and later semi-solidified large droplets.



Quantitative FTIR – LWIR Hemispherical Reflectance

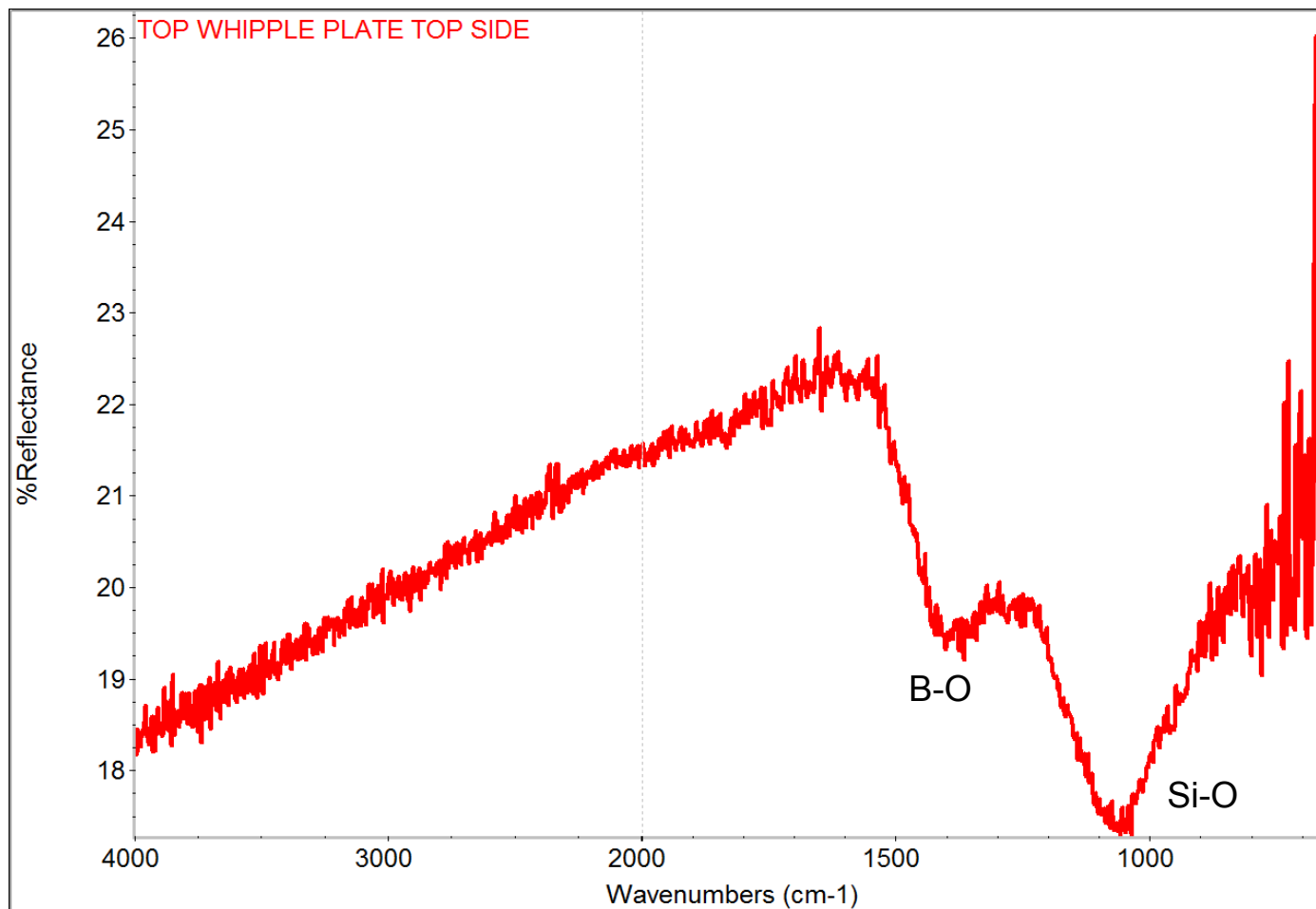


Significant decrease in reflectance – “darkening”. Note- underside of Whipple plate had a very thin deposit – compare with hold down plate.



Top Whipple Plate FTIR (post test)

Two reflectance minima occur from transmission through silicate material and reflectance off underlying metal

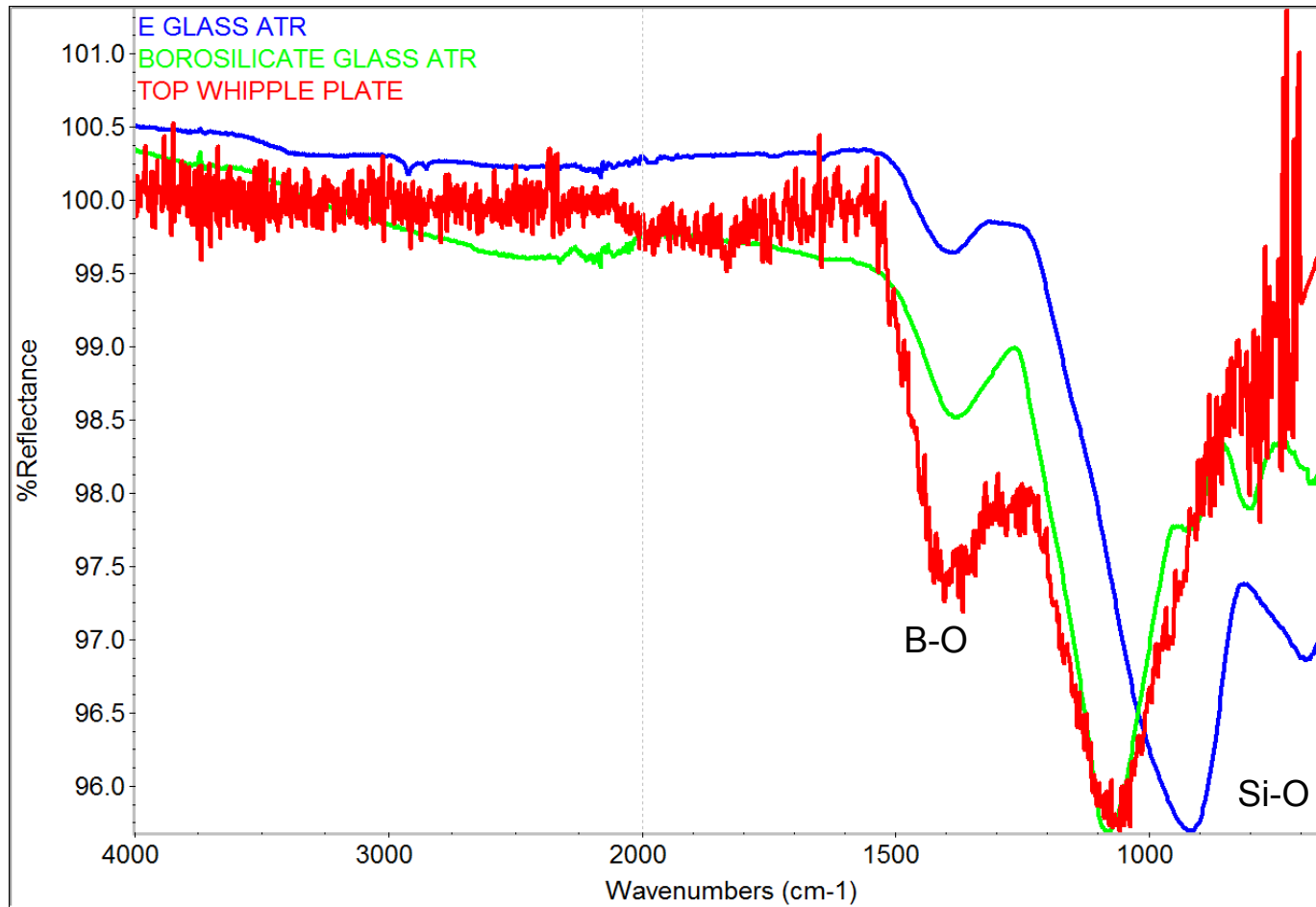


Feature at 1070 cm^{-1} is from Si-O bonds in a silicate. Feature at 1400 cm^{-1} is from “borate” in borosilicate.



Infrared Spectra of Silicate Glasses

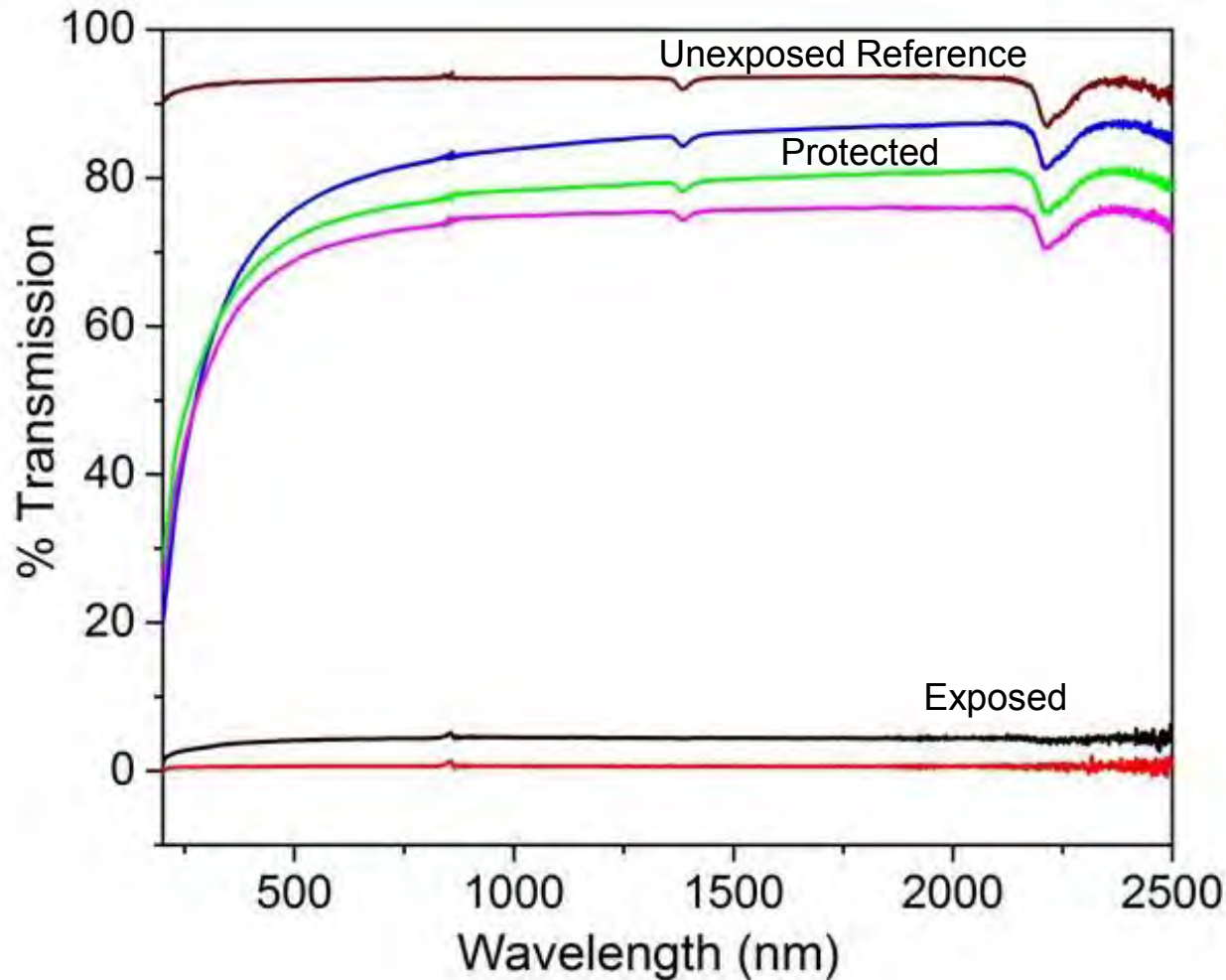
Attenuated total reflectance (ATR) and diffuse reflectance (Whipple plate)



Silicate peak shifts from 910 cm^{-1} in E-glass to 1070 cm^{-1} implies a change in composition and Si-O bond frequency .



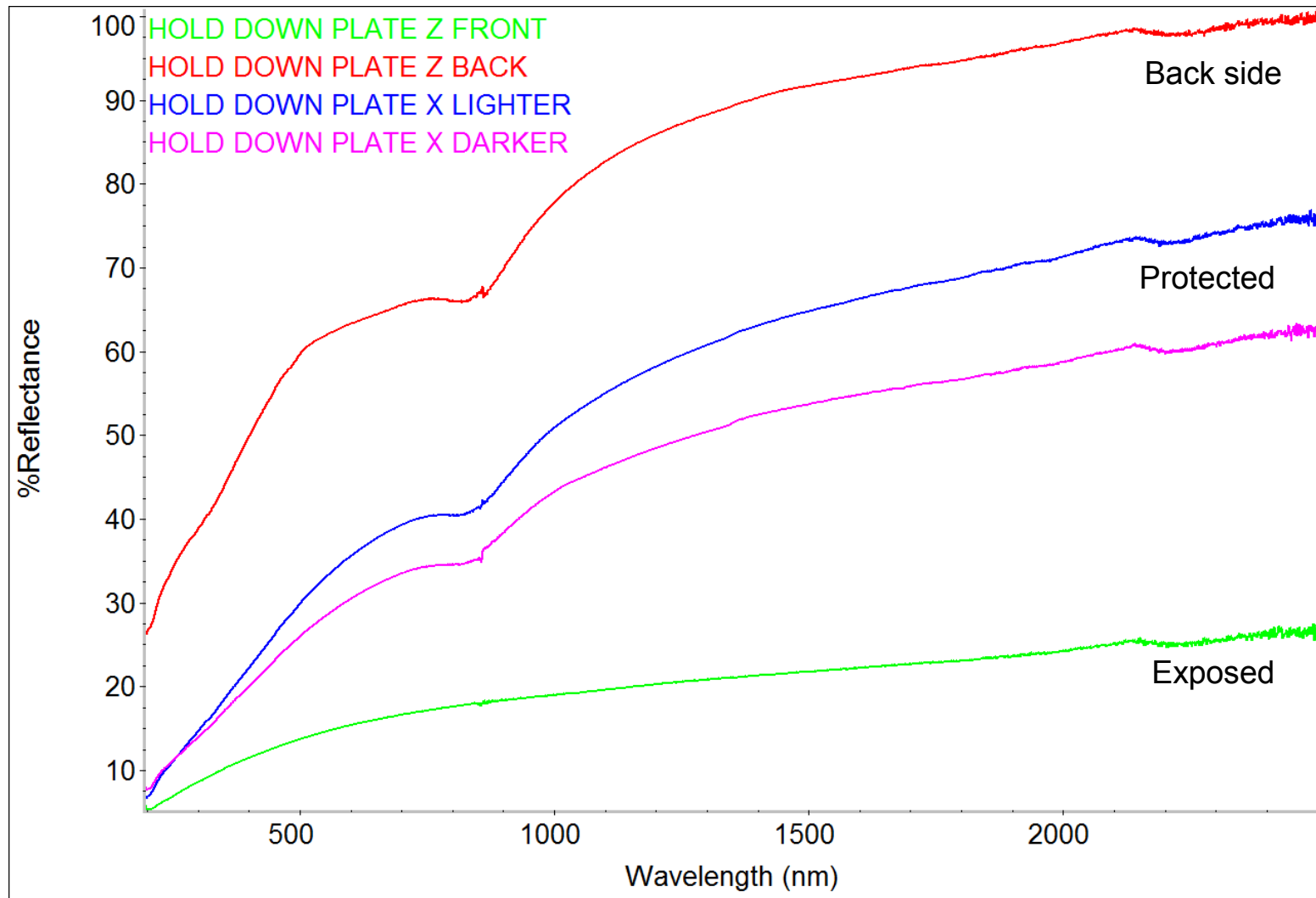
UV-VIS-NIR Spectroscopy (transmission) – SiO₂ Witness Plates



Protected samples show a 10-20% drop in transmission while exposed samples are nearly opaque.



UV-VIS-NIR Spectroscopy (reflectance) – Hold Down Plates



Significant decrease in reflectance on exposed surfaces.
Less so on protected surfaces.



Summary of Observations

- The material on the witness plates forms a layer ~10 microns thick consisting of solidified molten droplets of two types of phases that have a complex intermixed flow structure.
- Consists of an Fe-Cr-Ni rich phase and oxide-rich phases.
 - In general more of the Fe-Cr-Ni phase arrived earlier and more of the oxide phases later.
 - The Fe-Cr-Ni phase is crystalline while the oxide phases are amorphous.
- Larger semi-solidified droplets were deposited on the surface of the layer with the flow structure.
 - Droplets have a slightly different composition from underlying oxide layers.
- The two types of phases are not simple physical mixtures of molten stainless steel and E-glass.
 - Chemical changes have occurred as a result of the impact.



Summary of Observations (cont.)

- The Fe-Cr-Ni proportions in the Fe-Cr-Ni phase are not significantly different from 304 SS – no segregation/partitioning.
 - Unlike that seen in meteorite impacts and simulations thereof.
- The Fe-Cr-Ni rich phase also contains significant Al and Si.
 - O and Ca are generally lacking, or at very low levels.
 - Si and Al are soluble in Fe up to 10-20 atomic %.
 - Al and Si are about equal in early arriving Fe-Cr-Ni
 - The later arriving Fe-Cr-Ni is Si rich and Al is low to absent.
 - There is less flow structure and individual droplets tend to retain their shape implying they were already semi-solidified when deposited.
- There is a Ca-Al oxide phase mixed with the Fe-Cr-Ni with complex flow patterns.



Summary of Observations (cont.)

- The oxide phases have a range of compositions
 - The early oxide phase mixed with Fe-Cr-Ni is primarily Ca-Al oxide with little/no Si.
 - Later oxide droplets are larger (to 100-200 microns) and show less to little flow structure but some gas bubbles.
 - Later oxide droplets have significant Si and many have a composition similar to E-glass.
- The integrated (Ca-Al-Si) composition of the early phases with the complex flow patterns is significantly enriched in Al with respect to E-glass implying **significant Al came from the projectile.**
 - Aluminum has the lowest melting point of the starting materials.
 - M.P. of Al = 660C
 - T_g (glass transition temp.) of E-glass ~ 850C
 - M.P. of 304 SS = 1400 -1450C



Summary of Observations (cont.)

- The first three bumpers that were perforated were fiberglass (1st, 2nd) and stainless steel (3rd).
 - These bumpers were closely spaced, with a relatively larger spacing between bumpers #3 and #4. The witness plate was located between SS bumper #3 and E-glass bumper #4.
 - Molten droplets consisting of Fe-Cr-Ni and Al-Ca oxide may have condensed from a mixed gas phase formed from the bumpers and the projectile.
 - Si and Al dissolved in the Fe-Cr-Ni leaving Al and Ca in an oxide phase, or Al and Ca combined with all the O leaving Si and excess Al to dissolve in the SS?
 - Additional Al (16-18%) came from the Al projectile.
 - These droplets arrived first in a very fluid state were immiscible and physically mixed and flowed together in complex patterns.



Summary of Observations (cont.)

- The fourth and last bumper to be perforated was fiberglass.
 - Molten droplets from this bumper probably arrived later and appeared to be less fluid and show less flow structure.
 - Droplets would have to be ejected up range.
 - Droplet sizes are larger (to 100-200 μm) with compositions more consistent with E-glass
 - Some Fe-Cr-Ni droplets also present. Droplets show little to no flow mixing. They retain their shape implying they were partially solidified when deposited.
 - There appears to be less aluminum in these late deposits.
 - Projectile has slowed down and possibly broken up depositing less energy and producing lower temperatures than in the first three bumpers.



Summary of Observations (cont.)

- Significant darkening of adjacent structures occurred as a result of impact and the deposition of molten metal and oxide/silicate droplets.
 - Decrease from 90-95% to 20-25% reflectance across UV-VIS-NIR-LWIR wavelengths.
 - This dramatic decrease in reflectance occurred without the presence of carbon, which has been attributed to observed darkening on orbit.
 - Most deposition on the witness plate assembly appears to have been at a steep angle based on shadowing produced by the Whipple plates.
- LWIR spectral features are related to silicate and borate from the E-glass bumpers that were penetrated.
 - Silicate feature shifts as a result of change in composition (Si-O bond distance/frequency).



Conclusions

- Molten droplets (100s μm to 10s nm) from the projectile and target materials (E-glass and stainless steel) were formed as a result of the hypervelocity impact.
 - Some of the molten droplets may have condensed from a vapor phase.
 - Compositions not seen in the original materials were formed as a result of the energy imparted by the impact.
- These droplets were deposited on adjacent surfaces and increased scattering at UV to LWIR wavelengths.
- This resulted in a decrease in reflectance (albedo) – i.e. darkening.
- At LWIR wavelengths Si-O absorption bands from the silicate phase derived from the E-glass were observed.
- A hypervelocity impact may be inferred if absorption bands (or reststrahlen bands) from an “infrared active” material appear on surfaces where they normally are not present?
 - Strongly “infrared active” materials include silicates, some oxides and most organics.
 - Metals are not “infrared active” so they leave no characteristic signature but contribute to the overall “darkening” by increasing scatter.



Appendix 1

Supplemental Information and Analyses



Introduction (cont.)

- Debris-LV (Pre Shot) conducted 1 April 2014
 - Further validated performance of projectile and facility and served as a dress rehearsal for the DebrisSat test.
 - The 15 kg target consisted primarily of empty tanks and was constructed by Patti Sheaffer from materials representative of a launch vehicle (LV) upper stage.
 - Primarily aluminum and titanium with lesser amounts of copper and stainless steel.
 - Test chamber was lined with “soft catch” foam panels to trap fragments for size distribution analysis.
 - A witness plate assembly was constructed by Aerospace in order to catch and sample debris and returned to Aerospace after the test for analysis.
 - Aerospace also placed SEM stub witness plates into soft catch for post test retrieval and analysis.
 - Aerospace TOR-2014-03577, Debris-LV Hypervelocity Impact Post-Shot Physical Results Summary, P. M. Sheaffer

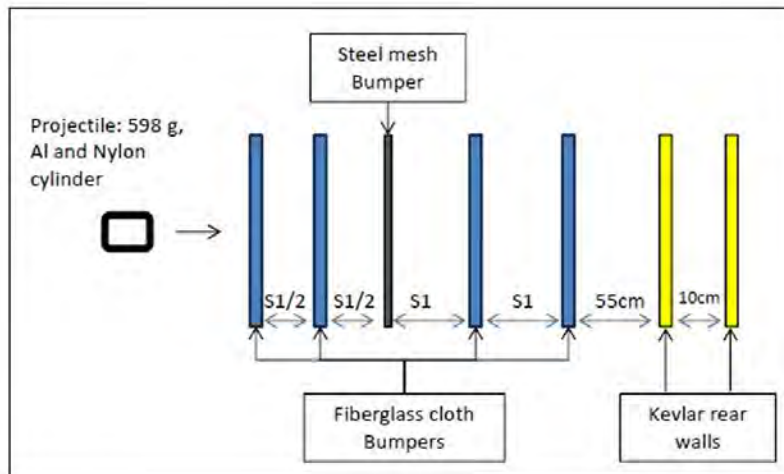


Introduction (cont.)

- Debris-Sat conducted 15 April 2014
 - The 50 kg target was constructed by the University of Florida from materials representative of a modern LEO satellite.
 - Aerospace Concept Design Center advised on selection of materials for various subsystems.
 - Test chamber lined with “soft catch” foam panels to trap fragments for size distribution analysis.
 - A witness plate assembly was constructed by Aerospace in order to catch and sample debris and returned to Aerospace after the test for analysis.
 - Aerospace also placed SEM stub witness plates into soft catch for post test retrieval and analysis.
 - Aerospace TOR-2014-03201, Time-resolved Spectroscopy of Hypervelocity Impact Flash on DebrisSat, Gouri Radhakrishnan.
 - Aerospace ATM-2014-03659, DebrisSat Hypervelocity Impact Fragmentation Modeling, Naoki Hemmi



Target



Target being loaded into chamber.
Target is 2.63 meters long and weighs
about 700 lbs.

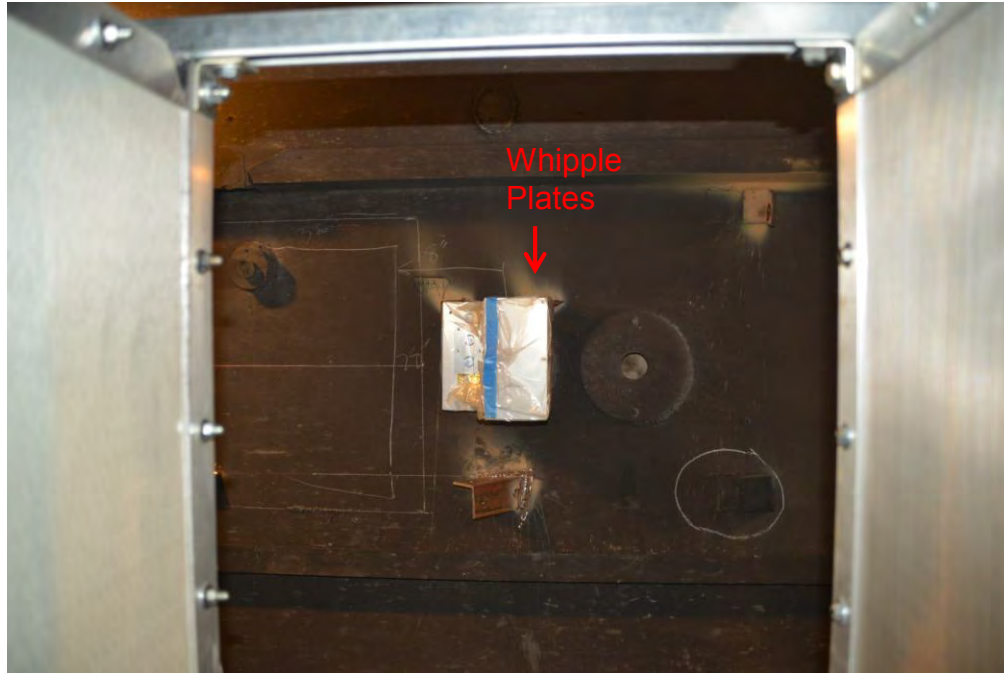
Image by AEDC

The distance S1 = 61 cm

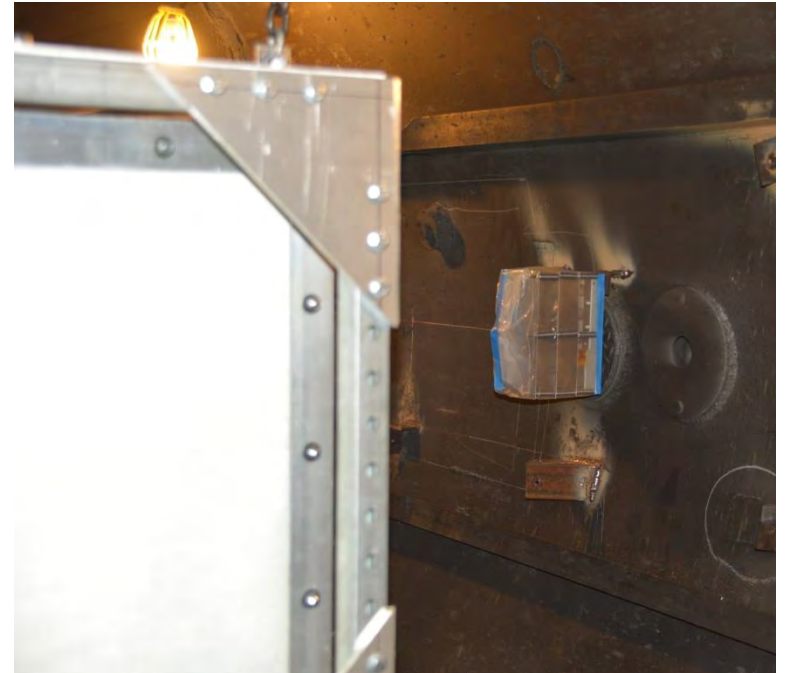


Target and Witness Plate Mounted in Chamber

Witness plate assembly is covered in plastic.



Bumper #4



Bumper #3

Bumper #1

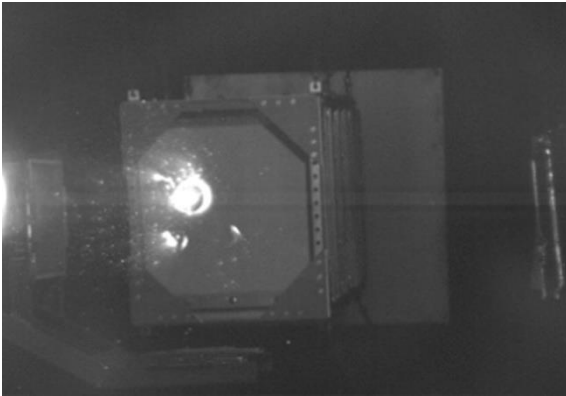
The witness plate assembly was positioned on the side of the chamber between bumpers #3 and #4. The Whipple plate side was up range. The hold down plates are positioned vertically. The distance to the target is about 1m.

Images by AEDC

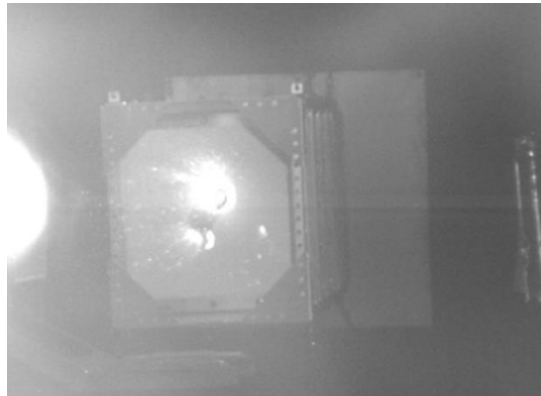


Frames from High Speed Video

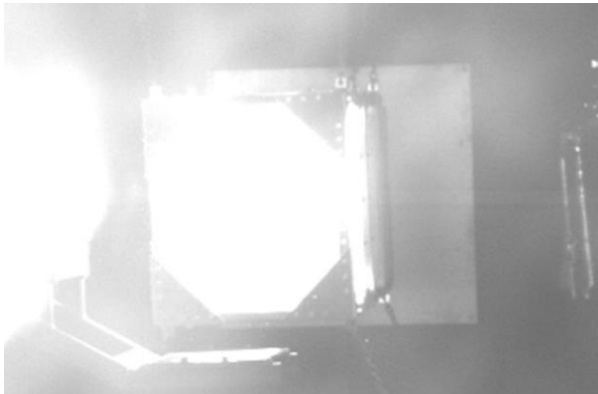
$T = -288 \mu\text{s}$



$T = \sim 0 \mu\text{s}$



$T = +36 \mu\text{s}$



$T = +72 \mu\text{s}$



$T = +108 \mu\text{s}$

Video from AEDC: 28,006 fps



Witness Plates Post Test: Whipple Plates

Bottom

Middle

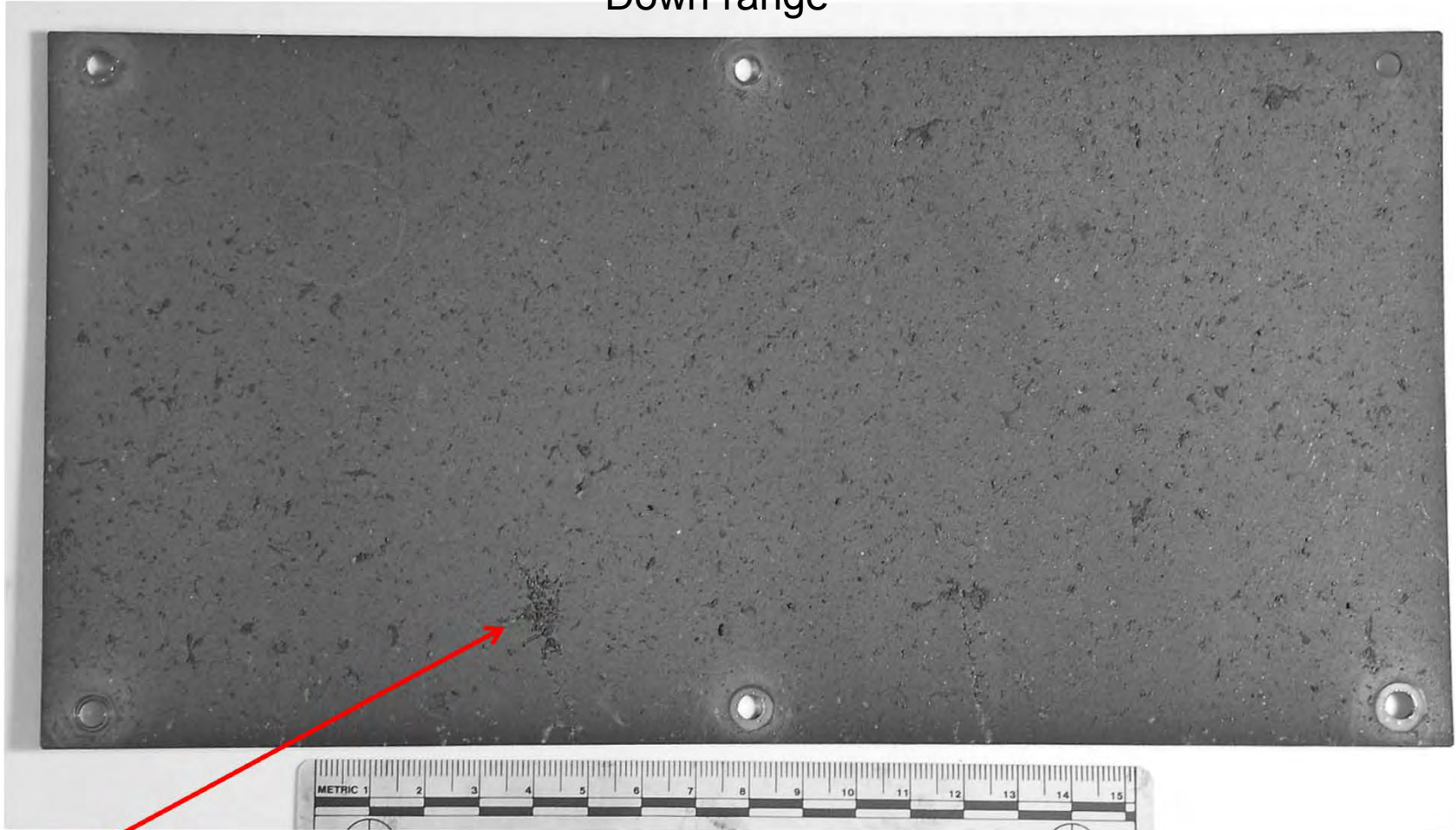
Top



Up range is to the right – note sharp band of deposits on up range side (right) of middle and lower Whipple plates

Top Whipple Plate: Post Test

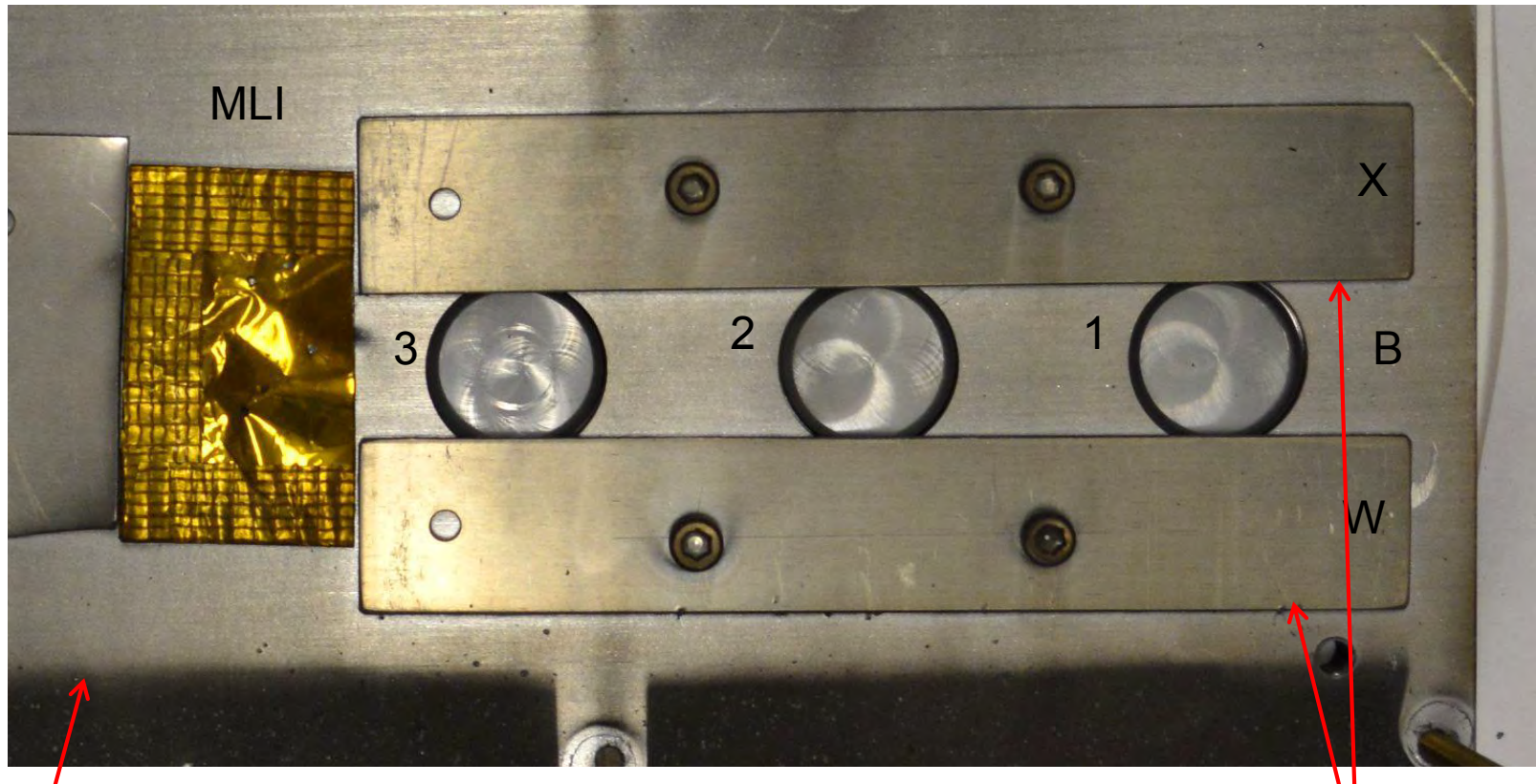
Down range



Large deposits are partially melted glass fibers

Witness Plates: Post Test (protected)

Down range



Up range

Note very sharp boundary between thick up range deposits (dark) and protected area.

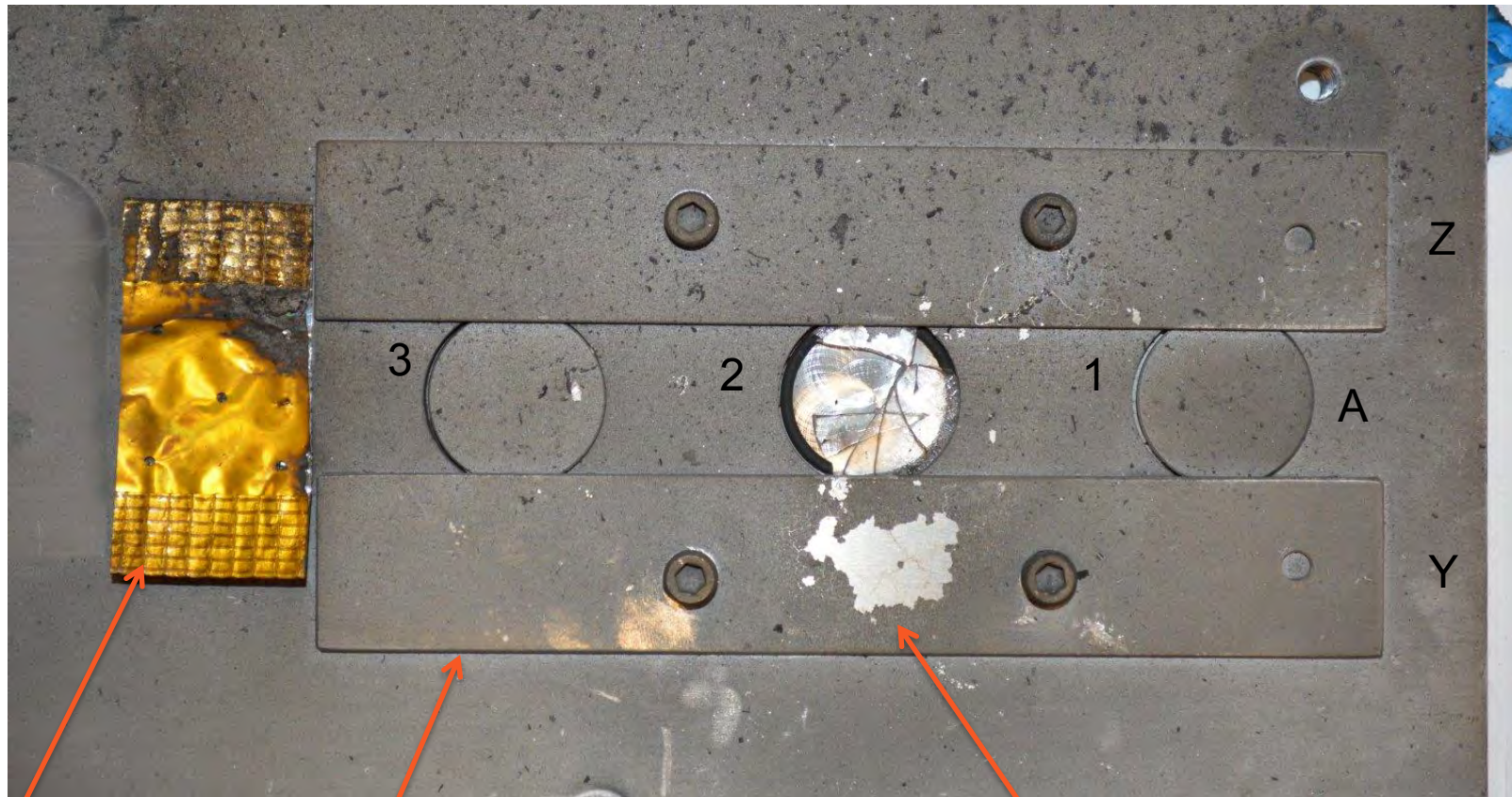
Edges of plates facing up range have thick accumulations of deposits. Opposite edges less so.

Surfaces of samples under Whipple plates are relatively clean. Deposition appears to be at a very high angle based on sharpness of debris shadow.



Witness Plates: Post Test (unprotected)

Down range



Multi layer
insulation

Hold down plate

Up range

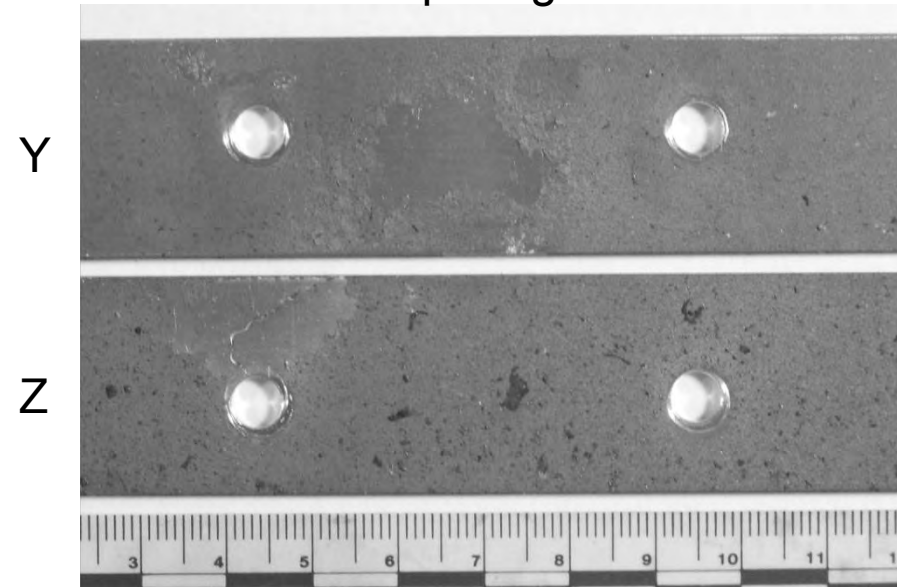
Note blistered and peeled coating and
fractured quartz window

Exposed surfaces are covered with a matte gray coating and fine debris.
Note larger deposits are concentrated toward the down range side of the plate.



Hold down plates: Post test

Up range



Note larger deposit fragments on the down range plate. Similar larger deposits were observed on the top Whipple plate. The Whipple plates probably shielded the up range hold down plate from larger fragments/deposits? This assumes the source was up range.



Close up of larger deposits on down range side plate.

Laboratory Instrumentation

- Field Emission Scanning Electron Microscopy (FESEM)
 - JEOL JSM-7600F SEM.
 - In-lens secondary electron detector (SEI mode).
 - High resolution imaging.
 - Lower secondary electron detector (LEI mode).
 - Less charging.
 - Enhances topography.
 - Backscatter electron detector (LBE mode)
 - Atomic number (Z) image contrast.
- Energy Dispersive (X-ray) Spectroscopy (EDS) in the SEM
 - Oxford X-Max silicon drift detector.
 - AZTec software.
- Wavelength Dispersive (X-ray) Spectroscopy (WDS) in the SEM
 - Oxford WAVE spectrometer.
 - INCA software.
- Electron Backscatter Diffraction (EBSD) and Transmission Kikuchi Diffraction (TKD) in the SEM
 - Oxford (hkl) Nordlys EBSD System



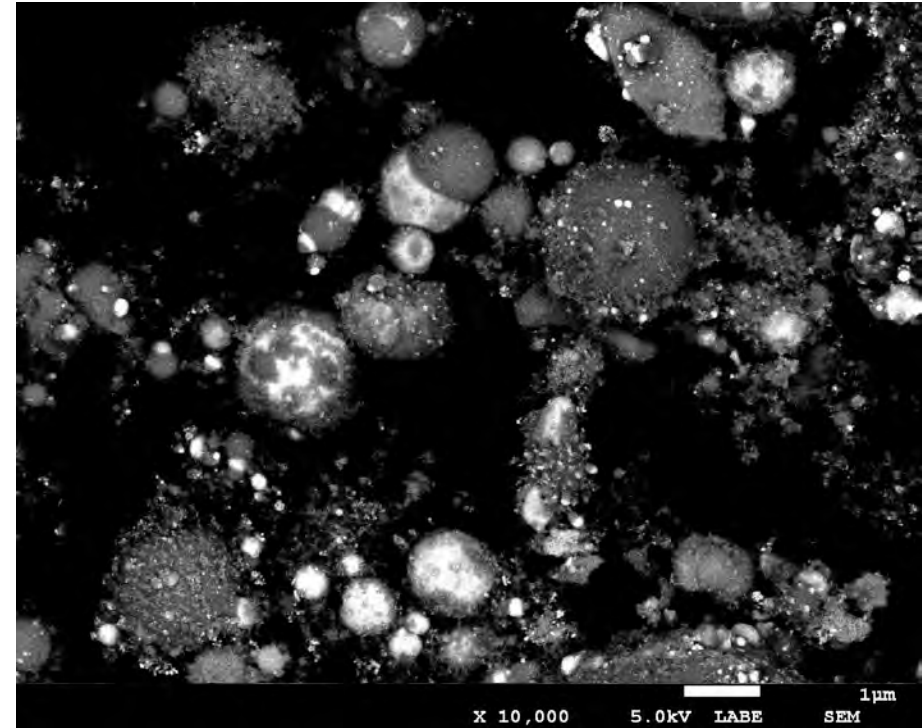
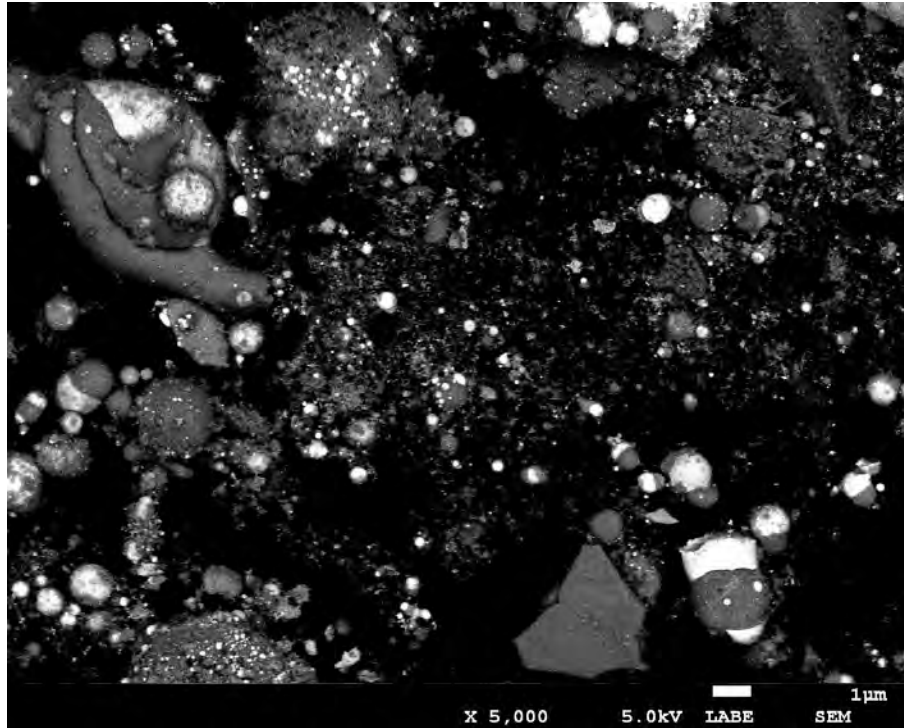
Laboratory Instrumentation (cont.)

- Fourier Transform Infrared (FTIR) spectroscopy
 - Nicolet 6700 spectrometer
 - Harrick Scientific “praying mantis” diffuse reflectance accessory
 - Qualitative reflectance
 - Mercury cadmium telluride (MCT) detector
 - Fast analysis with excellent signal to noise
 - Can only analyze small samples ($< 1''$)
 - Labsphere hemispherical reflectance accessory
 - Quantitative reflectance
 - Long scan time with poor signal to noise
- X-ray Diffraction
 - PANalytical X'Pert Pro Diffractometer
 - Copper radiation
 - X'Celerator detector
- UV-VIS-NIR Spectroscopy
 - Perkin Elmer Lambda 900 Spectrometer
 - Diffuse transmission and reflectance with integrating sphere.



Top Whipple Plate Tape Lift

Backscatter SEM 5KX 10KX

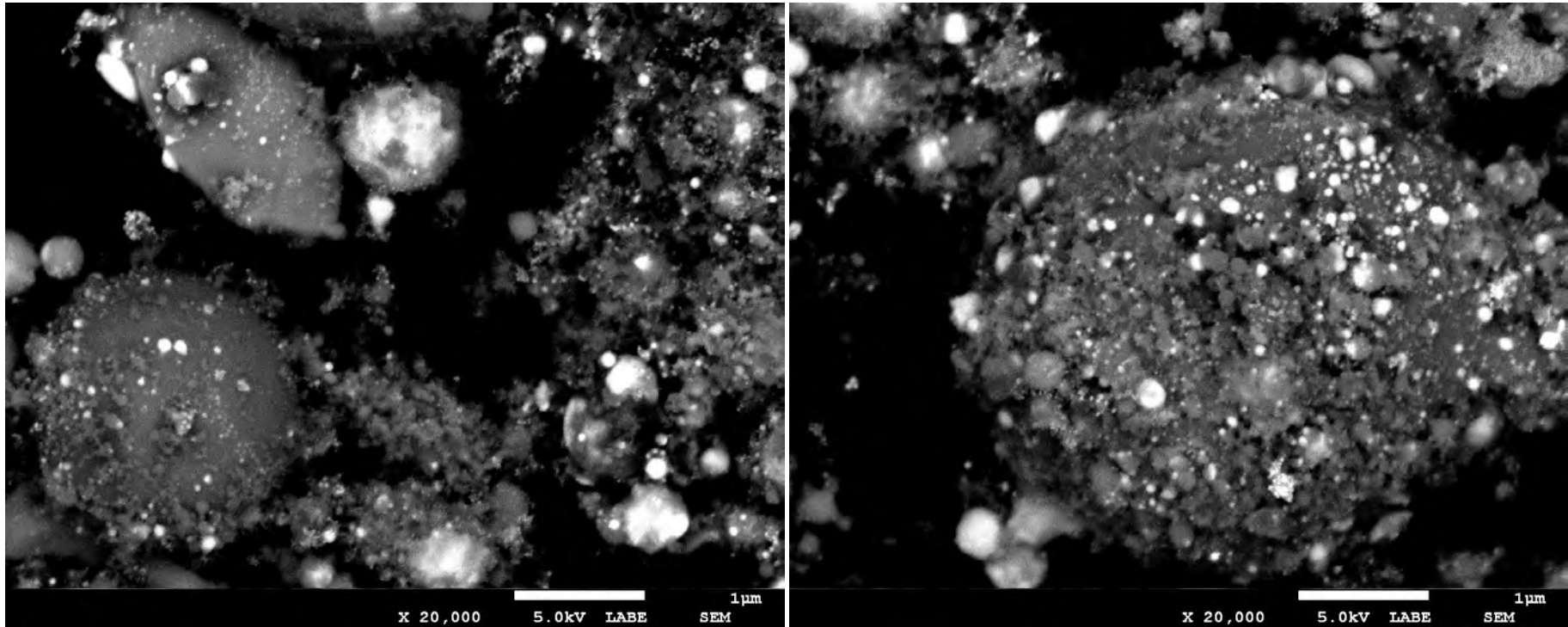


- Solidified molten droplets range from 10 μm to 10 nm.
- High Z/bright = Fe, Cr rich Low Z /gray = silicate, oxide
- Black background = carbon tape



Top Whipple Plate Tape Lift

Backscatter SEM 20KX



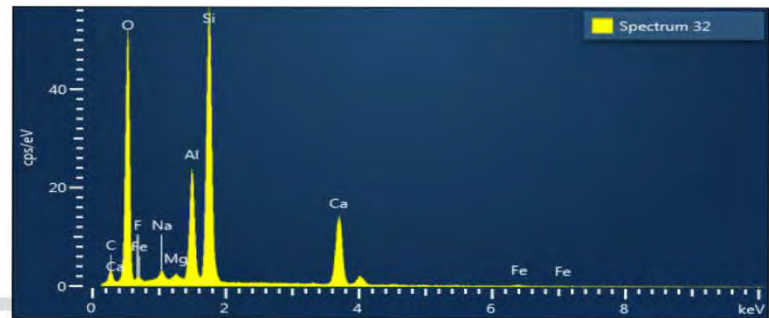
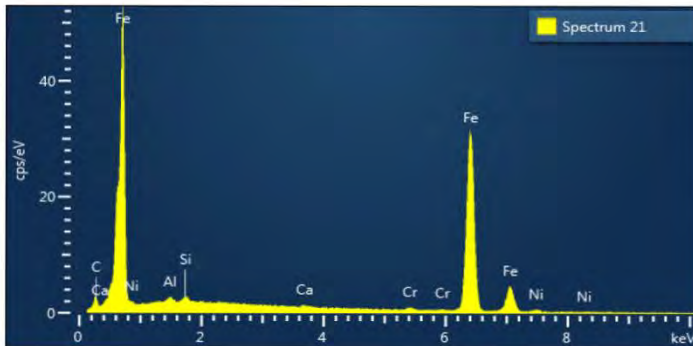
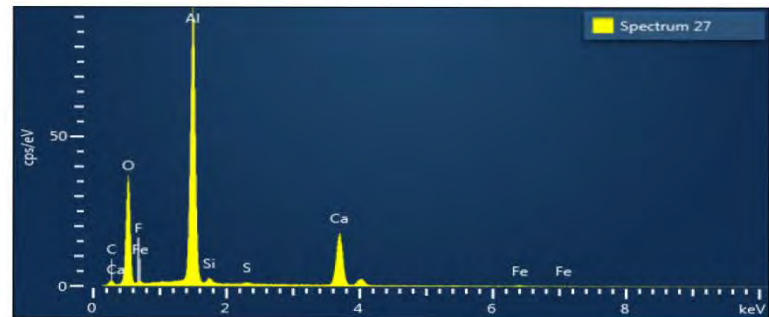
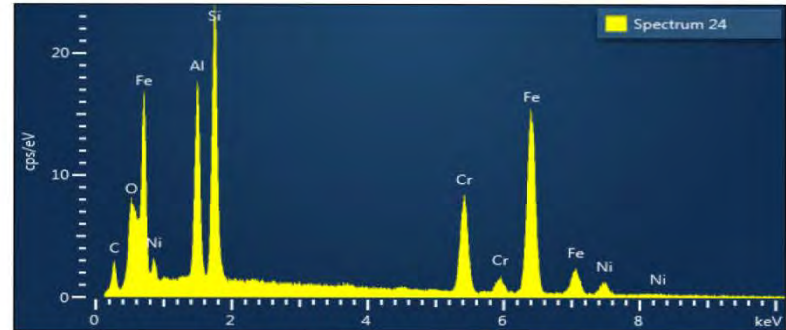
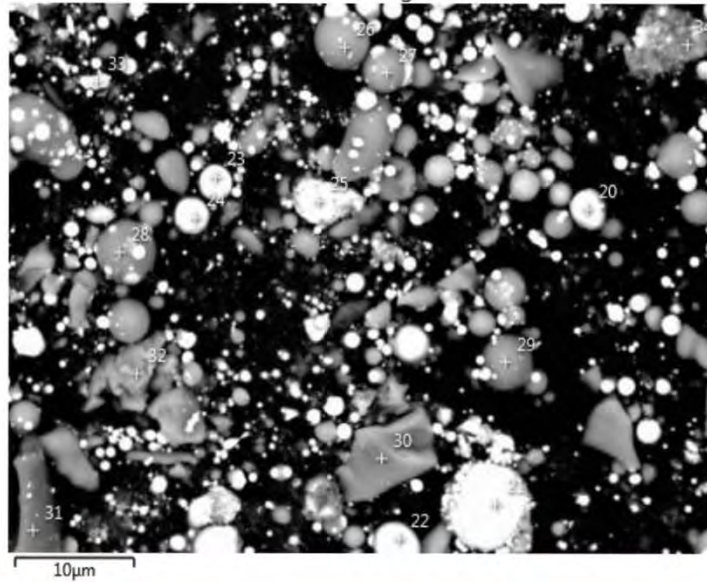
Solidified molten droplets:
Note droplets to nm scale.



SBU Marking

Top Whipple Plate Tape Lift

SEM - EDS Spectra

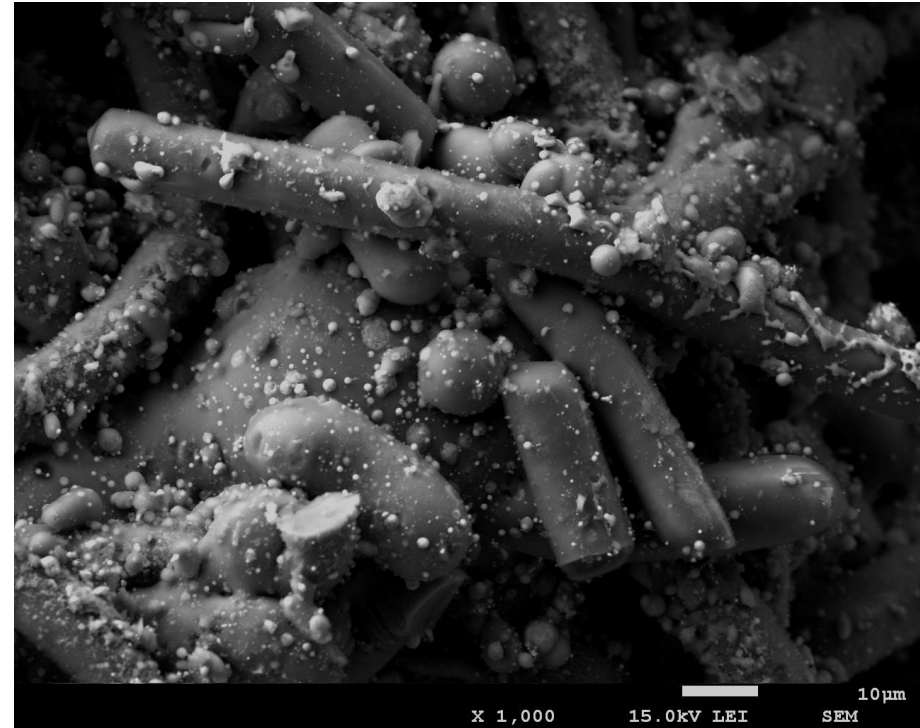
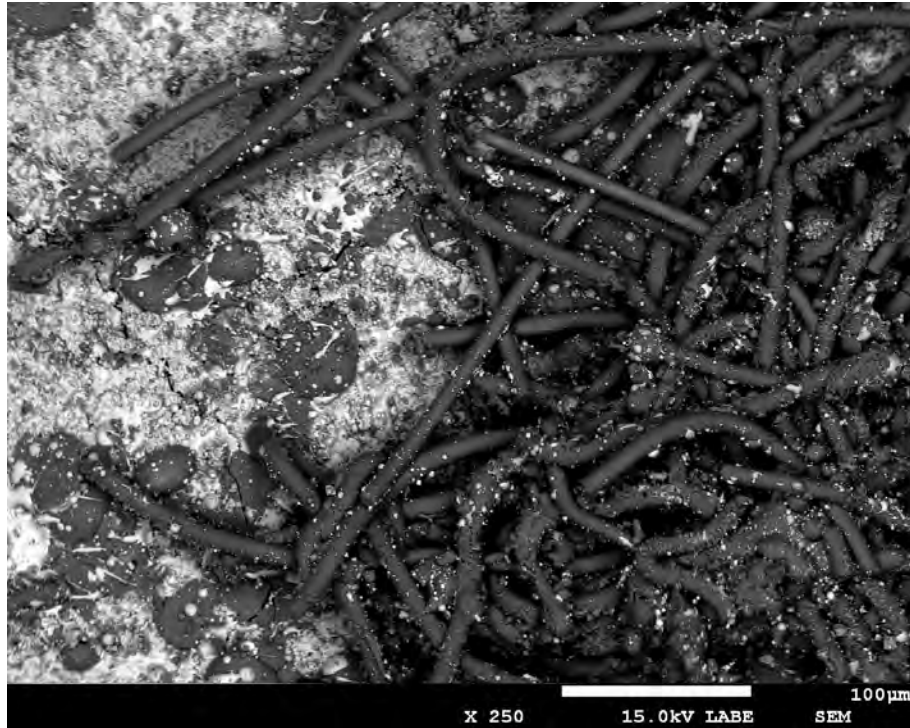


Particles contain Fe, Cr, Ni, Si, Al, Ca, O – elements in E-glass and SS

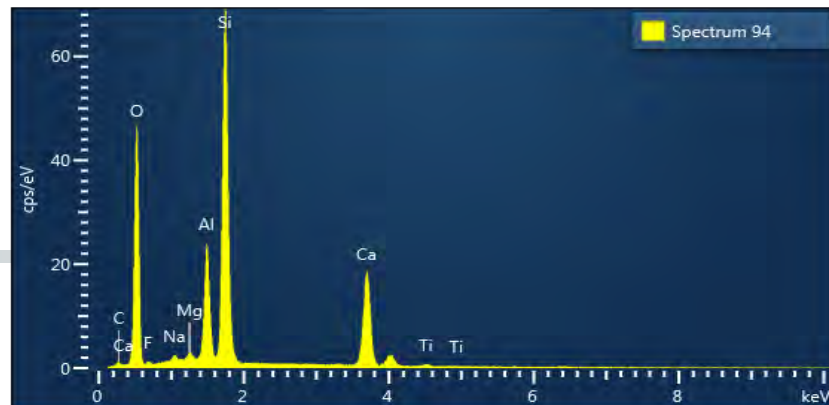


Exposed Hold Down Plate (Z)

Backscatter SEM

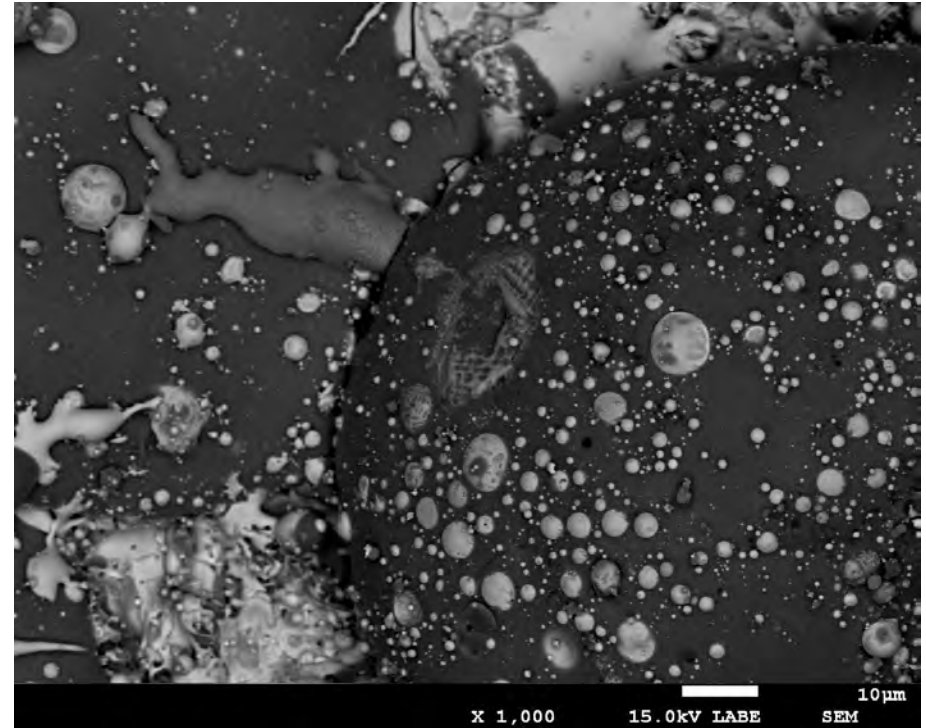
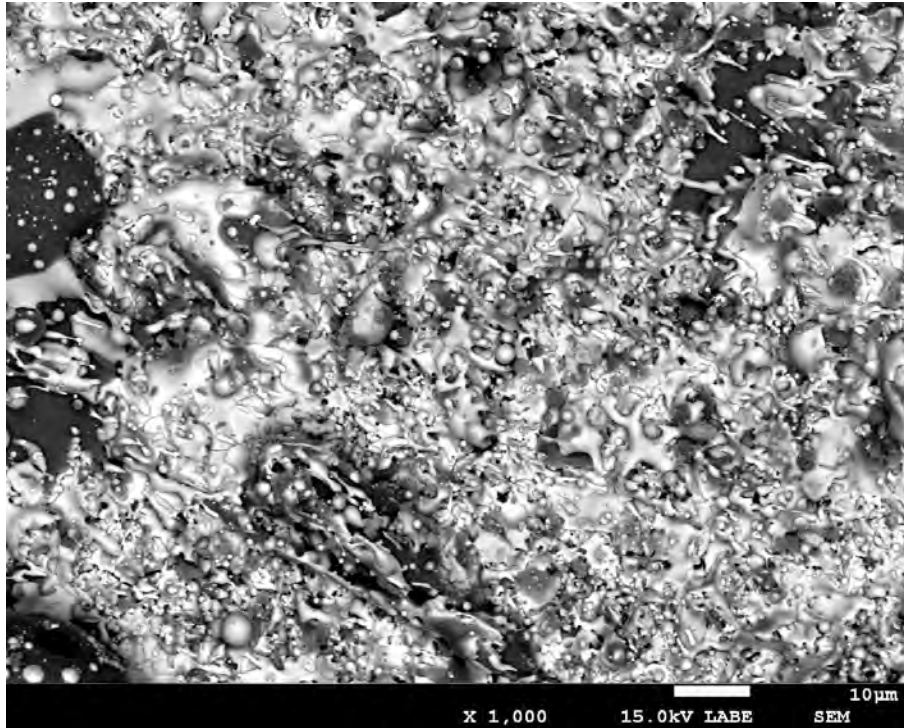


Remains of unmelted E-glass fibers.
E-glass = Ca-Al borosilicate



Exposed Hold Down Plate (Z)

Backscatter SEM – 1KX

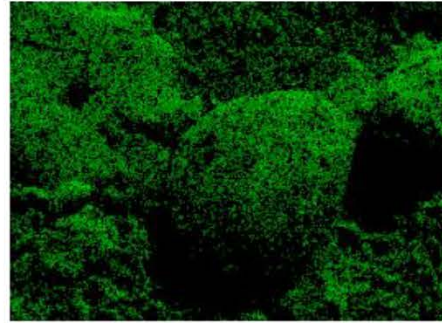
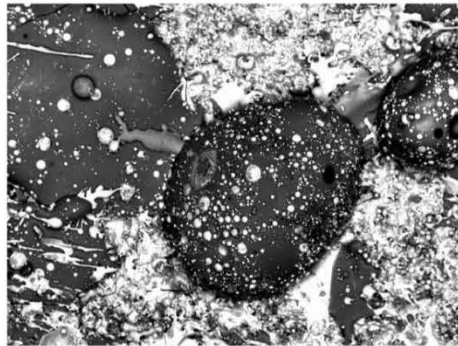


Coalesced solidified molten droplets with complex flow structure in higher Z material.

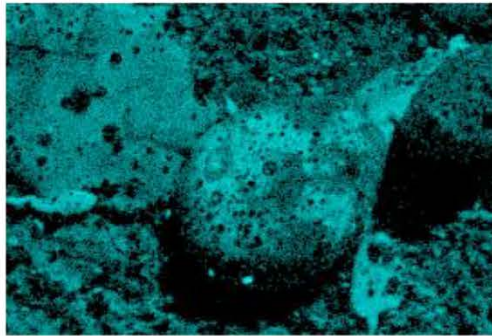


Exposed Hold Down Plate (Z)

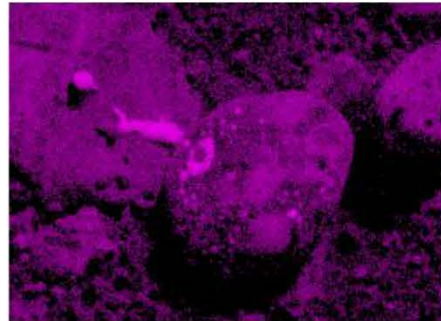
SEM - EDS Elemental Maps



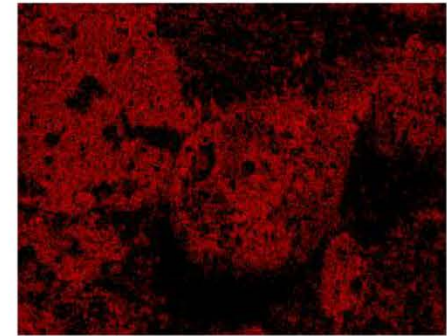
Al K series



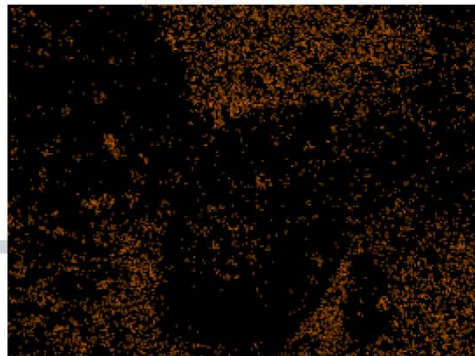
Si K series



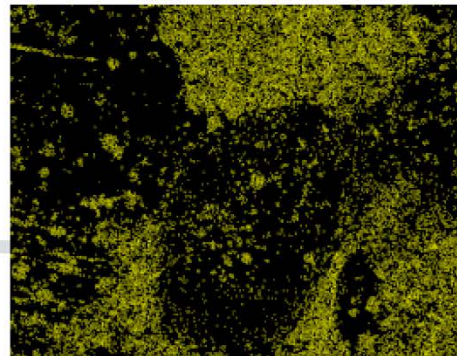
Ca K series



Cr K series



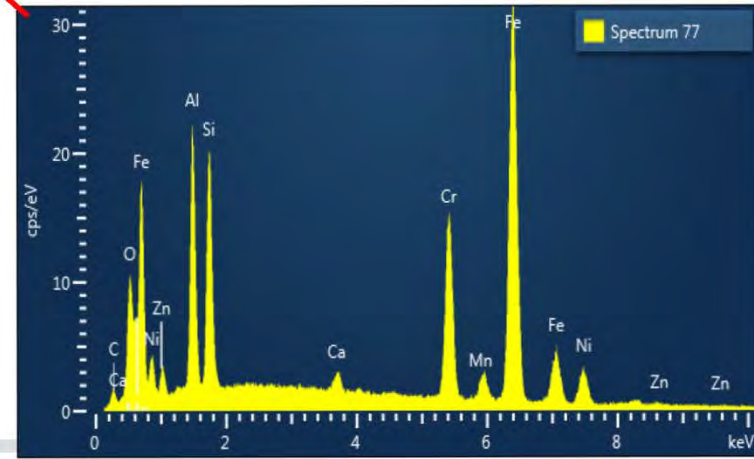
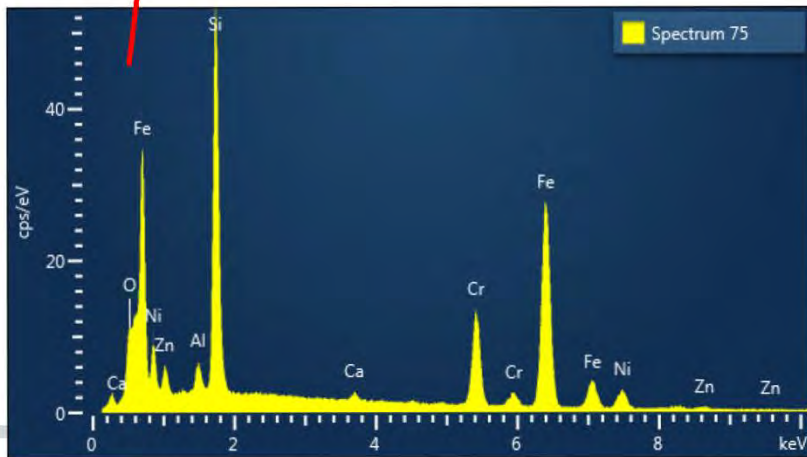
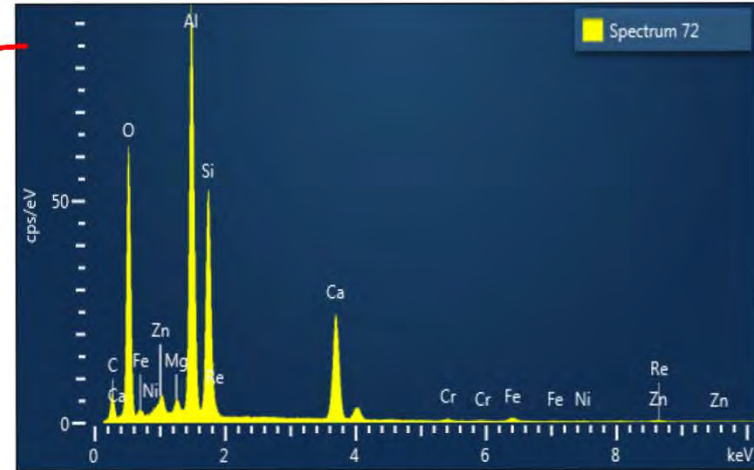
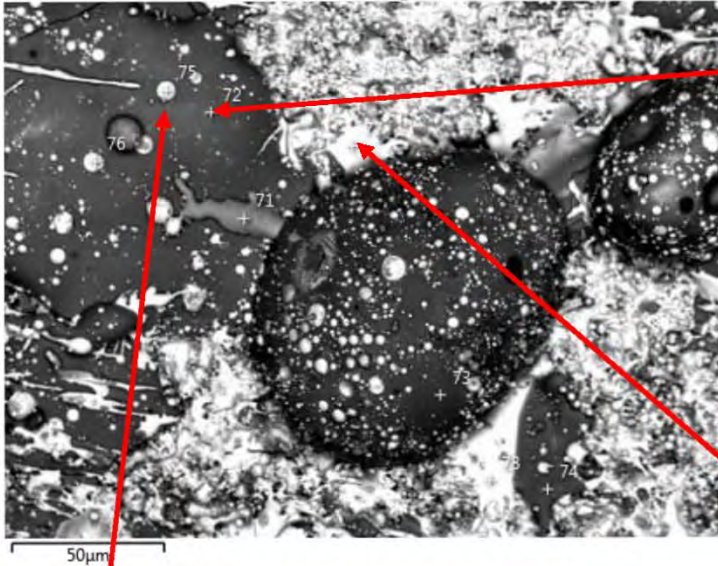
Fe K series



SBU Marking

Exposed Hold Down Plate (Z)

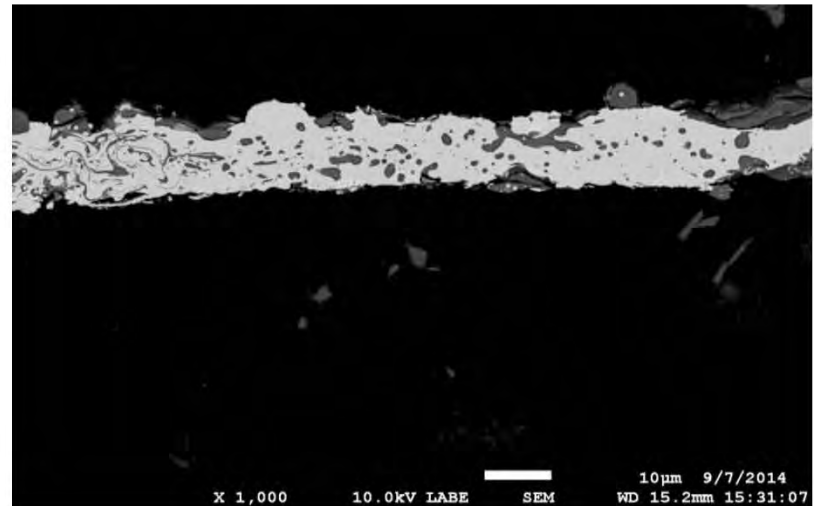
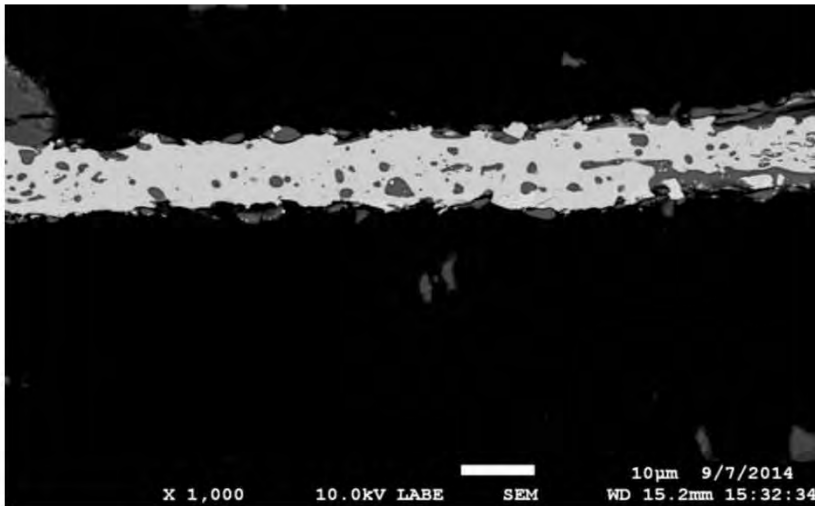
SEM - EDS Spectra



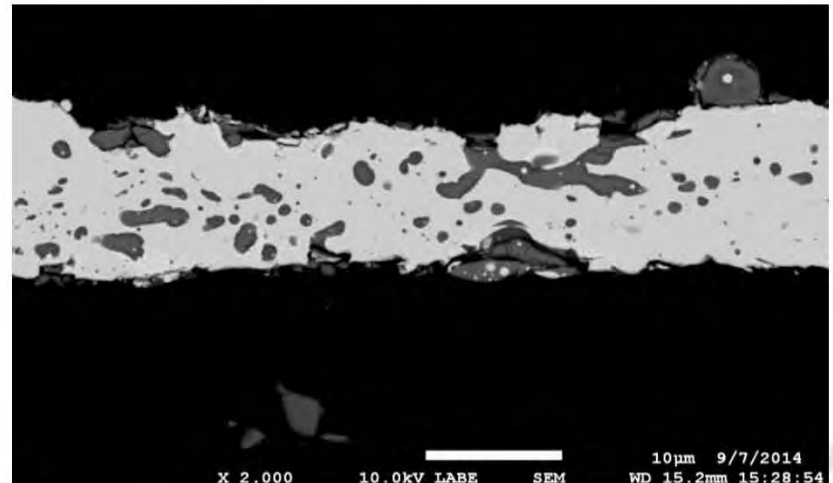
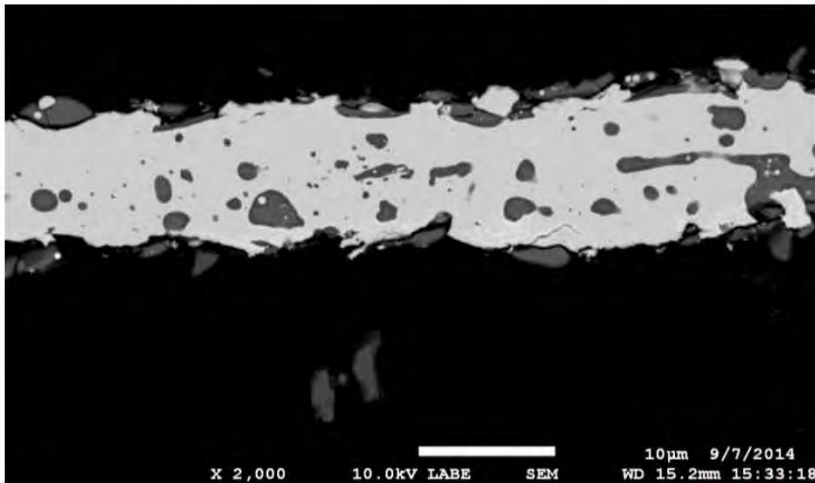
Al – Si also present in Fe-Cr phase. Variable Si-Al-Ca stoichiometry



SBU Marking
Exposed Hold Down Plate (Z) Cross Sectioned Flake
Backscatter SEM 1KX, 2KX



1KX



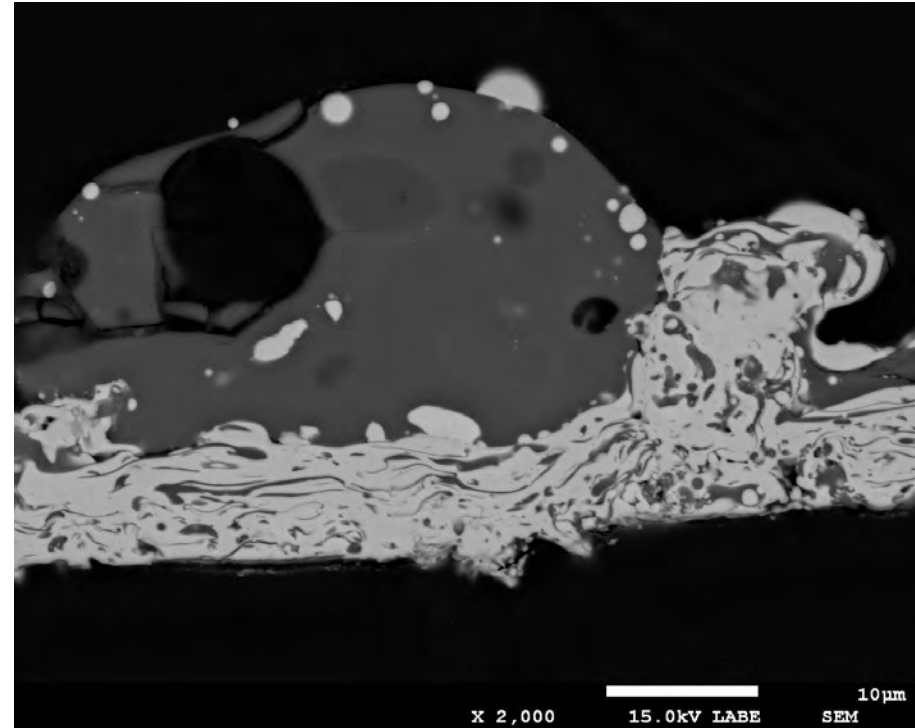
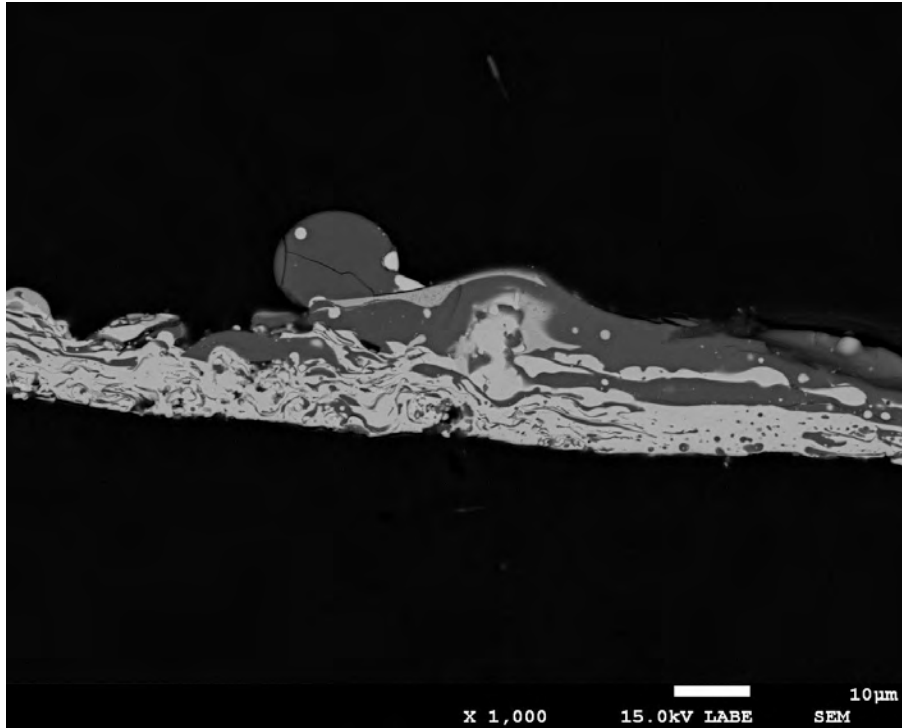
2KX

Isolated areas show less complex flow structure.



Exposed Hold Down Plate (Z) Cross Sectioned Flake

Backscatter SEM 1-2 KX

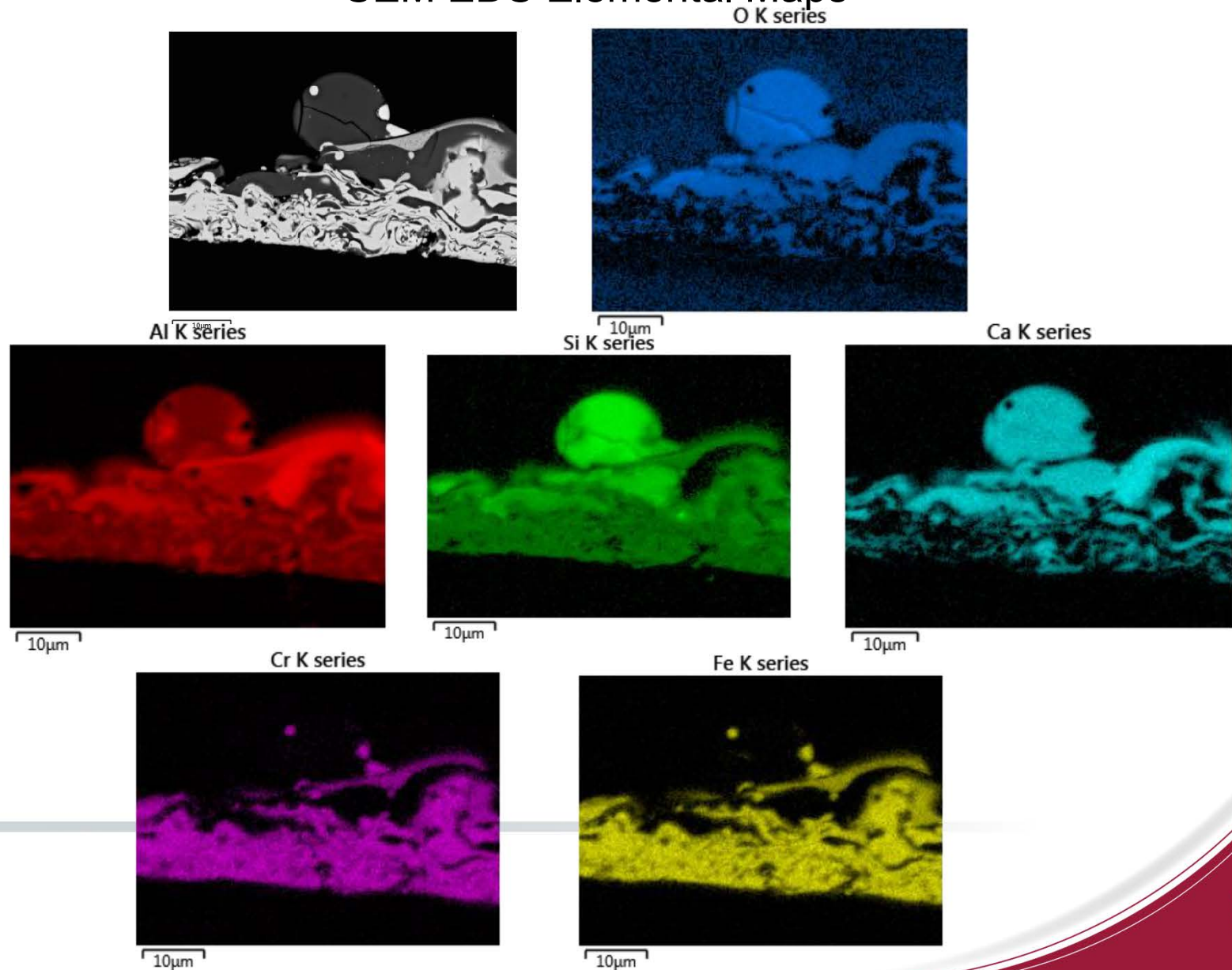


- The first two bumpers that were perforated were fiberglass and the 3rd was stainless steel.
- Molten droplets from these arrived earlier in a very fluid state and physically mixed and flowed together but did not homogenize (were not miscible?).
- The fourth and last bumper to be perforated was fiberglass.
 - Less energy delivered by projectile.
 - Droplets from this bumper arrived latter and were less fluid.



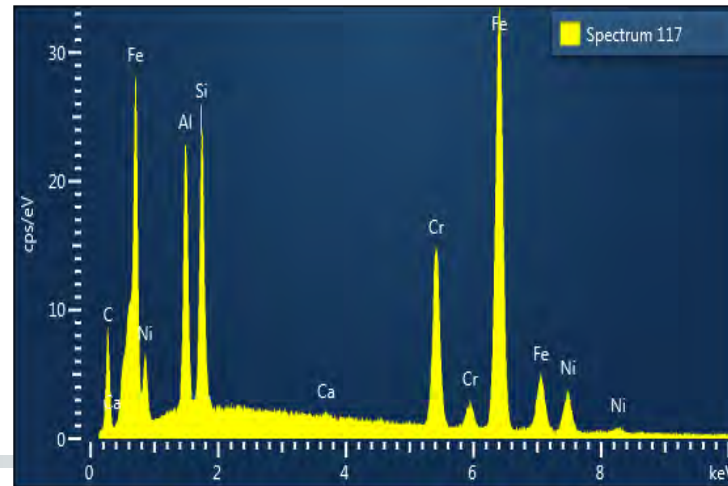
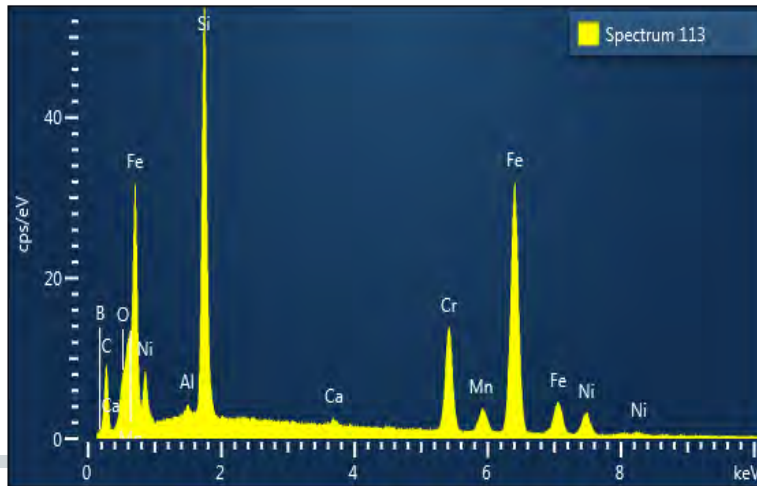
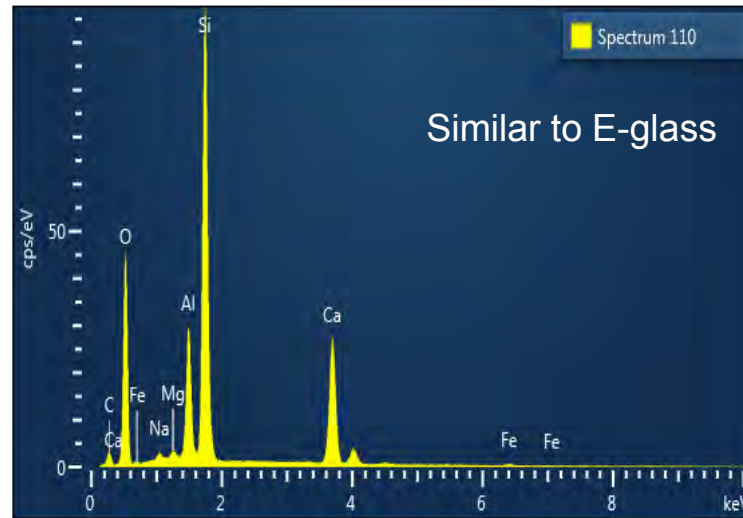
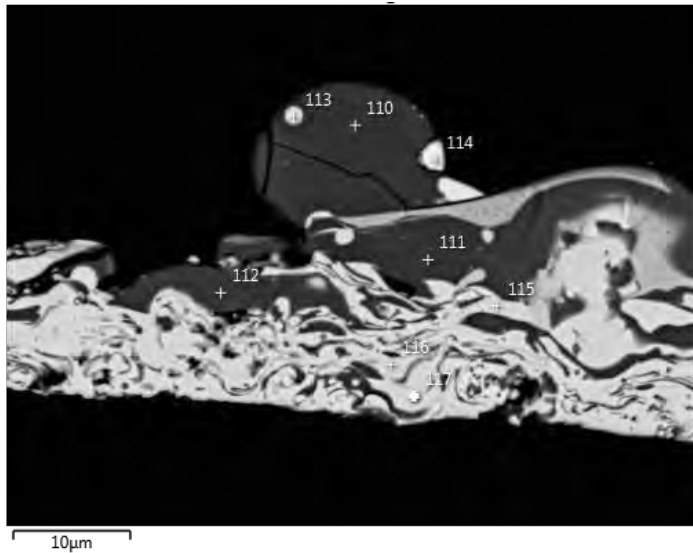
SBU Marking

Exposed Hold Down Plate (Z) Cross Sectioned Flake SEM EDS Elemental Maps



Exposed Hold Down Plate (Z) Cross Sectioned Flake

SEM EDS Spectra



Early Fe-Cr-Ni phase contains Al-Si but proportions vary.

76 Late Ca-Al silicate droplets are similar to E-glass

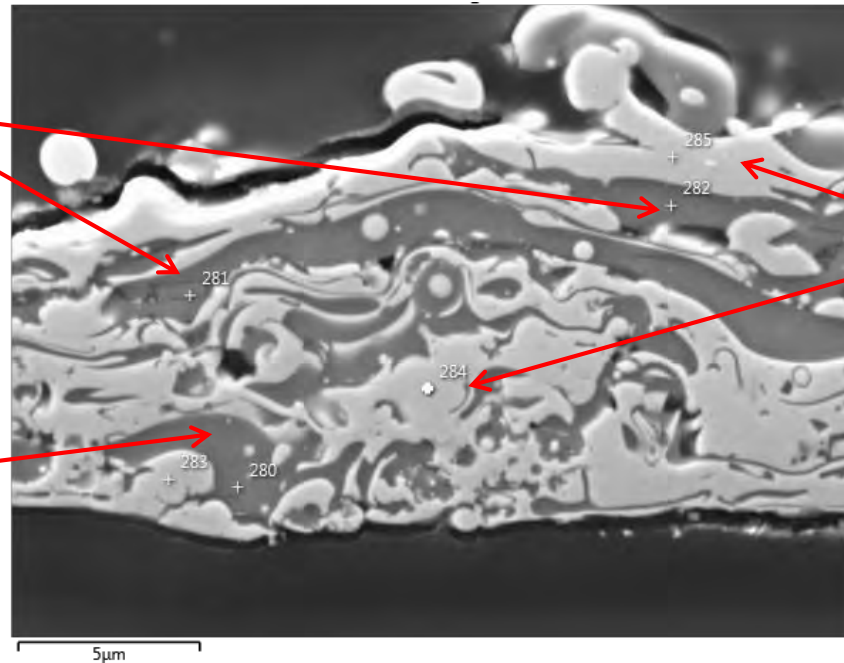


Exposed Hold Down Plate (Z) Cross Sectioned Flake

EDS Semi-quantitative Analyses

Later oxide phase has more Si

Early oxide phase mixed with Fe-Cr-Ni is rich in Al and Ca, little Si



Fe-Cr-Ni phase has significant Al and Si and no Ca

Element	E-Glass	280	281	282	283	284	285	Steel
O	65.3	58.38	61.29	56.74	3.29	3.41	4.08	
Na	0.4							
Mg	0.4		0.88	0.76				
Al	5.9	28.83	20.26	20.51	5.81	12.31	14.13	
Si	19.4	0.46	6.32	7.86	10.85	10.28	9.06	1.0
Ca	8.4	12.34	11.25	10.56				
Mn								1.4
Cr				0.88	10.22	12.88	12.44	19.3
Fe		0.00		2.68	57.26	53.98	50.44	68.2
Ni				0.00	12.56	7.15	9.86	10.2
Total	99.8	100.00	100.00	100.00	100.00	100.00	100.00	100.0

← Sample location

All values are atomic %

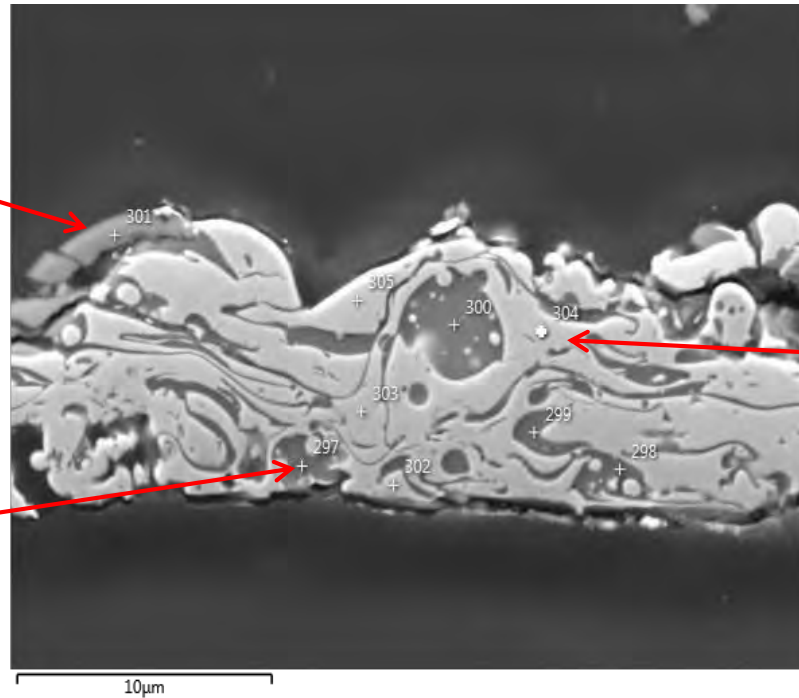


Exposed Hold Down Plate (Z) Cross Sectioned Flake

EDS Semi-quantitative Analyses

Later oxide phase has more Si

Early oxide phase mixed with Fe-Cr-Ni is rich in Al and Ca, little Si



Fe-Cr-Ni phase has significant Al and Si, no Ca

Element	E-Glass	297	298	299	300	301	302	303	304	305
O	65.3	56.90	54.57	58.58	58.11	62.14	5.25	8.24	7.58	3.12
Na	0.4									
Mg	0.4					1.02				
Al	5.9	28.49	25.57	28.24	29.28	16.53	15.57	16.85	16.16	9.53
Si	19.4	0.88	1.45	0.57	0.91	10.63	7.43	7.39	9.84	12.42
Ca	8.4	12.20	12.01	11.96	10.62	8.96		1.14	0.78	
Cr		0.56	1.47	0.65		0.72	11.83	11.91	12.21	14.61
Fe		0.98	4.93	0.00	1.08		51.08	45.67	45.44	51.42
Ni		0.00	0.00	0.00			8.84	8.79	7.98	8.91
Total	99.8	100.0	100.00	100.00	100.00	100.00	100.00	100.00	100.00	100.00

← Sample location

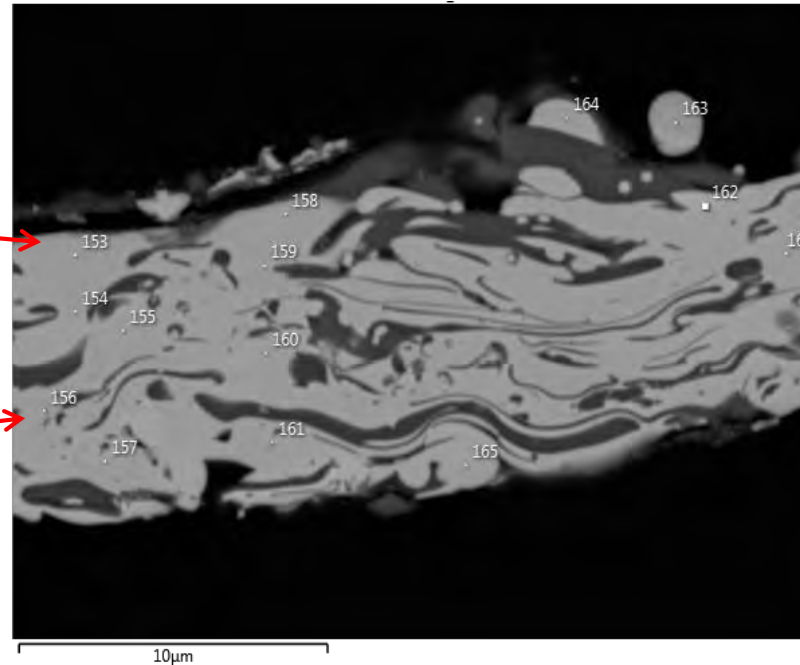
All values are atomic %



Exposed Hold Down Plate (Z) Cross Sectioned Flake EDS Semi-quantitative Analyses

High Si and little Al in
later Fe-Cr-Ni

Early Fe-Cr-Ni has
about equal amounts
of Al and Si



All values are atomic %

	153	154	155	156	157	158	159	160	161	162	163	164	165	166
O	3.23	2.85	2.73	7.76	3.27	3.80	4.18	3.77	5.83	3.82	5.44	3.86	2.70	1.51
Al	2.16	13.70	16.37	16.52	13.27	2.22	14.07	12.90	13.54	5.63	0.92	14.12	14.91	8.24
Si	29.37	10.29	9.98	9.02	11.73	32.24	10.43	11.67	12.03	13.81	28.89	12.21	9.12	11.72
Ca				1.06										
Cr	11.91	12.10	12.63	12.22	12.45	13.14	12.39	12.06	12.64	15.52	12.68	12.91	12.64	14.84
Fe	46.44	52.37	51.01	45.31	51.58	48.61	52.20	53.03	48.40	61.23	44.81	56.91	52.31	56.07
Ni	6.89	8.69	7.28	8.11	7.70	0.00	6.73	6.56	7.56	0.00	7.27	0.00	8.31	7.62
Total	100.00	100.00	100.00	100.00	100.00	100.00	100.00	100.00	100.00	100.00	100.00	100.00	100.00	100.00

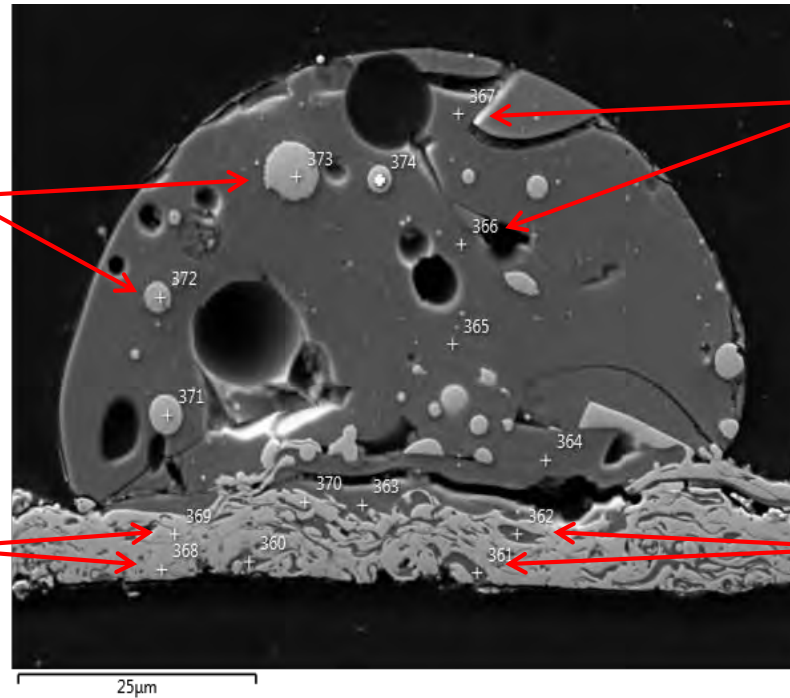
← Sample location

Some late arriving Fe-Cr droplets are enriched in Si and depleted in Al



Exposed Hold Down Plate (Z) Cross Sectioned Flake

EDS Semi-quantitative Analyses



Later more isolated Fe-Cr-Ni has more Si and little Al

Late large oxide droplet has composition more similar to E-glass with significant Si

Early Fe-Cr-Ni has significant Al and Si

Early oxide phase mixed with Fe-Cr is rich in Al and Ca, little Si

	360	361	362	363	364	365	366	367	368	369	370	371	372	373	374
O	48.93	58.96	61.35	62.30	61.81	62.15	61.61	61.21	4.01	4.06	4.17	3.40	4.31	2.71	3.75
Na							0.47	0.37							
Mg			0.58	1.67	1.11	0.68	0.55	0.60							
Al	25.14	28.37	22.47	14.84	15.09	13.95	14.21	14.67	15.91	12.28	15.30				
Si	2.47		3.61	13.20	12.47	14.25	14.22	14.28	10.02	17.94	9.08	18.08	38.49	16.03	21.63
Ca	9.62	12.67	11.99	7.99	9.51	8.98	8.94	8.87							
Cr	3.15								12.75	13.21	12.50	13.77	11.93	15.31	14.02
Fe	10.68								50.46	46.51	51.30	56.81	39.58	56.39	52.35
Ni	0.00								6.84	6.00	7.66	7.94	5.70	9.56	8.24
Total	100.	100.	100.	100.	100.	100.	100.	100.	100.	100.	100.	100.	100.	100.	100.

← Sample location

All values are atomic %

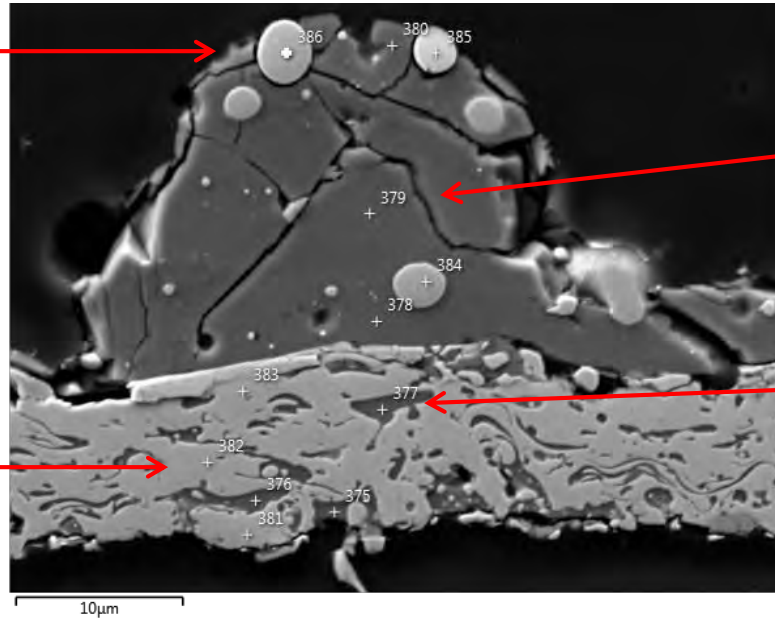


Exposed Hold Down Plate (Z) Cross Sectioned Flake

EDS Semi-quantitative Analyses

Later more isolated Fe-Cr has significant Si and little Al

Early Fe-Cr-Ni has significant Si and Al



Later larger droplets have composition more similar to E-glass but enriched in Al

Early oxide phase has significant Al and Ca – no Si

	375	376	377	378	379	380	381	382	383	384	385	386
O	56.19	59.88	60.02	61.11	61.70	60.28	3.51	2.83	2.75	2.22	3.83	4.39
Na				0.33								
Mg				0.51	1.13	1.07						
Al	27.13	27.81	28.24	16.62	12.94	19.01	12.29	14.63	2.19	1.20		
Si	1.02			12.77	13.74	10.86	11.53	9.96	27.19	25.71	25.98	28.92
Ca	10.48	12.31	11.74	8.67	10.48	8.78						
Cr	1.16						11.64	12.28	11.97	14.47	13.73	13.01
Fe	4.01						53.60	49.74	46.72	47.92	48.52	47.63
Ni	0.00						7.44	10.57	9.18	8.48	7.93	6.06
Tot.	100.	100.	100.	100.	100.	100.	1000	100.	100.	100.	100.	100.

← Sample location

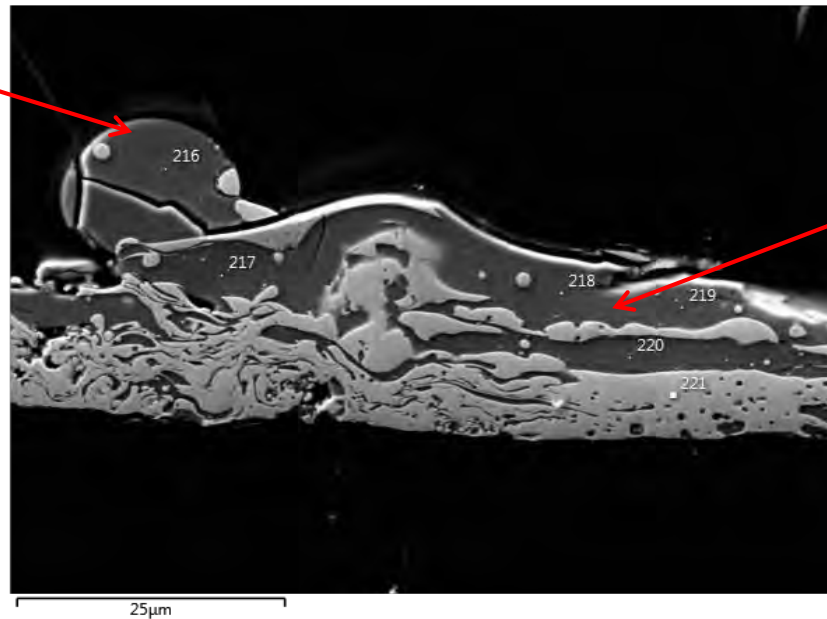
All values are atomic %



Exposed Hold Down Plate (Z) Cross Sectioned Flake

EDS Semi-quantitative Analyses

More Si-rich and
relatively Al-poor.
More like E-glass.
Arrived semi-
solidified.



Al-rich, Si-poor.
Arrived in fluid state.

Element	E-Glass	216	217	218	219	220	221
O	65.3	66.89	62.86	57.74	58.94	62.08	0.00
Na	0.4					0.53	
Mg	0.4		0.60			0.72	
Al	5.9	5.76	12.60	30.00	29.01	15.39	16.25
Si	19.4	19.32	14.67	0.72	1.36	12.59	10.89
Ca	8.4	8.03	9.27	11.54	10.69	8.69	
Cr							10.68
Fe							52.90
Ni							9.27
Total	99.8	100.00	100.00	100.00	100.00	100.00	100.00

← Sample location

All values are
atomic %

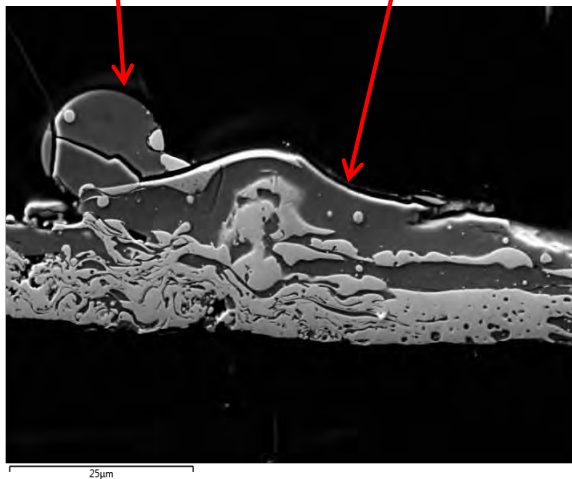
Earlier arriving silicate droplets can have different compositions – more Al-rich than E-glass.



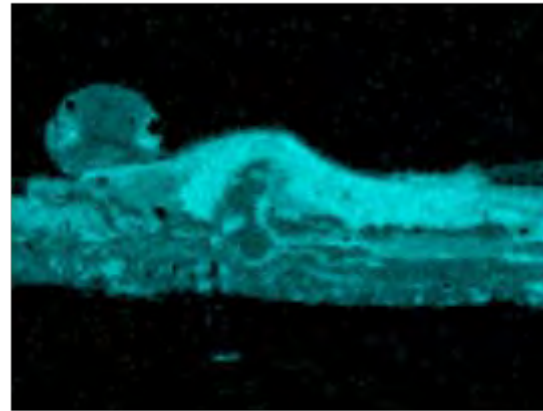
Exposed Hold Down Plate (Z) Cross Sectioned Flake EDS Maps

More Si-rich
Al-poor –
late droplet

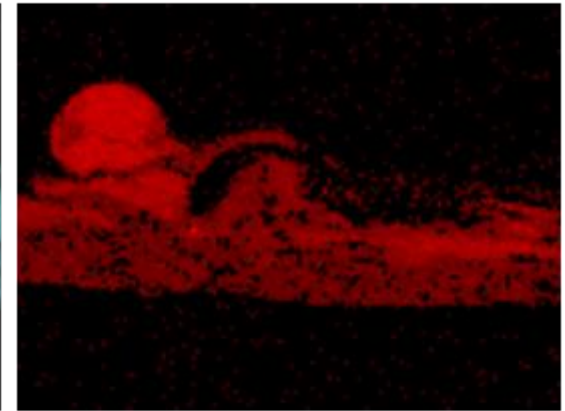
Al-rich, Si-poor
early droplet?



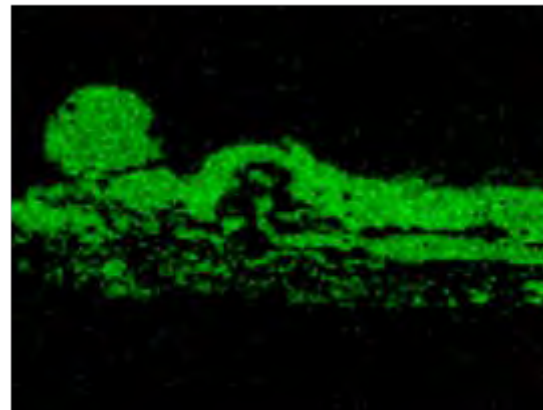
Al K series



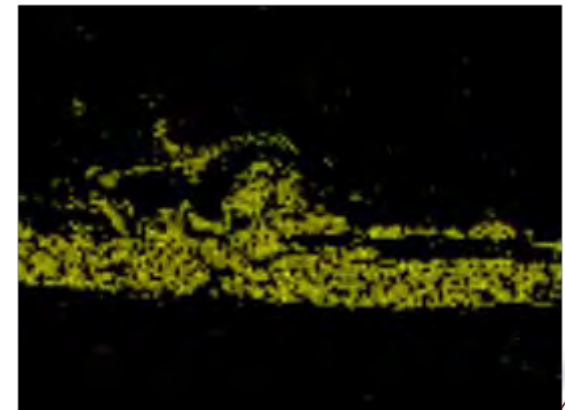
Si K series



Ca K series

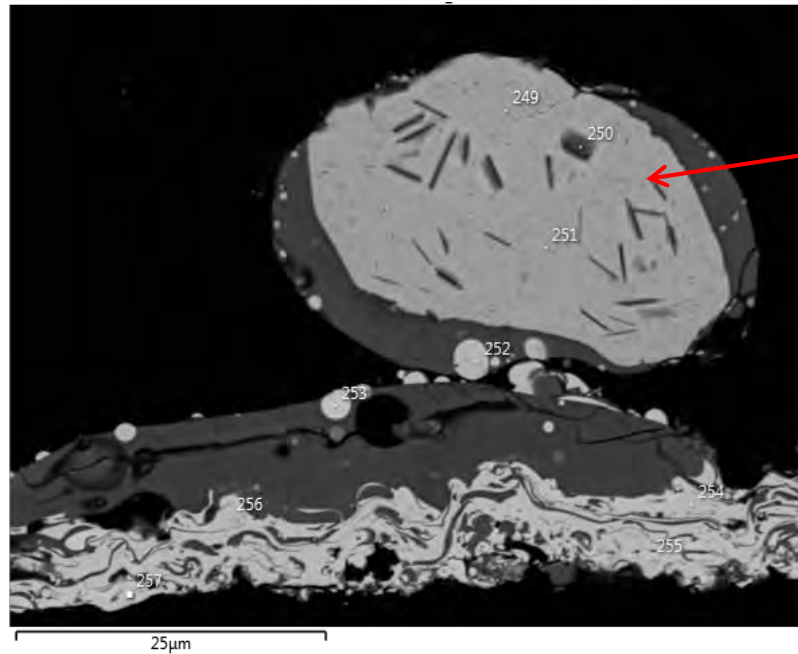


Fe K series



Exposed Hold Down Plate (Z) Cross Sectioned Flake

EDS Semi-quantitative Analyses



Significantly enriched in aluminum – from projectile? Arrived later.

Element	249	250	251	252	253	254	255	256	257
O	4.19	42.95	3.53	4.04	3.26	2.91	4.71	3.98	3.91
Al	46.21	34.22	40.91	5.16	1.82	15.35	12.36	13.12	13.64
Si	7.36	3.09	6.82	30.45	23.25	10.61	11.70	12.69	9.46
Cl		2.64							
Cr	9.57	3.25	6.58	9.20	11.77	12.37	13.95	13.99	12.46
Fe	32.67	13.84	34.80	51.15	50.38	48.12	57.29	56.22	50.25
Ni	0.00	0.00	7.35	0.00	9.53	10.64	0.00	0.00	10.28
Total	100.0	100.00	100.00	100.00	100.00	100.00	100.00	100.00	100.00

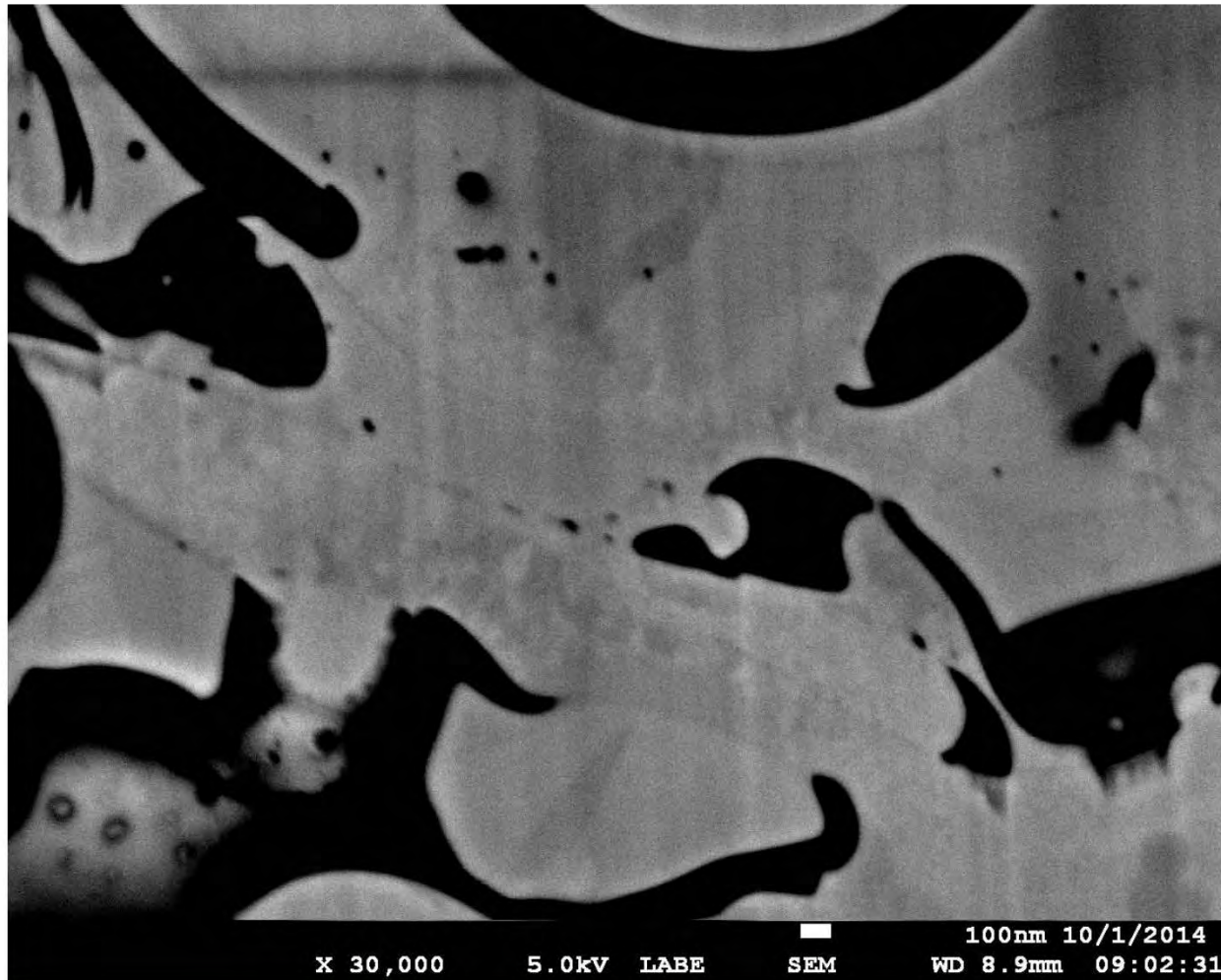
← Sample location

All values are atomic %

This is an isolated particle



SBU Marking
FIB/TEM Cross Section of Hold Down Plate Flake
Backscatter SEM 30KX

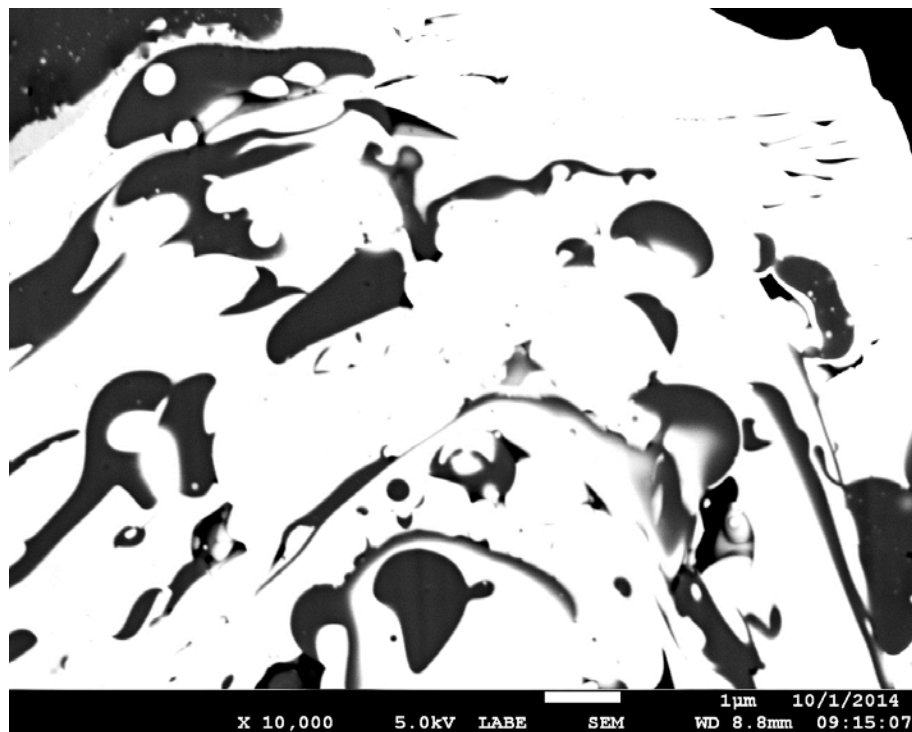


Channeling contrast in Fe-Cr-Ni phase shows crystalline grain boundaries. Crystallites are relatively large (to 1 μm). Finer grains in localized areas imply faster cooling.

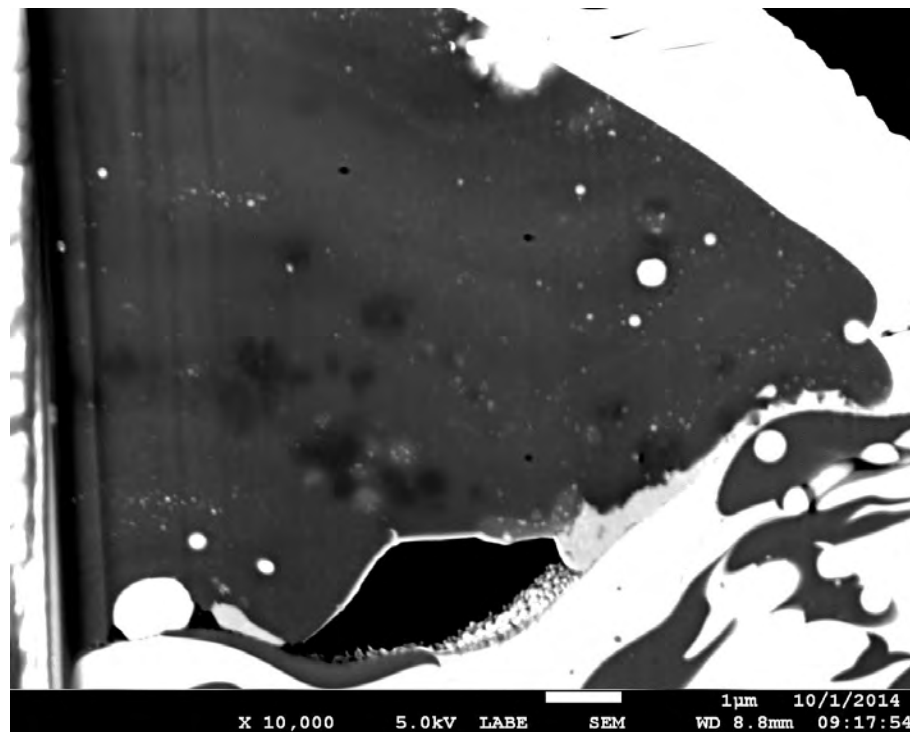


FIB/TEM Cross Section of Hold Down Plate Flake

Backscatter SEM 10KX

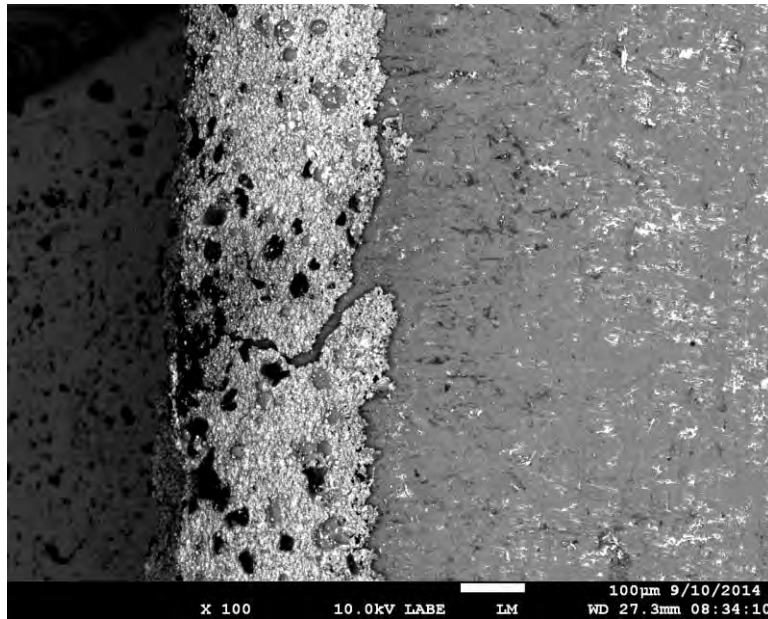


Ca-Al oxide phase shows no channeling contrast grain boundaries- is amorphous.



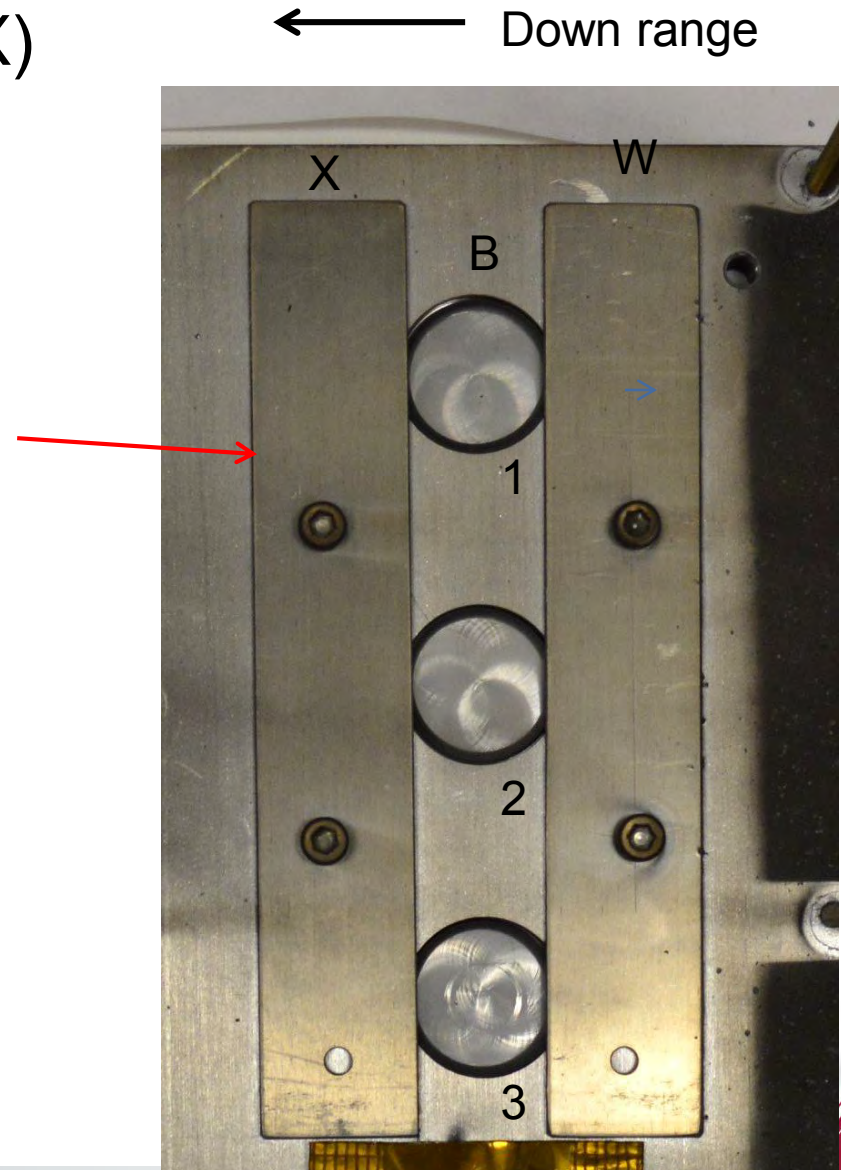
Note dispersed nano higher Z droplets.

Protected Hold Down Plate (X)



The down range edge of plate has accumulated a layer of molten deposits.

The up range edge is relatively clean.



Most molten droplets must have impinged at a relatively high angle since the Whipple plates effectively shadowed the witness plates underneath.



Protected Hold Down Plate (X)

Backscatter SEM 500X

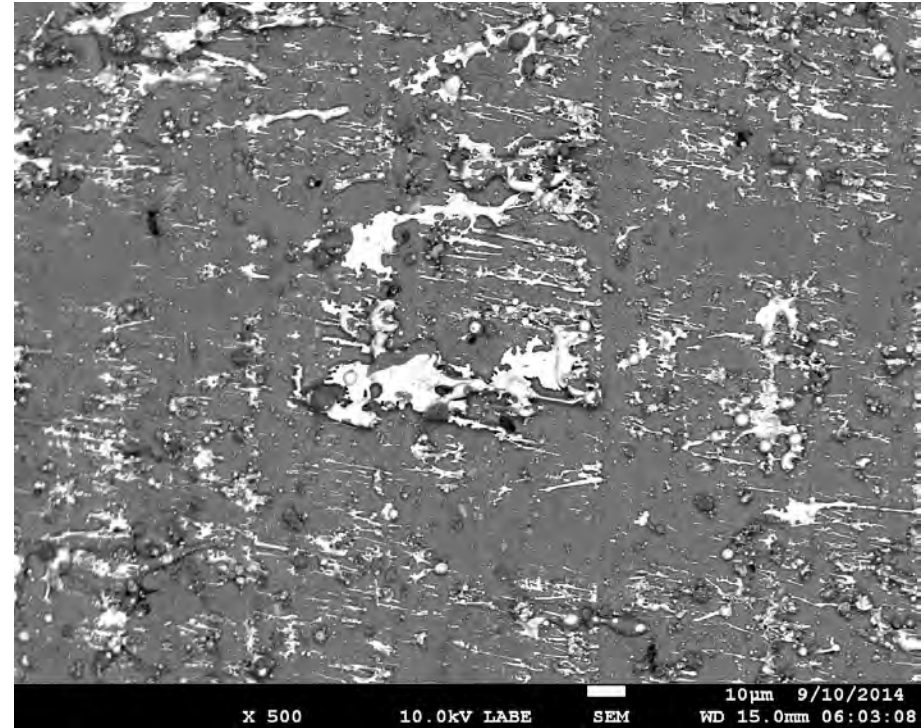
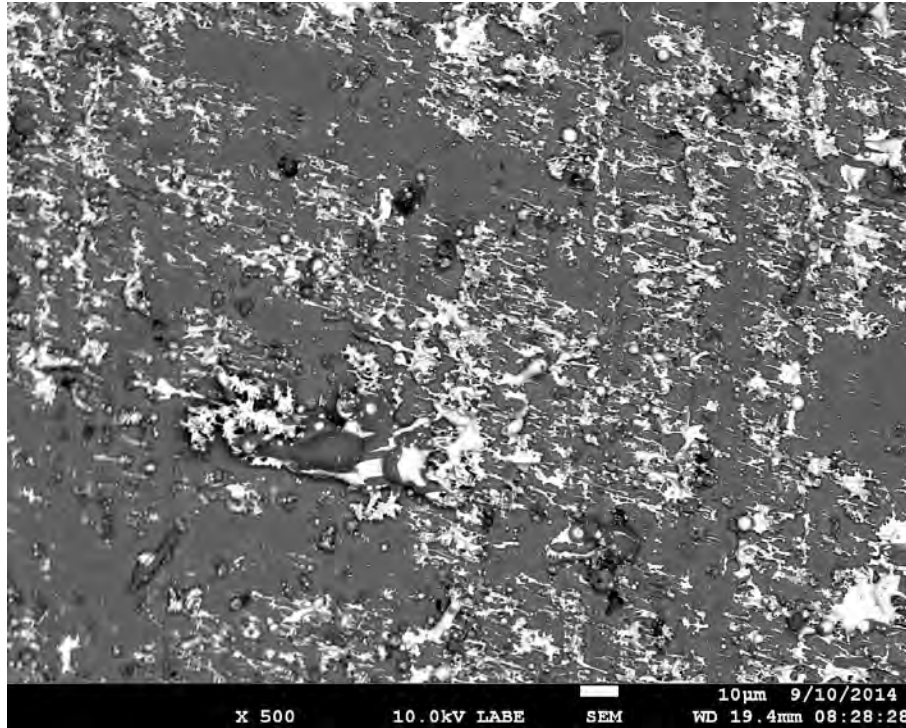


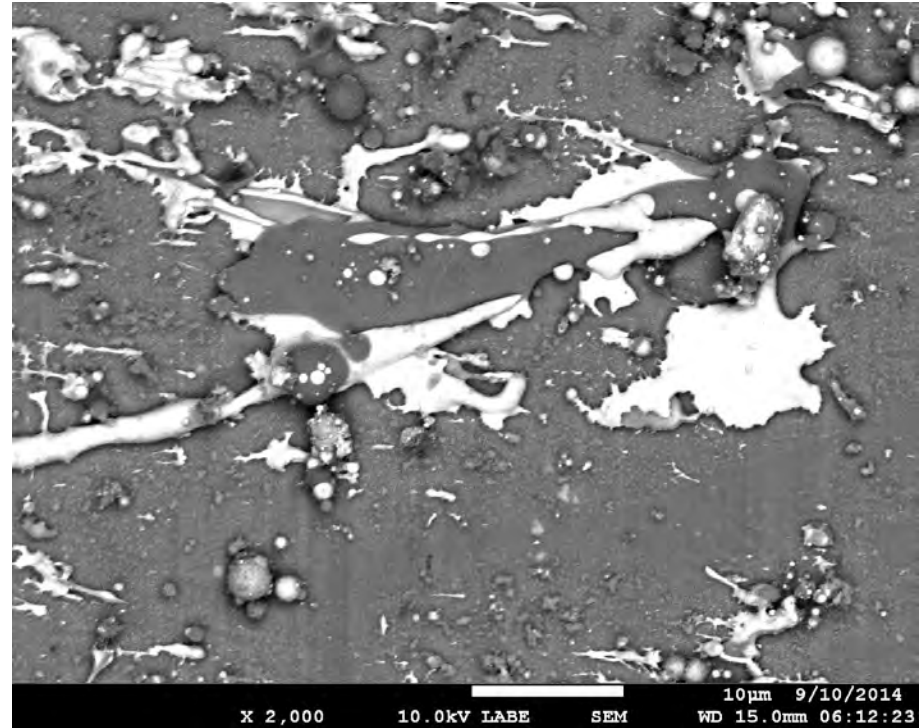
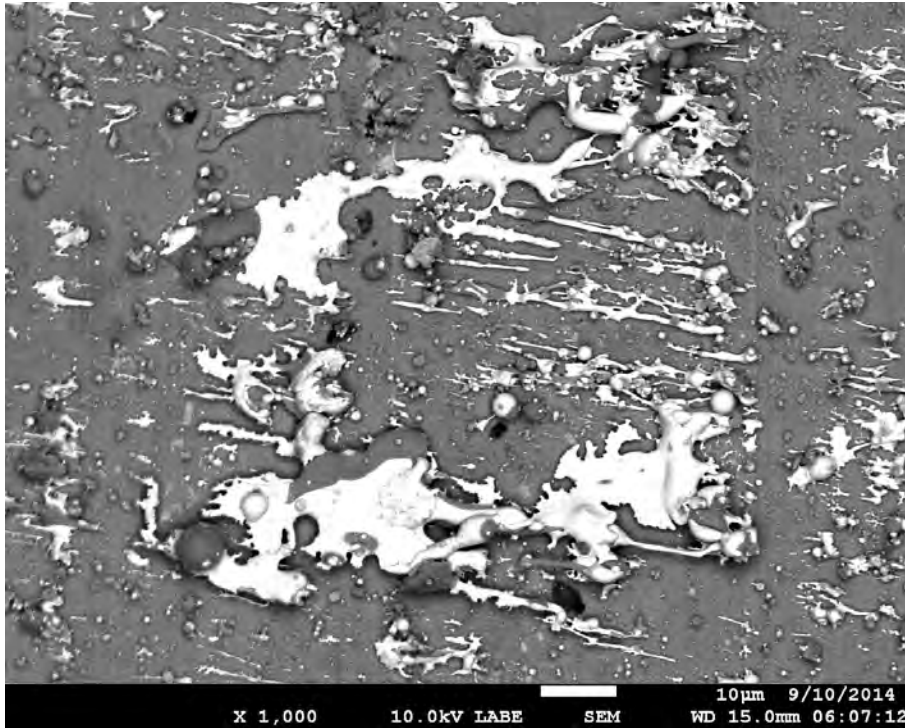
Plate (X) has slightly more elongated molten droplets oriented perpendicular to the long dimension of the plate, than plate (W). Implies the source was down range? Vertical striations are from rolling the aluminum plate.

The direction of flow of the droplets is up range based on the accumulation on the down range edge.



Protected Hold Down Plate (X)

Backscatter SEM 1KX, 2KX

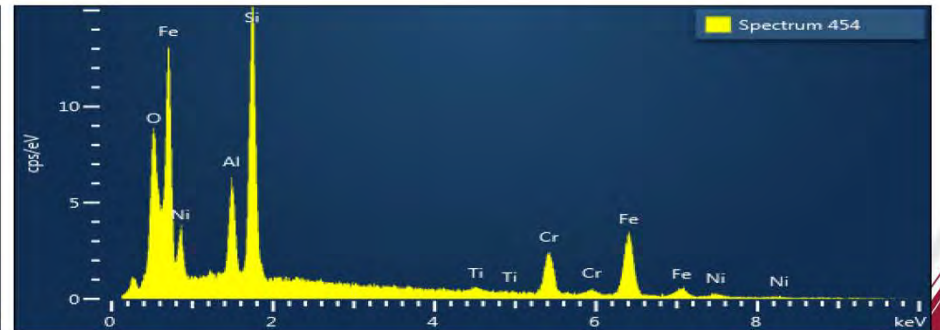
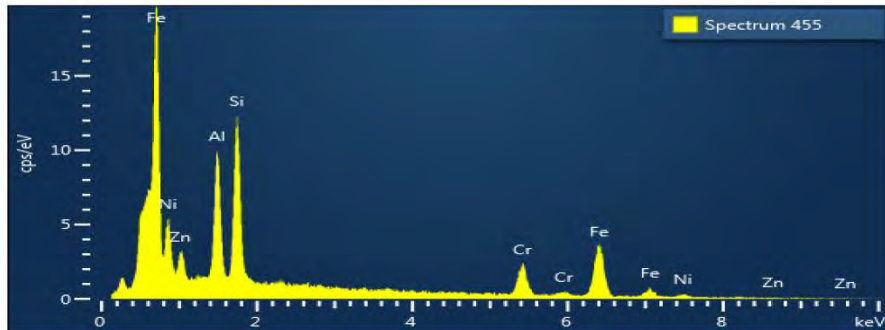
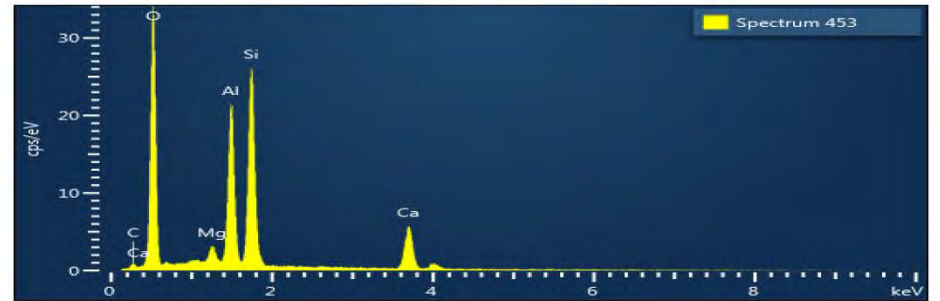
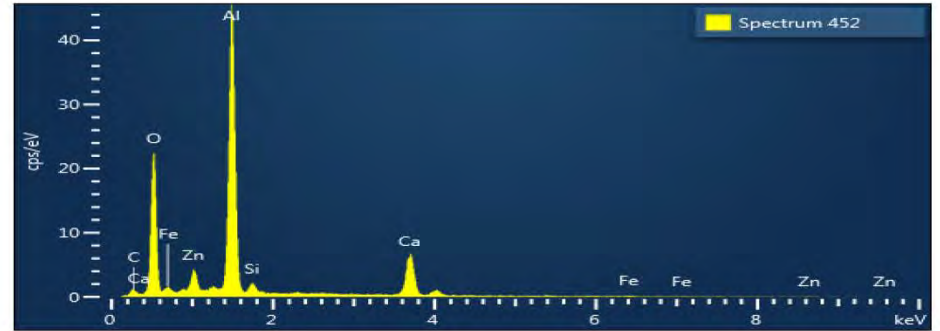
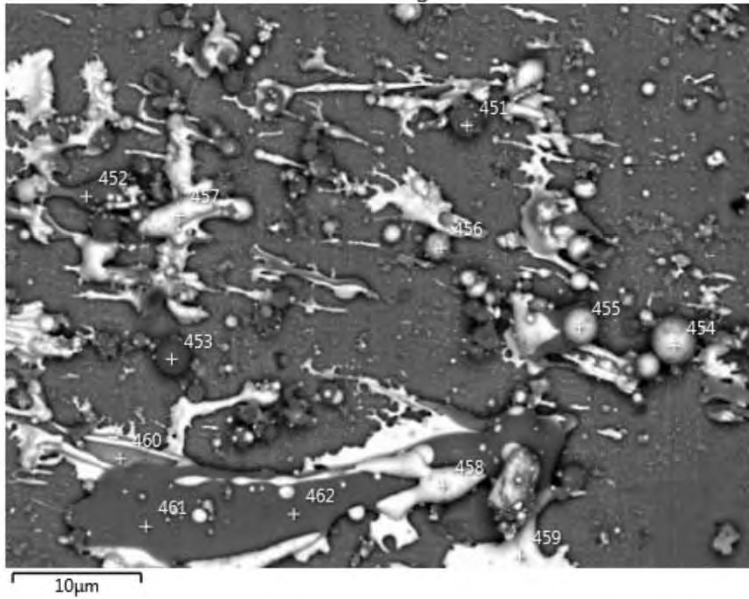


Molten droplets are Fe-Cr-Ni rich (light) and Ca-Al-oxide or silicate (gray). Gray background is the clean aluminum plate.



Protected Hold Down Plate (X)

SEM EDS

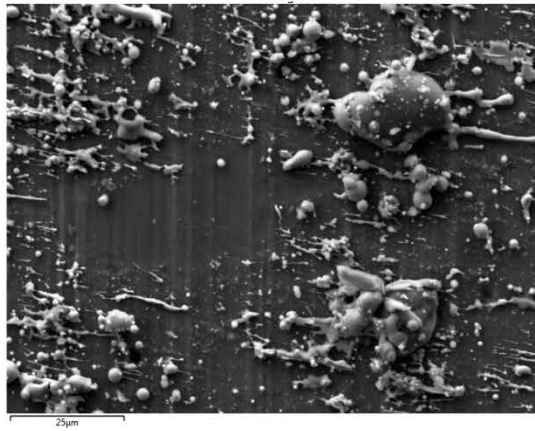


Droplets have similar compositions to what are seen on exposed hold down plate.

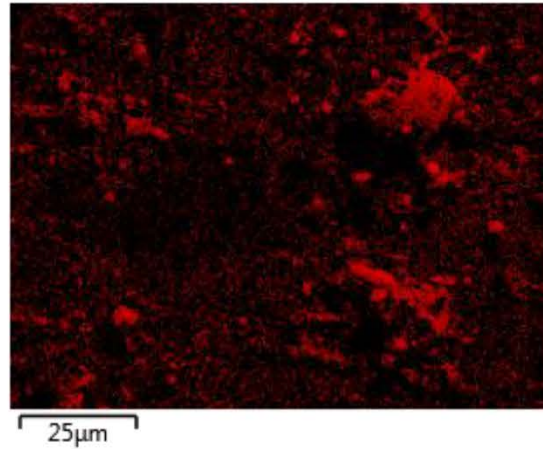


Protected Hold Down Plate (X)

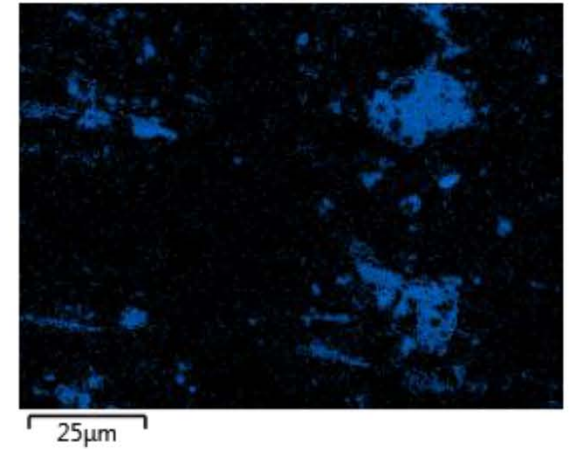
SEM EDS Maps



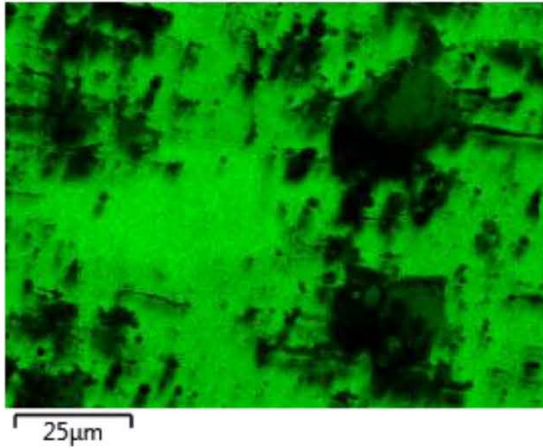
O K series



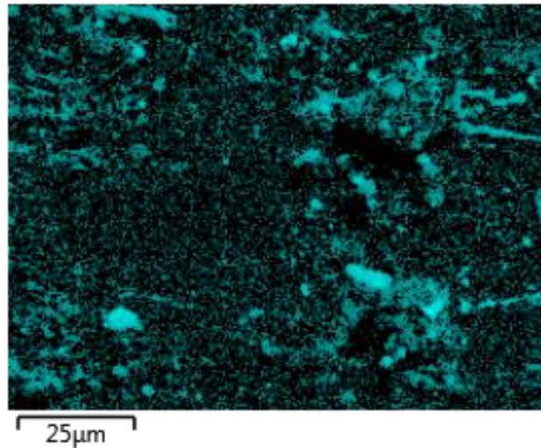
Ca K series



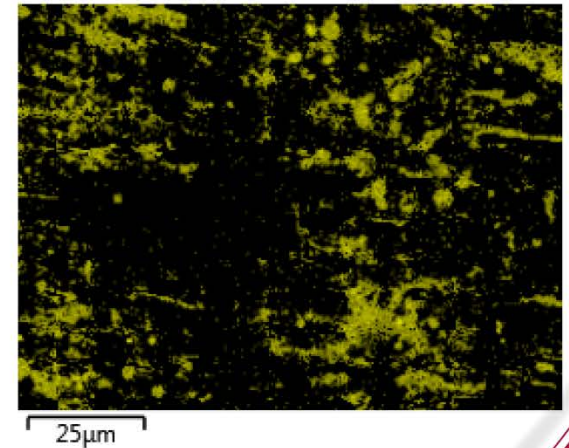
Al K series



Si K series

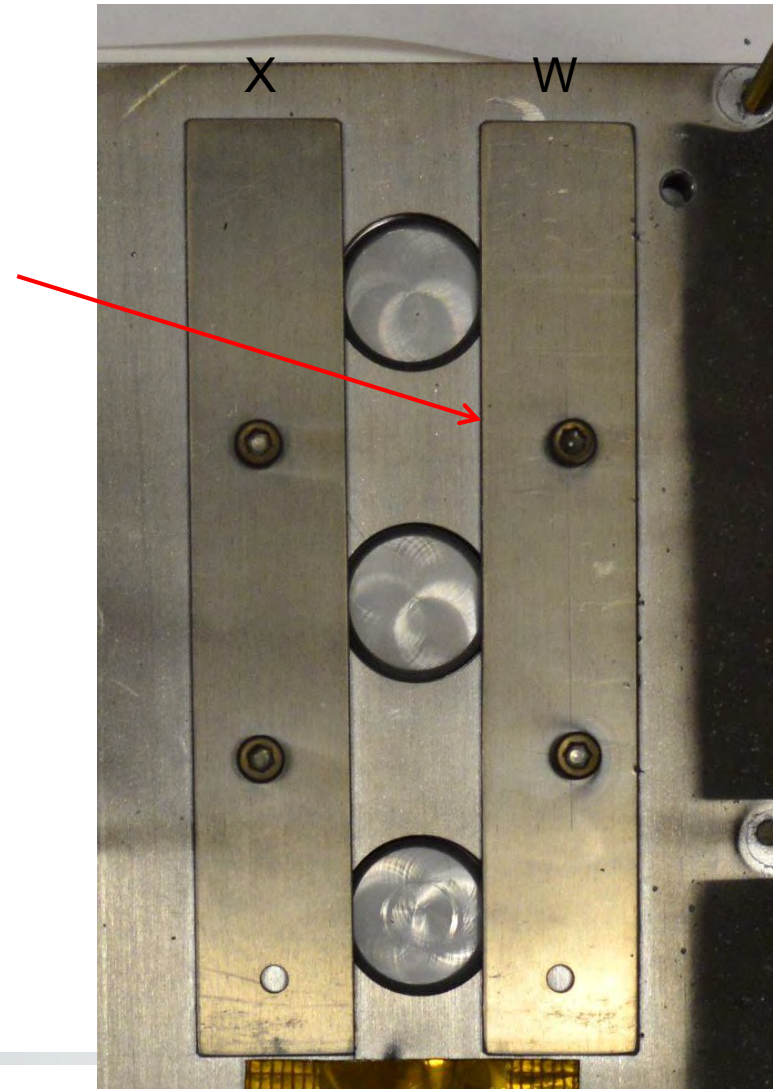
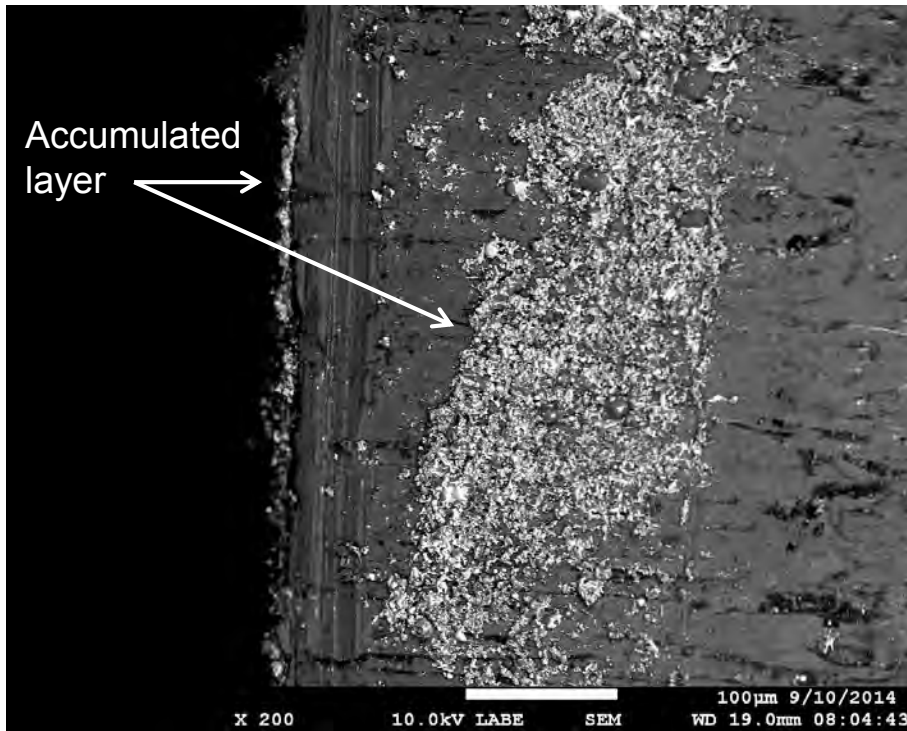


Fe K series



Protected Hold Down Plate (W)

← Down range



Down range edge of plate has accumulated a layer of molten deposits. The deposit is not as thick as that on the edge of plate (X)

Protected Hold Down Plate (W)

Backscatter SEM 500X, 2KX

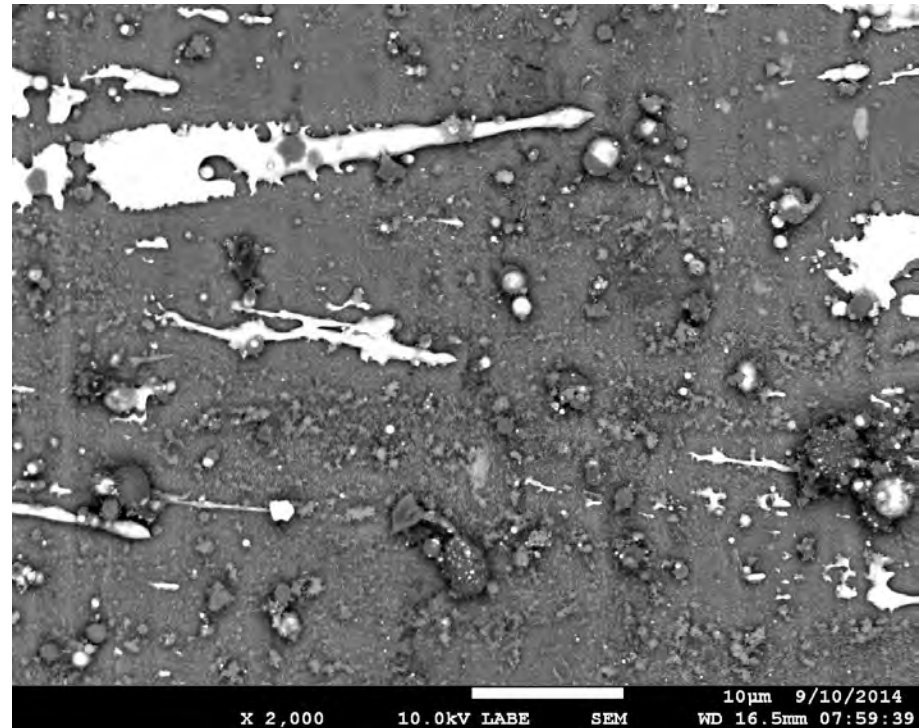
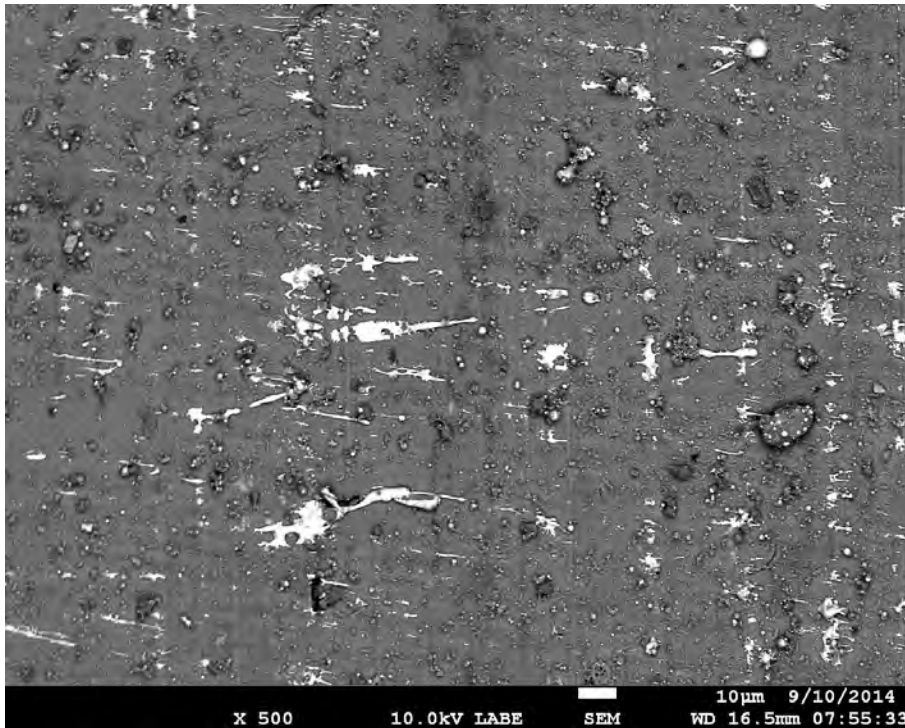


Plate is relatively clean with sparse elongated molten droplets oriented perpendicular to the long dimension of the plate. Vertical striations are from rolling the aluminum plate. The direction of flow of the droplets is probably up range (from left to right).

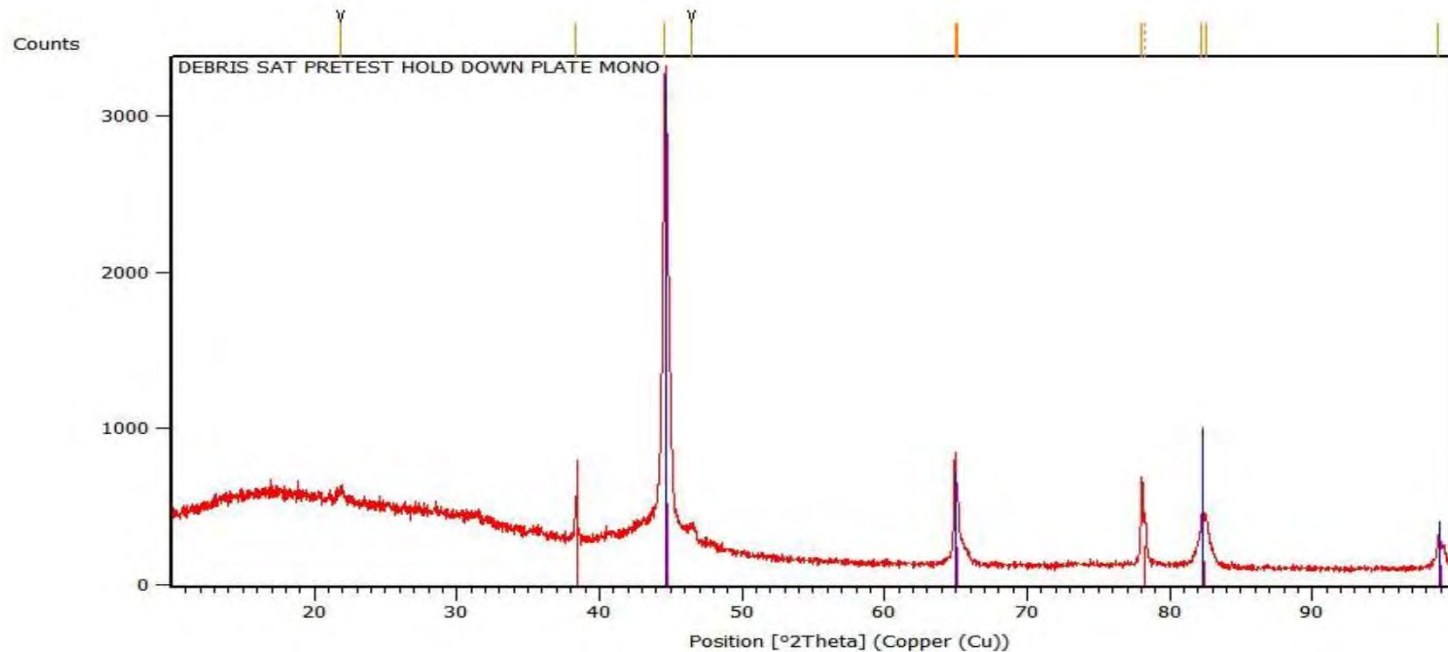
Deposits are loosely adhering and can easily be wiped off.



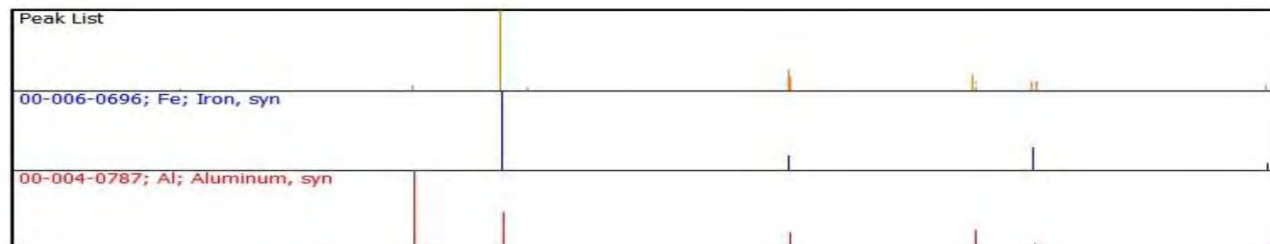
SBU Marking

Exposed Hold Down Plate (Z) Flake

X-ray Diffraction



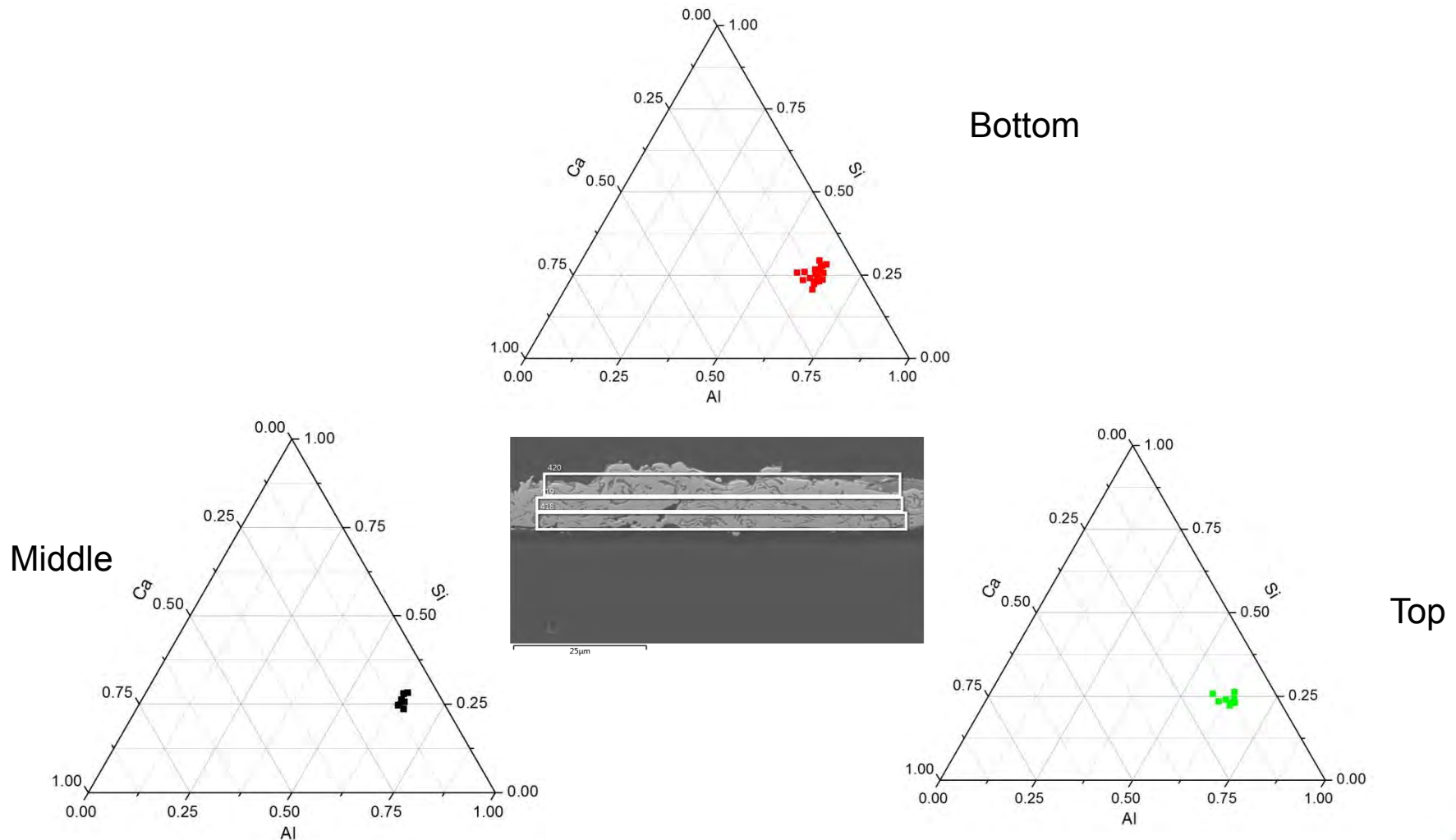
XRD Library Matches



Solidified molten material is partially crystalline.
 α Fe-Cr-Ni phase is body-centered cubic “iron”.
Silicate/oxide phase is amorphous.



Integrated Ca-Al-Si Content of Fe-Cr-Ni and Ca-Al-Si Phases Complex Flow Structure



No significant change in bulk composition of layer with complex flow structure with depth/time. Did not sample large late arriving droplets or very top most surface.



Appendix 2



Technical Reports Addendum Asset Summary



TRAAS ID #: 2014082413085814820

Report Name: DebriSat Pre Preshot Laboratory Analyses

Aerospace Report Number: TOR-2014-03083

Start Date of Test: 2014-04-21

Created By: 14820 Adams, Paul M

JO: 8506-72

End Date of Test: 2014-11-30

First Aerospace Author / PI: 14820 Adams, Paul M

Program:

Description:

Keywords:

Asset: AAA123	Manufacturer: PERKIN ELMER CORPORATION	Model: LAMBDA 900	Usage Start Date: 2014-04-21	Usage End Date: 2014-10-30	Asset Comment:
Date:	Calibration Due Date:	Comment:	Certificate Number:		
2013-04-17	2014-08-17	TMT-NORMAL	fa6f32f7eed80b468d87b46e44dfec1aa		
2014-08-18	2016-03-13	TMT-NORMAL	777773c04920e64b8f107f76514d6a40		
Asset: AAA126	Manufacturer: PERKIN ELMER CORPORATION	Model: PELA-1000	Usage Start Date: 2014-04-21	Usage End Date: 2014-10-30	Asset Comment:
Date:	Calibration Due Date:	Comment:	Certificate Number:		
2013-04-17	2016-04-17	TMT-NORMAL	ed846df747a19149bb42006784ea95a7		
Asset: ABB367	Manufacturer: PANALYTICAL	Model: X'Pert Pro MPD	Usage Start Date: 2014-04-21	Usage End Date: 2014-09-30	Asset Comment:
Date:	Calibration Due Date:	Comment:	Certificate Number:		
2014-03-17	2015-07-12	TMT-NORMAL	ed56d88fa3e45747818a097cc86c3027		
Asset: ABW501	Manufacturer: THERMO-NICOLET	Model: 6700	Usage Start Date: 2014-04-21	Usage End Date: 2014-09-30	Asset Comment:
Date:	Calibration Due Date:	Comment:	Certificate Number:		
2014-03-17	2015-08-16	TMT-NORMAL	c0ad25e310e49243ae8a043b67c2c0f1		
Asset: ACR364	Manufacturer: JEOL (USA) INC.	Model: JSM-7600F	Usage Start Date: 2014-04-21	Usage End Date: 2014-09-30	Asset Comment:

Wed Dec 24 07:51:55 PST 2014

Page 1 of 2



SBU Marking

Date:	Calibration Due Date:	Comment:	Certificate Number:
2014-02-05	2015-07-05	TMT-NORMAL	d498d9360ad1224f85d04309c6869674
Asset: ACR429 Manufacturer: OXFORD INSTRUMENTS Model: X-MAX Usage Start Date: 2014-04-21 Usage End Date: 2014-09-30 Asset Comment:			
Date:	Calibration Due Date:	Comment:	Certificate Number:
2013-02-08	2014-06-08	TMT-NORMAL	106f65e49dfc8043869a5da06587e7fa
2014-06-02	2015-12-27	TMT-NORMAL	f840182f4f92e2449d541c92c3465ec2
Asset: ACR822 Manufacturer: OXFORD INSTRUMENTS Model: HKL Usage Start Date: 2014-04-21 Usage End Date: 2014-11-30 Asset Comment:			
Date:	Calibration Due Date:	Comment:	Certificate Number:
2013-04-10	2014-08-10	TMT-NORMAL	1a28e3eb00681541b3a79b3818cc734c
2014-06-02	2015-12-27	TMT-NORMAL	ead709f42b3e744fb9d90107a3f68844

*Support and Auxiliary Equipment are not calibrated.



DebrisSat Pre Preshot Laboratory Analyses

Approved Electronically by:

David J. Gorney, EXECUTIVE VP
OFFICE OF EVP/SSG

Anthony T. Salvaggio, PRINC DIRECTOR
ENGINEERING DIRECTORATE
ENGINEERING & INTEGRATION DIVISION
OFFICE OF EVP/SSG

Technical Peer Review Performed by:

Shant Kenderian, DIRECTOR DEPT
MATERIALS PROCESSING DEPT
SPACE MATERIALS LABORATORY
ENGINEERING & TECHNOLOGY GROUP

© The Aerospace Corporation, 2015.

All trademarks, service marks, and trade names are the property of their respective owners.

SC2477

External Distribution

REPORT TITLE

Debrisat Pre Preshot Laboratory Analyses

REPORT NO.

TOR-2014-03083

PUBLICATION DATE

March 27, 2015

SECURITY CLASSIFICATION

UNCLASSIFIED

David E Davis
SMC/ENE
david.davis.3@us.af.mil

J.-C. Liou
NASA-JSC
jer-chyi.liou-1@nasa.gov

Norman Fitz-Coy
University of Florida
nfc@ufl.edu

Thomas Huynh
SMC/ENC
thomas.huynh@us.af.mil

John Opiela
NASA-JSC
john.n.opiela@nasa.gov

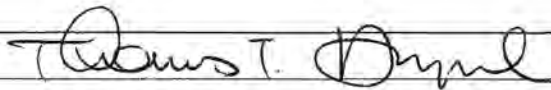
Heather Cowardin
NASA-JSC
heather.cowardin@nasa.gov

Jesse Edwards
SMC/ENC
esse.edwards.4@us.af.mil

Mitch Nolen
AEDC
mitchell.nolen.ctr@us.af.mil

Brian Roebuck
AEDC
brian.roebuck.ctr@us.af.mil

APPROVED BY
(AF OFFICE)



DATE

2 Mar 2015

2477